

**The endocytic adaptor AP-2 interacts with γ -TuRC components to
maintain centrosome integrity in neural progenitor cells**

Dissertation

zur

Erlangung des Doktorgrades

Dr. rer. nat

der Mathematisch-Naturwissenschaftlichen Fakultät

der Universität zu Köln

vorgelegt von

Santiago Manuel Camblor Perujo

Aus Langreo

2022

Berichtersteller/in: Prof. Dr. Natalia L. Kononenko

Prof. Dr. Elena I. Rugarli

TABLE OF CONTENT

TABLE OF CONTENT	IV
LIST OF FIGURES	VIII
ABBREVIATIONS	X
SUMMARY	XIII
ZUSAMMENFASSUNG	XIV
1. INTRODUCTION	1
<i>1.1 Brain development</i>	<i>1</i>
1.1.1 Neural Progenitor Cells (NPCs) and the neurogenic process	2
1.1.2 Cell cycle and neurogenesis	4
<i>1.2 Centrosomes and cell cycle</i>	<i>7</i>
1.2.1 The centrosome cycle	7
1.2.2 Centrosome-related disorders	9
<i>1.3 Endocytosis</i>	<i>10</i>
1.3.1 Phagocytosis and Macropinocytosis	11
1.3.2 Receptor-Mediated Endocytosis, CIE, CME, and AP-2.....	12
1.3.3 Endocytosis functions in the brain, cell cycle, and neurogenesis	14
2. AIMS OF THE STUDY	23
3. RESULTS	24
<i>3.1 AP-2 deletion has severe consequences for NPCs proliferation and mitosis</i>	<i>24</i>
<i>3.2 AP-2 is required for cell cycle entry in the G1-S transition</i>	<i>28</i>
<i>3.3 AP-2 KO induces senescence-associated cell death and DNA-damage p53-dependent</i>	<i>30</i>
<i>3.4 Disturbance of p53 signaling rescues the AP-2 KO phenotype</i>	<i>33</i>

3.5 AP-2 interacts with centrosomal proteins and stabilizes centrosome structure.....	35
3.6 AP-2 role in cell cycle and centrosome is independent of Clathrin-Mediated Endocytosis	41
3.7 AP-2 KO increases ciliation, but cilia removal does not rescue the phenotype in astrocytes	43
3.8 AP-2 is essential for MTOC activity and new-born neurons migration	45
4. DISCUSSION.....	50
4.1 AP-2 is essential for G1 to S transition, and AP-2 deletion results in cell cycle arrest.....	50
4.2 AP-2 novel interactions with centrosomal components are vital for a proper centrosome structure and function.....	52
4.3 AP-2 KO defective centrosomes have physiological effects on microtubule activity and cell migration.	53
4.4 AP-2 role in centrosome and cell division is independent of CME.	55
4.5 Possible hypothesis	56
4.5.1 AP-2 traffics γ -Tubulin components to the centrosome from the basal body in the plasma membrane.	57
4.5.2 AP-2 helps stabilize the centrosome structure binding to γ -Tubulin components	57
4.5.3 AP-2 binding to γ -Tubulin components at the centrosome is necessary for spindle formation .	58
4.5.4 AP-2 mediates local protein translation at the centrosome	58
4.5.5 AP-2 acts at the transcriptional level in the nucleus	59
5. CONCLUDING REMARKS AND DIRECTIONS FOR FUTURE WORK.....	61
6. MATERIALS AND METHODS.....	64
6.1 Materials.....	64
6.1.1 General laboratory equipment	64
6.1.2 Chemicals	65
6.1.3 Reagents.....	68
6.1.4 Kits and other equipment	69

6.1.5 Antibodies	70
6.1.6 Oligonucleotides and vectors	73
6.1.7 Mouse models	74
6.1.8 Solutions and Media	74
6.2 Methods	78
6.2.1 Animals.....	78
6.2.2 Genotyping	78
6.2.3 Preparation of cell cultures and transfections	79
6.2.5 EdU Pulse Labelling	82
6.2.6 β -Gal Senescence Assay.....	82
6.2.7 Neurosphere Migration Assay.....	82
6.2.8 Immunocytochemistry of cultured cells	82
6.2.9 Immunostaining of Tubulin1 α	83
6.2.10 Microscope picture analysis	83
6.2.11 STED imaging	84
6.2.12 Live imaging of cultured neurons	84
6.2.13 Propidium Iodide Flow Cytometry	84
6.2.14 Western blotting	84
6.2.15 Co-immunoprecipitation assays	85
6.2.16 Mass Spectrometry analysis of AP-2 α binding partners	85
6.2.17 Proteomics	86
6.2.18 Statistical Analysis	87
7. REFERENCES	88
8. PUBLICATIONS	116

ACKNOWLEDGMENTS117

EIDESSTÄTTLICHE ERKLÄRUNG118

CV.....119

LIST OF FIGURES

Figure 1. Neuronal progenitor cells lineage determination.....	2
Figure 2. Schematic illustration of neural progenitor cell division modes and neurogenesis process.....	3
Figure 3. Cell cycle diagram.....	6
Figure 4. Diagram of the centrosome cycle.....	8
Figure 5. Structure of the γ -tubulin complex and its association with the centrosome.	9
Figure 6. Several centrosomal proteins are linked to disorders.	10
Figure 7. Different endocytosis mechanisms.....	11
Figure 8. AP-2 complex and CME.....	14
Figure 9. Duality of endocytic proteins.	19
Figure 10. Tamoxifen treatment completely deletes AP-2 after 72 hours.....	24
Figure 11. The proliferation of NPCs is compromised upon deletion of AP-2.	25
Figure 12. Mitotic cells are reduced with time upon AP-2 deletion.....	26
Figure 13. AP-2 KO NPCs present mitotic spindle anomalies and lagging chromosomes.	27
Figure 14. Reintroduction of AP-2 μ rescues the mitotic phenotypes of AP-2 KO cells.....	27
Figure 15. Proteins and pathways essential for cell cycle progression are affected in KO cells.	28
Figure 16. The proliferation of NPCs is reduced when AP-2 KO is induced.....	29
Figure 17. AP-2 KO arrest cells in the G1-S phase transition with increased dead cells.....	30
Figure 18. Senescence is increased in AP-2 KO cells.....	31
Figure 19. p53 is activated in AP-2 deleted NPCs.....	32
Figure 20. DNA damage is increased in AP-2 KO cells.....	32
Figure 21. Mitosis is reduced and abnormal in MEFs upon AP-2 depletion.....	33

Figure 22. Mitosis phenotypes are rescued upon p53-pathway inhibition in iMEFs.	34
Figure 23. AP-2 subunit α interacts with components of the γ -tubulin complex, essential for centrosome structure and function.	36
Figure 24. AP-2 subunits α and μ interact physically with GCP3.	37
Figure 25. GCPs distribution and levels are altered upon AP-2 KO in NPCs.....	38
Figure 26. GCP2 distribution and levels are altered upon AP-2 KO in NPCs.....	39
Figure 27. AP-2 KO NPCs present abnormal centrosomes.	39
Figure 28. AP-2 KO cells have normal centrioles but abnormal pericentriolar matrix.....	40
Figure 29. CME-inhibited cells do not present any mitotic defect or cell cycle arrest.	41
Figure 30. AP-2 KO NPCs present abnormal centrosomes.	42
Figure 31. AP-2 KO NPCs have increased ciliation and elongated cilia.....	43
Figure 32. Disrupted CME NPCs do not present increased ciliation nor increased cilia length ..	44
Figure 33. Astrocytes have proliferation defects that are not rescued by cilia KO.....	45
Figure 34. Evidence of possible AP-2 trafficking to the centrosome.	46
Figure 35. Microtubules are affected in AP-2 KO NPCs, but microtubule nucleation is not disrupted.....	46
Figure 36. Microtubule activity is affected in AP-2 KO NPCs.....	47
Figure 37. Microtubule activity is not rescued in AP-2+Ift88 KO astrocytes.	48
Figure 38. AP-2 KO NPCs have disturbed migration.	49
Figure 39. Graphic representation of potential AP-2 roles in cell cycle.	60

ABBREVIATIONS

AD	Alzheimer Disease
ALS	Amyotrophic Lateral Sclerosis
ANOVA	Analysis of variance
AP-2	Adaptor Protein Complex 2
APO	Apochromat
APS	Ammonium peroxodisulfate
ARL13	ADP-ribosylation factor-like protein 13B
BDNF	Brain-derived Neurotrophic Factor
b-FGF	Basic fibroblast growth factor 2
BRCA1	Breast cancer type 1 susceptibility protein
BSA	Bovine Serum Albumin
C	Celsius
C57BL6	C57 black 6
CASP2	Caspase-2
CCP	Clathrin-Coated Pit
CCV	Clathrin-Coated Vesicle
CEP63	Centrosomal Protein 63
CHC	Clathrin heavy chain
CME	Clathrin-mediated endocytosis
CNS	Central Nervous System
DAPI	4',6-diamidino-2-phenylindole
DIC	Differential interference contrast
DIV	Days In Vitro
DMEM	Dulbecco's modified eagle medium
DMEM/F-12	Dulbecco's Modified Eagle Medium/Nutrient Mixture F-12
DMSO	Dimethyl sulfoxide
DNA	Deoxyribonucleic acid
dNTP	Nucleoside Triphosphate
DTT	Dithiothreitol
E12.5	Embryonic day 12.5
E2F	Transcription factor E2F
EAP	Endocytic Accessory Proteins
EB3	Ending binding protein 3
ECL	Enhanced chemiluminescence (ECL)
EDTA	Ethylenediaminetetraacetic acid
EGF	Epidermal Growth Factor
EGTA	Egtazic Acid
FBS	Fetal bovine serum
FDR	False Discovery Rate
G0	Quiescent stage

G1	Growth 1 phase
G2	Growth 2 phase
GAPDH	Glyceraldehyde 3-phosphate dehydrogenase
GCP	Gamma-tubulin Complex Protein
GFAP	Glial Fibrillary Acidic Protein
GFP	Green fluorescent protein
HBSS	Hanks' Balanced Salt Solution
HD	Huntington Disease
HEPES	4-(2-hydroxyethyl)-1-piperazineethanesulfonic acid
ICC	Immunocytochemistry
IGEPAL	Octylphenoxypolyethoxyethanol
KD	Knockdown
kDa	Kilodalton
KO	Knockout
LANUV	Landesamt für Natur, Umwelt und Verbraucherschutz
LAS	Leica Application Suite
LB	Lysogeny broth
LED	Light-emitting diode
M	Mitosis
mCh	mCherry protein
MEF	Mouse Embryonic Fibroblast
MEM	Minimum Essential Media
MS	Mass spectrometry
MT	Microtubule
MTOC	Microtubule Organising Center
NGS	Normal Goat Serum
NLS	Nuclear Localization Sequence
NPC	Neural Progenitor Cell
NSC	Neural stem cell
ON	Overnight
PB	Phosphate-buffer
PBS	Phosphate-buffered saline
PCM	Pericentriolar Matrix
PCM1	Pericentriolar Material 1
PCNT	Pericentrin
PCR	Polymerase chain reaction
PD	Parkinson Diseases
PDL	Poly-D-Lysine
PFA	Paraformaldehyde
PIPES	2,2'-(Piperazine-1,4-diyl)di(ethane-1-sulfonic acid)
RB	Retinoblastoma protein
RFP	Red fluorescent protein

RGC	Radial Glial Cells
RIPA	Radioimmunoprecipitation assay
RNA	Ribonucleic acid
ROI	Region Of Interest
Rpm	Revolution per minute
RT	Room temperature
S	Synthesis Phase
SAC	Spindle
SAK/PLK4	Sak kinase
SDS	Sodium Dodecyl Sulfate
SDS-PAGE	Sodium Dodecyl Sulfate - Polyacrylamide Gel Electrophoresis
SGZ	Subgranular zone
sHH	Sonic Hedgehog
STED	Stimulated Emission Depletion
SV40	Simian vacuolating virus 40
SVZ	Subventricular Zone
TBE	Tris/Borate/EDTA
TBS	Tris-buffered saline
TEAB	Tetraethylammonium bromide
TEMED	Tetramethylethylenediamine
TGF-β	Transforming Growth Factor Beta
Tmx	Tamoxifen-inducible line
TRK-B	Tyrosine receptor-like B
WB	Western Blot
WT	Wild Type
αTAT	α -Tubulin Acetyltransferase
γ-TuRC/TuRC	γ -tubulin ring complex
γ-TuSC/TuSC	γ -tubulin small complex

SUMMARY

Neurogenesis is the process by which a population of cells called Neural Progenitor Cells (NPCs) produces neurons and glia within the central nervous system. This is a crucial process for development, and it has been shown that in the adult brain continues in restricted areas to support functions like learning, memory formation, or injury recovery. NPCs can divide differently to maintain the pool of progenitor cells and produce newly differentiated cells. These different division modes are tightly modulated by the cell cycle, and disturbances in it can result in severe disorders in development and aging. Centrosomes are cellular structures essential for cell cycle progression, and the correct structure of this organelle in cycling cells is pivotal for the generation of neurons, and disruption of it leads to neurodevelopmental and neurodegenerative disorders.

Interestingly, several studies have highlighted alternative roles of endocytic machinery proteins in the cell cycle, also called moonlighting. This thesis reports a novel role of Adaptor Protein Complex-2 (AP-2) in centrosome structure and cell cycle progression. AP-2 was found to interact with components of the γ -tubulin ring complexes (γ -TuRC), a set of proteins crucial for centrosome formation and microtubule (MTs) nucleation. NPCs deficient for AP-2 reveal defects in centrosome formation and p53-dependent G1/S phase cell cycle arrest together with senescence-related cell death. This function of AP-2 in regulating NPC proliferative capacity is independent of clathrin and requires its association with components of γ -TURC. AP-2-dependent γ -TuRC assembly at the centrosome prevents premature NPC differentiation. Taken together, our data identify a novel non-canonical function of the endocytic adaptor AP-2 in regulating the proliferative capacity of NPC and set directions for identifying novel therapeutic strategies for the treatment of neurodevelopmental and neurodegenerative disorders with AP-2 complex dysfunction.

ZUSAMMENFASSUNG

Neurogenese ist der Prozess, bei dem eine Zellpopulation, die so genannten neuronalen Vorläuferzellen (NVZ), sich zu Neuronen und Glia ausdifferenzieren im Zentralnervensystem. Dieser Prozess ist für die Entwicklung von entscheidender Bedeutung, und es hat sich gezeigt, dass er auch im erwachsenen Gehirn in begrenzten Hirnarealen fortgesetzt wird, um Funktionen wie z.B. das Lernen, die Gedächtnisbildung oder die Heilung von Verletzungen zu unterstützen. NVZ können sich auf unterschiedliche Weise teilen, um den Pool der Vorläuferzellen zu erhalten und/oder neue differenzierte Zellen zu produzieren. Diese verschiedenen Teilungsmodi werden durch den Zellzyklus streng reguliert, und Störungen in diesem Zyklus können zu schwerwiegenden Störungen in der Entwicklung und im Alterungsprozess führen. Zentrosomen sind zelluläre Strukturen, die für die Progression des Zellzyklus unerlässlich sind. Die korrekte Struktur dieser Organelle in zyklischen Zellen ist entscheidend für die Bildung von Neuronen, und eine Störung dieser Struktur führt zu neurodegenerativen Störungen.

Interessanterweise haben mehrere Studien alternative Rollen von Proteinen der endozytischen Maschinerie im Zellzyklus aufgezeigt, die auch als „Moonlighting“ bezeichnet werden. In dieser Arbeit wird über eine neue Rolle des Adaptor-Protein-Komplexes-2 (AP-2) bei der Zentrosomenstruktur und der Zellzyklusprogression berichtet. Es wurde festgestellt, dass AP-2 mit Komponenten der γ -Tubulin-Ring-Komplexe (γ -TuRC) interagiert, einer Gruppe von Proteinen, die für die Zentrosomenbildung und die Nukleation von Mikrotubuli (MTs) entscheidend sind. NVZs, denen AP-2 fehlt, weisen Defekte bei der Zentrosomenbildung und einen p53-abhängigen G1/S-Phasen-Zellzyklusstillstand sowie einen seneszenzbedingten Zelltod auf. Diese Funktion von AP-2 bei der Regulierung der proliferativen Kapazität von NVZ ist unabhängig von Clathrin und erfordert seine Assoziation mit Komponenten von γ -TURC. Die AP-2-abhängige γ -TuRC-Assemblierung am Zentrosom verhindert eine vorzeitige NPC-Differenzierung. Zusammengefasst identifizieren unsere Daten eine neuartige, nicht-kanonische Funktion des endozytischen Adapters AP-2 bei der Regulierung der Proliferationsfähigkeit von NVZs und weisen den Weg für die Identifizierung neuartiger therapeutischer Strategien zur Behandlung von neurodegenerativen und neurodevelopmentalen Erkrankungen mit AP-2-Komplex-Dysfunktion.

1. INTRODUCTION

1.1 Brain development

Multicellular organisms are created from a fusion of two haploid gametes (sperm and egg) into a diploid cell, the zygote (Molè *et al*, 2020). Eventually, it will become an embryo, in which the three germ layers (ectoderm, endoderm, and mesoderm) formed after gastrulation will start to form the organs that will compose the body in a process called organogenesis (Gilbert & Barresi, 2016). Cells in the germ layers will undergo a complex cascade of signals that will specialize these cells for their role in the mature tissues and organs (Hobert, 2008, 2011; Young, 2011). We call this process differentiation, which is critical for adult organism formation since defective differentiation during development can compromise proper organ formation and function (Cai *et al*, 2021; Langen *et al*, 2017; Ping *et al*, 2014), and in adults, it can degenerate in tumorigenesis (Luo *et al*, 2008; Shats *et al*, 2007). While differentiated cells have only self-renewal capacity, stem and progenitor cells have a multipotent differentiation potential, producing different cell types or a restricted number in the case of progenitor cells (Zakrzewski *et al*, 2019). The cell microenvironment strongly determines this capacity, and each cell layer will give rise to different cells and organs (Bloom & Zaman, 2014). The endoderm will form tissues that will assemble into the lungs, thyroid, and pancreas; the mesoderm, muscles, kidneys, and red blood cells; and the ectoderm will form skin and brain cells (Gilbert & Barresi, 2016). The brain has a complex structure and a heterogeneous population of specialized cells. This cellular diversity arises from a single population of cells called Neural Progenitor Cells (hereafter refer as NPCs), undifferentiated cells that produce neurons and glia within the central nervous system (CNS) (Gotz & Huttner, 2005; Martinez-Cerdeno & Noctor, 2018).

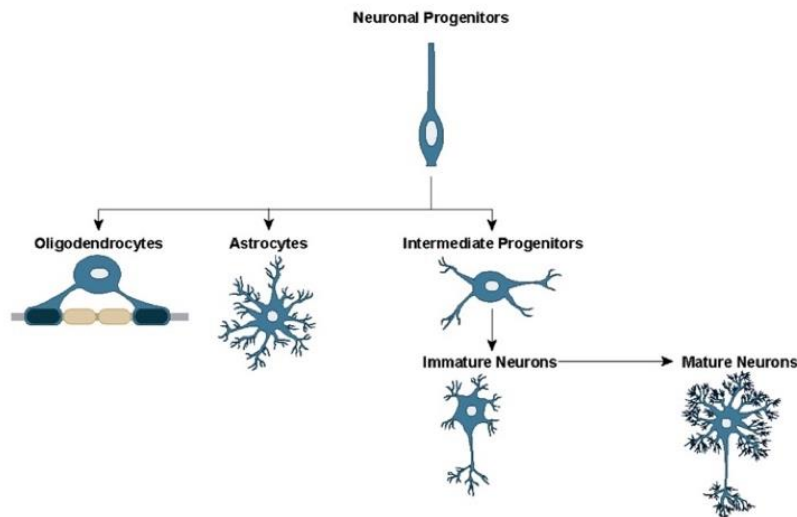


Figure 1. Neuronal progenitor cells lineage determination. NPCs in response to different stimuli can differentiate into different cell types. They can divide into another NPC maintaining the progenitors pool, differentiate into oligodendrocytes, myelinating cells of the CNS, astrocytes, supportive cells of the CNS or neuronal intermediate progenitors, which will eventually turn into neurons. Illustration reproduced courtesy of Cell Signaling Technology, Inc. (www.cellsignal.com).

1.1.1 Neural Progenitor Cells (NPCs) and the neurogenic process

NPCs are characterized as being able to divide in different ways. Before organogenesis, they divide symmetrically into two identical NPCs, expanding the population of cells with neurogenic capacity. This initial expansion of the progenitors' pool is crucial to ensure that the correct number of neurons and glia are produced during neurogenesis (Kriegstein *et al*, 2006; Takahashi *et al*, 1994). If proliferation is compromised, it can result in several neurodevelopmental disorders, e.g. a decrease in the progenitor pool will result in a smaller brain size, called microcephaly (Rhinn *et al*, 2022; Woods & Basto, 2014), or, in the opposite case, an increase in the pool will augment brain size, macro- or megalencephaly (Mirzaa *et al*, 2013). Upon neurogenesis start, around embryonic day 12.5 (E12.5), they can divide either symmetrically and eventually give rise to two differentiated cells (symmetric terminal differentiation) or asymmetrically, into one NPC and one differentiated cell (Caviness *et al*, 2003; Franco & Muller, 2013; Noctor *et al*, 2004).

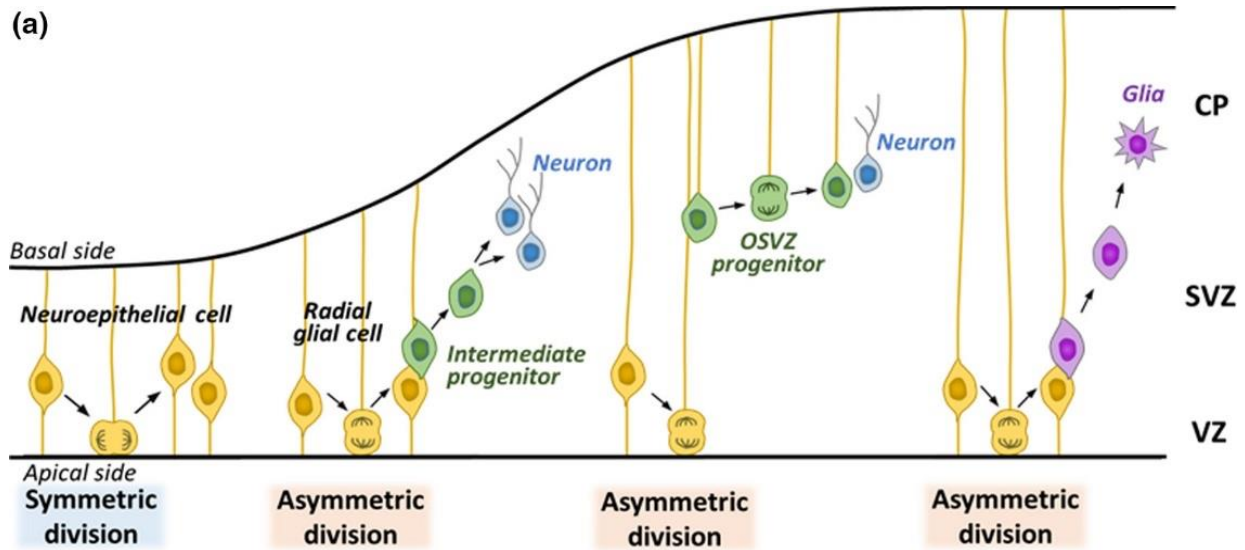


Figure 2. Schematic illustration of neural progenitor cell division modes and neurogenesis process. NPCs can divide into two different ways. 1) Before neurogenesis, NPCs will only divide symmetrically into two NPCs, expanding the pool of progenitors in preparation for neurogenesis. 2) At the onset of neurogenesis at E12.5, they will also make neurogenic divisions, which can be symmetric (in the case of the generation of two differentiated cells) or asymmetric (the division will result in one NPC and one differentiated cell). Additionally, Radial Glial Cells (RGCs) protrusion will guide cell migration to the cortical plate during development. Image modified from (Sueda & Kageyama, 2020).

The generation and differentiation of cells is only one part of this process. Cells must reach the right place within the developing brain with the help of NPCs, called Radial Glial Cells (RGCs), which will serve as migration guidelines for the newly generated cells (Gregg & Weiss, 2003). During asymmetric division, the daughter RGCs long projection will allow the differentiated daughter cell to adhere starting the migration process (Arno *et al*, 2014; Noctor *et al.*, 2004; Rakic, 1971, 1974). At the right moment, the cell should be able to detach from the process and continue its migration to its destination (Elias *et al*, 2007; Jossin & Cooper, 2011; Mestres *et al*, 2016; Shieh *et al*, 2011). After the NPCs complete their neurogenic cycle, they can stop cycling in different ways. They can arrest the cell cycle reversibly, in a process called quiescence (Otsuki & Brand, 2018; Terzi *et al*, 2016), which is crucial to avoid exhausting the progenitor pool. There are two irreversible options, the first one is a terminal division (the two daughter cells undergo terminal differentiation) to produce a pair of neurons (Haubensak *et al*, 2004; Miyata *et al*, 2004; Noctor *et al.*, 2004; Noctor *et al*, 2008), further migrating to the cortical plate (Martinez-Cerdeno & Noctor, 2018). Such directional migration requires polarized membrane remodeling and concerted cycles

of adhesions and deadhesion events (Vitriol & Zheng, 2012; Webb *et al*, 2002). The last one is senescence, which is an irreversible state in which damaged or aged cells are permanently arrested (Fridlyanskaya *et al*, 2015; Serrano, 2010; Terzi *et al.*, 2016) this permanent arrest degenerates in cell death, in order to clear defective cells (Lim *et al*, 2021; Nguyen *et al*, 2021; Wickman *et al*, 2012).

Despite being primarily embryonic, neurogenesis continues in restricted areas in the adult brain. Those areas are the Subventricular zone (SVZ), which generate cells that will migrate to the olfactory bulb to differentiate into interneurons that will participate in the sense of smell, and the Subgranular zone (SGZ) in the hippocampus, where granule cells are produced, which are crucial for memory formation and learning (Eriksson *et al*, 1998; Kuhn *et al*, 1996; Shohayeb *et al*, 2018). Adult neurogenesis is also crucial in injury in pathology. In neurodegenerative diseases, reduced self-renewal of NSCs results in neuronal loss (Horgusluoglu *et al*, 2017). Reduced NSC proliferation has been found in Parkinson's Disease (PD) (Höglinger *et al*, 2004), Alzheimer's Disease (AD) (Mu & Gage, 2011), Huntington's Disease (HD) (Kandasamy *et al*, 2010), and Amyotrophic Lateral Sclerosis (ALS) (Lee *et al*, 2011). After brain insult in ischemic stroke, there is an increase of neurogenesis in the SVZ and migration of neuroblasts to the striatum (Jin *et al*, 2001; Jin *et al*, 2003). Neurogenesis is tightly related to the cell cycle, in the next section the cell cycle will be described and its implication in the neurogenic process.

1.1.2 Cell cycle and neurogenesis

The cell cycle is the process by which cells multiply in a process in which one mother cell will divide into two daughter cells (usually in a symmetric way been both daughter cells identical to each other) (Alberts *et al*, 2007). We can divide the cell cycle into two major phases, interphase, where the cell starts preparing all the requirements for division, and mitosis, the division of the cell into two daughter cells (Foster *et al*, 2010). In addition, there is one more state called quiescence or G0, a reversible state in which the cell is out of cycling (Otsuki & Brand, 2018; Terzi *et al.*, 2016). Interphase begins with the Growth Phase 1 (G1) after mitotic exit, in which the cell starts to duplicate all its components except for the genetic material, which will be duplicated during the DNA Replication Phase (S) and will finalize just before mitosis with the Growth Phase 2 (G2) in which any replication problem prior to mitosis is fixed. After G2 cells enter Mitosis, that will start with the pairing of sister chromatids and the beginning of the mitotic spindle formation during pro-/prometaphase. Afterward, the chromosomes are aligned thanks to the fully formed mitotic spindle in the Metaphase, and finally, the separation into two cells will start during Ana-

and Telophase to culminate with the membrane separation or cytokinesis (Alberts *et al.*, 2007). To ensure the correctness of the process, there are several control checkpoints in which the cell will look for potential defects and, in case of defects been found, the cell cycle is interrupted (Bower *et al.*, 2017). The first checkpoint is the G0/G1 Restriction Point, in which the cell commits to the cycle. Otherwise, it becomes quiescent (Pardee, 1989). The Rb/E2F signaling pathway is the primary mechanism behind this control, and when Rb releases transcription factors to the E2F gene, it starts a transcriptional cascade of gene activation, which is vital for the whole replication process (Classon & Harlow, 2002; Weinberg, 1995). The second one is the DNA-damage Checkpoint at the G1-S transition, which delays DNA replication if damage is found in the genetic code. This checkpoint is heavily dependent on the p53/p21/Mdm2 pathway, and p53 mutations or loss leads to a bypass of this point (Agarwal *et al.*, 1995; Brown *et al.*, 2009; Hartwell & Weinert, 1989; Menendez *et al.*, 2009). Following DNA damage or centrosomal defects, caspase-2 is activated to cleave MDM2, which is a p53 repressor inducing cell cycle arrest and apoptosis (Lim *et al.*, 2021). The Intra-S Checkpoint is a second DNA-damage checkpoint to ensure there are no genetic defects before mitosis after replication. If that is the case, inactivation of cyclins will delay the G2/mitosis entry (Morgan, 1995; Nigg, 1995). After ensuring an error-less DNA, the next control point is the Decatenation G2 Checkpoint that ensures that the sister chromatids are ready for mitosis, if that is not the case the cell will not enter mitosis (Downes *et al.*, 1994; Luo *et al.*, 2009; Skoufias *et al.*, 2004). Finally, the Spindle Assembly Checkpoint (SAC) acts in mitosis to ensure a perfect bipolar mitotic spindle in Anaphase and the equal segregation of the chromatids (Kung *et al.*, 1990; Musacchio, 2015; Taylor & McKeon, 1997; Wang *et al.*, 2004). The checkpoint is mainly mediated by the mitotic checkpoint complex (MCC) which includes the proteins BubR1, Bub3, Cdc20, and Mad2 (Alfieri *et al.*, 2016; Izawa & Pines, 2015; Sudakin *et al.*, 2001).

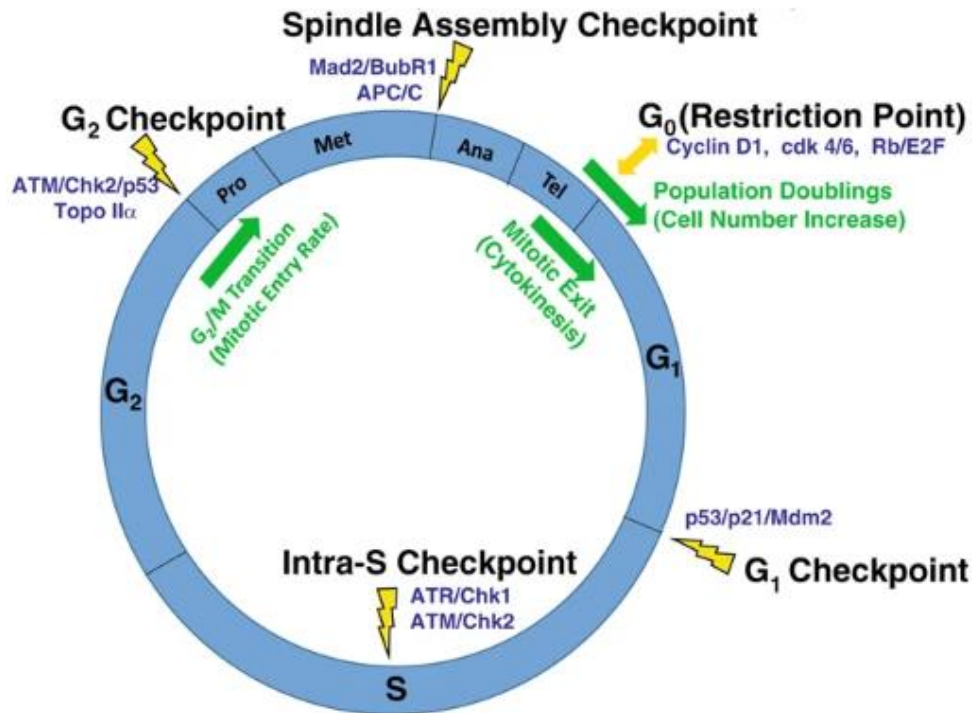


Figure 3. Cell cycle diagram. The cell cycle is controlled by different checkpoints that ensure the correction of DNA defects during interphase (from the G₁-S transition until the beginning of mitosis) and the correct segregation of the sister chromatids in mitosis. After mitosis exit, the G₀ restriction point will be the point of decision if the cell will divide or remain in quiescence. After this point, DNA quality controls will be done in G₁-S transition, at the middle of S-phase during DNA duplication, and on the onset of mitosis. Finally one more checkpoint will ensure the correct chromosomal alignment at the end of metaphase to extra the cell division. Image modified from (Bower *et al.*, 2017)

The division mode is tightly related to the cell cycle, and differences in the cycle length, incorrect assembly or duplication of cellular structures, or the positioning of the mitotic spindle will influence the promotion of proliferation or the differentiation of daughter cells (Calegari *et al.*, 2005; Calegari & Huttner, 2003; Lange *et al.*, 2009; Salomoni & Calegari, 2010). The probability of a proliferative or neurogenic division has been shown to depend on G₁ length, with shorter G₁ leading to proliferation and longer to cell differentiation (Calegari *et al.*, 2005; Calegari & Huttner, 2003). The mitotic spindle determines the cell's division angle, which will also determine how the cell will divide. If the cell presents abnormal spindles or a compromised microtubule activity, the cells will not be able to mediate a correct division (D'Aquino *et al.*, 2005; Pereira & Schiebel, 2005; Yeh *et al.*, 1995). Finally, cellular structures are crucial for the cell cycle and neurogenesis. The

centrosome will be examined in detail in the next chapter because of its essential role in division and neurogenesis.

1.2 Centrosomes and cell cycle

Centrosomes are organelles composed of two centrioles embedded in a protein matrix called the pericentriolar matrix (PCM) (Lin *et al*, 2022; Luders & Stearns, 2007), which are crucial for cell cycle progression, especially during the G1-S transition in which cyclin recruitment to the centrosome is required for S-phase initiation (Lin *et al.*, 2022; Mattaloni *et al*, 2013; Tsou & Stearns, 2006). Centrosomes are also the cell's primary microtubule-organizing center (MTOC). Proteins forming the PCM mediate microtubule nucleation, which is essential during mitosis in the formation of the mitotic spindle (O'Toole *et al*, 2012; Strome *et al*, 2001).

1.2.1 The centrosome cycle

The centrosome cycle consists of four phases synchronized to the cell cycle. Starting in anaphase and through the G1-phase, the centriole pair will start the disengagement to be duplicated simultaneously with the DNA in the S-phase. Once we have two centrosomes in the G2 phase, they will be disjunct and separated in preparation to have two mature centrosomes that will form the bipolar spindle for mitosis, ensuring the correct chromosomal separation (Fujita *et al*, 2016; Mazia, 1987; Meraldi & Nigg, 2002; Nigg & Stearns, 2011; Winey, 1999).

Out of the cell cycle (during G0), since the centrosome is not necessary, it will become a different structure, the basal body, that will assemble the primary cilium, a microtubule structure that will sense environmental conditions, if the conditions are suitable for cycling, the cilium will disassemble, and the cell cycle will start all over again (Plotnikova *et al*, 2009). The primary cilium is an important signaling center. It maintains cellular quiescent state by Sonic Hedgehog (Shh) and TGF- β signaling (Ghossoub *et al*, 2016; Molla-Herman *et al*, 2010; Pedersen *et al*, 2016). Interestingly this signaling is also crucial for development, for example, Shh is required for progenitor expansion cell migration in the brain (Spassky *et al*, 2008; Tobin *et al*, 2008; Willaredt *et al*, 2008).

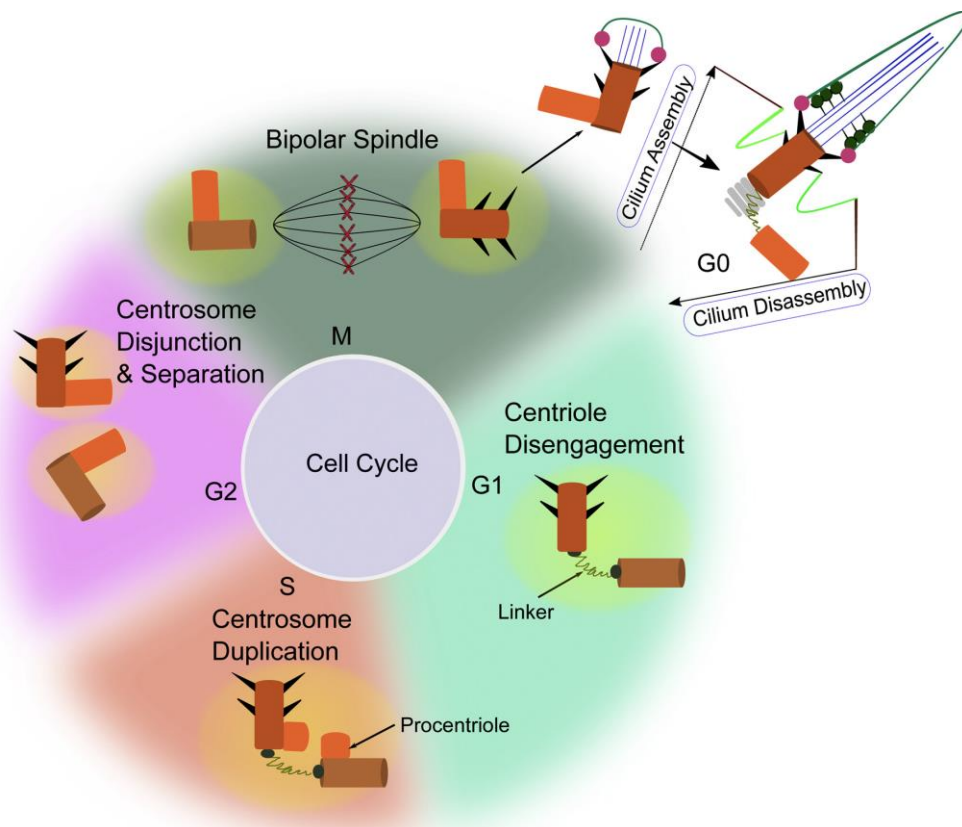


Figure 4. Diagram of the centrosome cycle. Cilium disassembly will start the centrosome formation and the start of the cell cycle. Centrosome starts to be formed during G1 after it is separated from the disassembled primary cilium. From this point, the procentriole will start to form during the S-phase allowing the duplication of the centrosome, to have two different centrosomes (mother and daughter centrosome) that will ensure a bipolar morphology of the cell in mitosis, and the formation of the mitotic spindle. After mitosis completion it will become again the basal body and the primary cilium will be assembled again. Image is taken from (Jaiswal & Singh, 2021)

The centrosome assembly is crucial for its progression towards the cell cycle, and several proteins and mRNAs are required to form a functional centrosome properly (Lin *et al.*, 2022; Mattaloni *et al.*, 2013; Tsou & Stearns, 2006) and if the centrosome is perturbed, it leads to genomic instability and disease (Conduit *et al.*, 2015). Crucial for microtubule nucleation at the centrosome, γ -Tubulin, a highly conserved member of the tubulin family (Ludueña, 2013; Oakley & Oakley, 1989), serves as a scaffold, combined with other proteins called GCPs, for the tubulin heterodimer formation (Oakley *et al.*, 2015; Petry & Vale, 2015; Thawani & Petry, 2021; Tovey *et al.*, 2018). γ -tubulin together with GCP2 and GCP3, will form the γ -Tubulin Small complex (γ -TuSC). When the

γ -TuSC binds to the other complex components (such as GCP4) will form the γ -Tubulin Ring Complex (γ -TuRC).

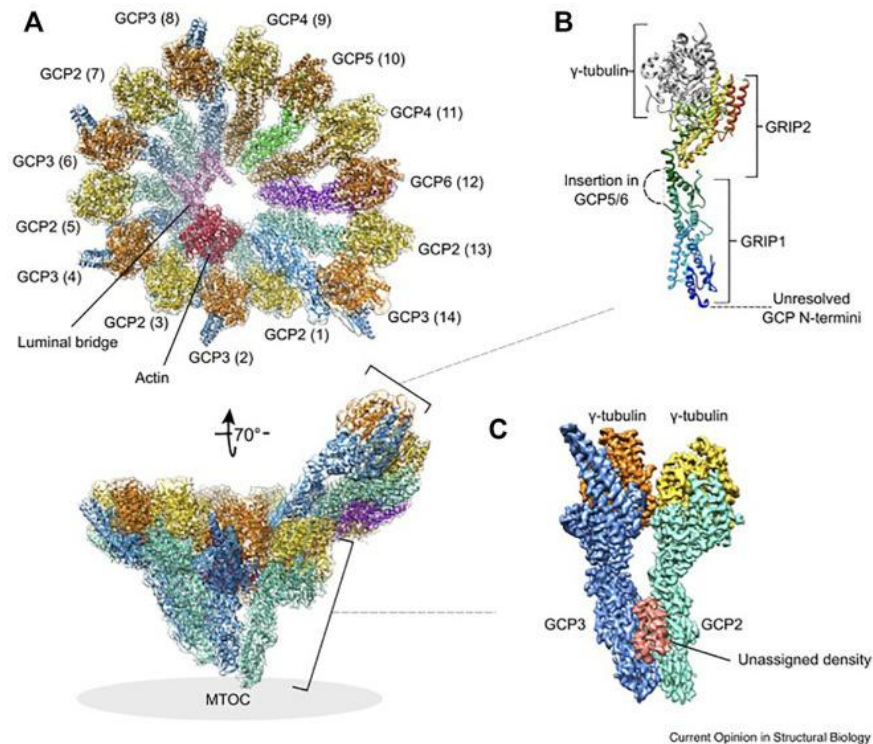


Figure 5. Structure of the γ -tubulin complex and its association with the centrosome. In C there is a representation of the γ -TuSC with two γ -tubulin molecules (in orange and yellow), a GCP2 molecule (green), and a GCP3 molecule (dark blue). In A, the γ -TuRC is represented with a typical ring organization with different components and attachment points to the MTOC. Image is taken from (Sulimenko *et al*, 2022)

1.2.2 Centrosome-related disorders

Despite early evidence of centrosomes' relation to disease, the mechanisms behind them have started to be elucidated recently, indicating that pathology causes in different tissues are diverse and specific (Bettencourt-Dias *et al*, 2011). We englobe centrosomal defects into structural defects, happening because of altered expression of protein leading to larger centrosome or reduced microtubule nucleation; and numerical changes in the number of centrosomes, it can happen by different causes such overexpression of regulators of centrosome duplication (e.g., PLK4/SAK) or mutations in oncogenes or tumor suppressors (e.g., p53, BRCA1) (Bettencourt-Dias & Glover, 2007; Fukasawa, 2007), prolonged G2 cell cycle arrest (Bourke *et al*, 2007; Loncarek *et al*, 2010; Robinson *et al*, 2007) or cell division failure (e.g., mitotic catastrophe and cytokinesis failure) (Hayashi & Karlseder, 2013). Errors in chromosome attachment are not

detected by the spindle assembly checkpoint and result in lagging chromosomes and genetic instability (Ganem *et al*, 2009; Silkworth *et al*, 2009).

As evidenced by its tight interaction with the cell cycle, most of the disorders associated with the centrosome have to do with cell cycle defects. Centrosome abnormalities are observed in different tumors (Lingle *et al*, 1998; Pihan *et al*, 1998). Moreover, decreasing p53, a tumor suppressor protein, results in a heterogeneous population of cells with multiple centrosomes and typical centrosome numbers. In the developing brain, centrosome integrity is pivotal for NPC cycle progression, and alterations of the centrosome result in severe defects (Chavali *et al*, 2014; Kaindl *et al*, 2010; Nano & Basto, 2017; Thornton & Woods, 2009; Woods & Basto, 2014). These disorders are defects of neural migration (such as lissencephaly), general growth defects with disproportional brain size (microcephalic osteoplastic primordial dwarfism type II (Griffith *et al*, 2008; Rauch *et al*, 2008)), and primary microcephalism (only brain size reduction).

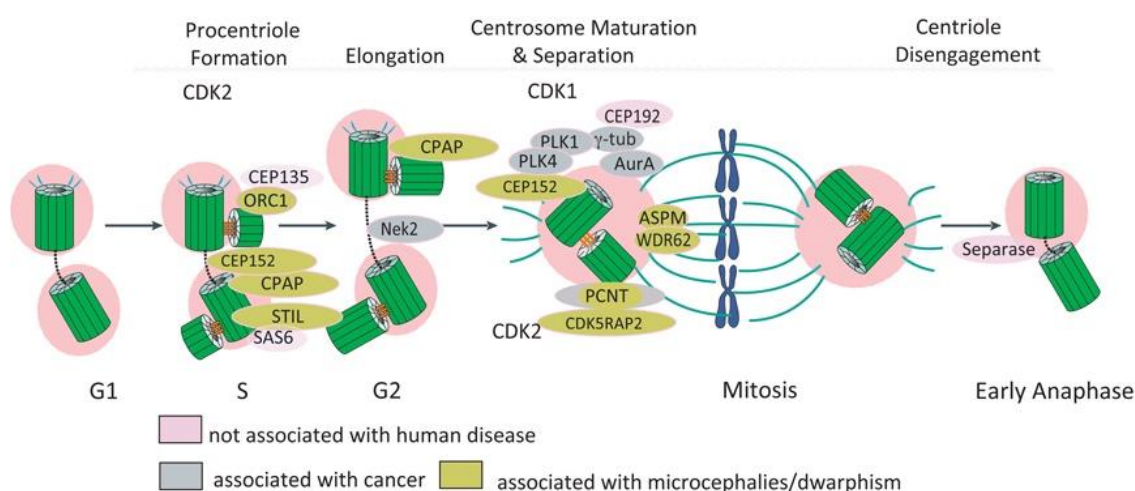


Figure 6. Several centrosomal proteins are linked to disorders. Centrosome function is crucial for cell cycle progression. Mutations of centrosomal proteins during S-phase (mostly important for centrosomal maturation) are primarily associated with microcephalism and dwarfism, while defects in G2 and Mitosis (most of these proteins important for bipolar mitotic spindle formation) can also be associated additionally with tumorigenesis. Image is taken from (Bettencourt-Dias *et al.*, 2011)

1.3 Endocytosis

Cells are isolated from the environment by a lipidic bilayer encrusted with proteins that separate the intracellular space from the environment called the plasma membrane (PM). Despite its protective function, it has mechanisms that facilitate the internalization of nutrients and molecules

into the cell that cannot diffuse through the membrane. Endocytosis can be described broadly as the invagination of the PM in order to engulf molecules or genetic material. As a result, the cell will internalize a membrane vesicle by scission of the PM. These vesicles are crucial for cellular functions such as cell signaling, nutrient uptake, or membrane remodeling (Conner & Schmid, 2003b; Kaksonen & Roux, 2018; McMahon & Boucrot, 2011).

We could roughly classify endocytosis into two big groups: one with two unspecific processes called phagocytosis and macropinocytosis in which the PM engulfs bulk amount of extracellular particles or volumes with high energy consumption (Lim & Gleeson, 2011). The second one is receptor-mediated endocytosis, which capitalizes on membrane receptors that bind to extracellular molecules with a lower energy demand than the previous modes described (Edeling *et al*, 2006; Kirchhausen, 2000, 2009).

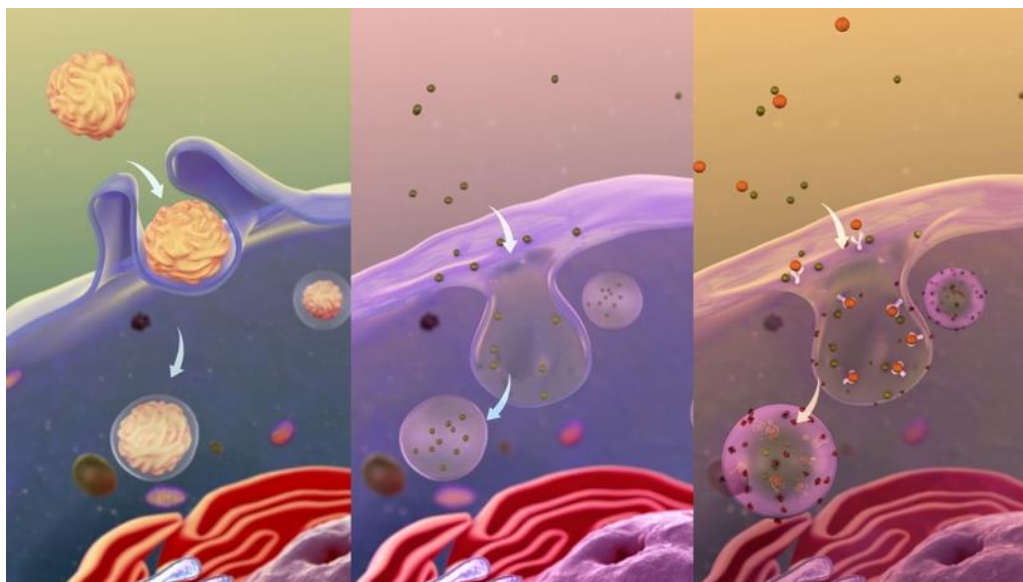


Figure 7. Different endocytosis mechanisms. Endocytosis englobes different internalization mechanisms, which differ in the specificity of the englobed substances and molecules involved. 1) Macro-/phago-/pinocytosis is the unspecific engulfing of bulk substances. 2) Receptor-Independent internalize smaller molecules without the involvement of clathrin, and finally 3) Clathrin-mediated endocytosis requires specific binding to membrane receptors and the complex molecular machinery behind it. Picture Image is taken from [scientificanimations.com](https://www.scientificanimations.com), CC BY-SA 4.0, via Wikimedia Commons.

1.3.1 Phagocytosis and Macropinocytosis

Macropinocytosis is a process by which actin-driven PM ruffling, also called macropinocytic cup, engulfs bulk particles in large vacuoles called macropinosomes (Swanson, 2008; Swanson &

Yoshida, 2019). This process is independent of receptors and cargo, and its mechanism still needs further investigation (Veltman *et al*, 2016). High macropinocytosis rates can be maintained for hours (Donaldson, 2019), a process which is vital for cancer cells obtaining of nutrients (Commisso *et al*, 2013) and immune cells in antigen presentation to T cells (Liu & Roche, 2015).

This process requires different proteins, such as several small GTPases, cytoskeletal proteins (e.g., WASP, ARP2/3), and inositol phospholipids (Buckley & King, 2017). From the first group, the most well-characterized is the RAS superfamily of GTPases (e.g., RAC1, CDC42, RAS, ARF6), essential for actin cytoskeleton rearrangement (Egami *et al*, 2014; Fujii *et al*, 2013; West *et al*, 2000). Three kinases are essential for macropinosome formation, the phosphoinositol (PI) 3-kinase (PI3K), the PI 4-phosphate 5-kinase (PI(4)P5K), and the phospholipase C-c-kinase (PLCc) (Yin & Janmey, 2003). From these, two can be activated by growth factor, PLCc and PI3K (Griner & Kazanietz, 2007; Rosse *et al*, 2010). PI3K and PI4P5K mediate the formation of membrane ruffles of PI to recruit and activate actin-regulatory proteins (Yin & Janmey, 2003). PI(4,5)P₂ is hydrolyzed by the action of PLC to produce inositol-1,4,5-trisphosphate (Ins(1,4,5)P₃) and diacylglycerol (DAG). DAG will recruit to the macropinocytic cup, and activate kinases such as protein kinase Ca (PKCa) and PKCe, promoting macropinosome formation (Mercer & Helenius, 2009).

1.3.2 Receptor-Mediated Endocytosis, CIE, CME, and AP-2

CIE is an internalization of membrane structures that does not require clathrin assembly around the pit/vesicle. There are several ways to classify CIE depending on several characteristics, such as crucial molecular components (endophilin-mediated endocytosis requires the molecule endophilin (Boucrot *et al*, 2015)), speed of the process (ultrafast endocytosis (Watanabe *et al*, 2013)), or PM markers associated to it (caveolin-associated endocytosis (Kovtun *et al*, 2015)). CIE is only activated by signals such as growth factors or cytokines and in response to pathogenesis (bacterial toxins and viruses) (Ferreira & Boucrot, 2018); (Lim & Gleeson, 2011; Mayor *et al*, 2014). CIE molecular mechanisms are not fully understood, but several key players have been identified, such as actin-polymerization factors, BAR domain proteins, and dynamin (Hinze & Boucrot, 2018; Renard *et al*, 2015; Watanabe *et al*, 2018; Watanabe *et al*, 2014).

Clathrin-Mediated Endocytosis (CME) is a process where the formation of a clathrin-coated pit (CCP), a triskelion-shaped scaffold protein, which will invaginate receptor-specific cargo in coated vesicles (Edeling *et al*, 2006; Kirchhausen, 2000, 2009). CME starts with the recruitment of

membrane bending-inducing proteins like epsin, AP180, or CALM (Chen *et al*, 1998; Ford *et al*, 2002; Koo *et al*, 2011; Miller *et al*, 2011; Schmid & McMahon, 2007) and cargo adaptors, such as FCHO (Henne *et al*, 2010), EPS15 (Benmerah *et al*, 1998), stonins (Walther *et al*, 2004), the assembly protein (AP) complex 2 (AP-2) (Conner & Schmid, 2003a) to the PM. Adaptors link clathrin to the PM via association with PI, such as PI(4,5)P2 (Owen *et al*, 2004). From all this, AP-2 is the major clathrin adaptor protein for CME (Robinson, 2004), is a heterodimer comprised of two binding subunits (α and β) and a stabilizing subunit (μ) (Kirchhausen, 1999), containing several PI(4,5)P2-binding sites (Honing *et al*, 2005; Rohde *et al*, 2002) and interacting with cargos containing either tyrosine- or dileucine-based motifs (Kadlecova *et al*, 2017; Kelly *et al*, 2008; Mattera *et al*, 2011). CME starts with the recruitment of AP-2 to the plasma membrane by phosphorylation of the μ 2 subunit by kinase AAK1 (Conner & Schmid, 2002; Ricotta *et al*, 2002). AP-2 can bind simultaneously to the PM and transmembrane cargo, modulating protein concentration to be internalized (Brodsky *et al*, 2001). Clathrin will bind to AP-2, starting the formation of the CCP by dynamin-dependent invagination. Membrane fission will generate a clathrin-coated vesicle (CCV). This fission it does not require only of dynamin, but several bin1/amphiphysin/RVS167 (BAR) domain protein family members (e.g., endophilin A1-3) and the actin cytoskeleton (Damke *et al*, 1994; Daumke *et al*, 2014; Ferguson *et al*, 2007; Gad *et al*, 2000; McMahon & Boucrot, 2011; Meinecke *et al*, 2013; Ringstad *et al*, 1999; Schuske *et al*, 2003; Takei *et al*, 1996). After fission CCV will disassemble their coating, in this process PI(4,5)P2-phosphatase synaptojanin-1 (SYNJ1) (Mani *et al*, 2007; Verstreken *et al*, 2003) and the clathrin disassembling chaperone heat-shock cognate 70 along with its cofactor auxilin (Prasad *et al*, 1993; Ungewickell *et al*, 1995) will mediate the correct uncoating of the vesicle. The uncoated vesicle be sent to the RAB5-positive early endosome (Mettlen *et al*, 2018), here there are two options for the cargo; to be recycled back to the PM (via the RAB11-positive recycling endosome) or sent to the lysosome for the degradation.

CME is the primary way of entry of surface receptors and ligands (Baschieri *et al*, 2020) and it is required for essential functions of the cell such as nutrient acquisition, the composition of the PM, cell surface receptor signaling (Polo & Di Fiore, 2006; Reider & Wendland, 2011), and regulation of cellular ion homeostasis (Lopez-Hernandez *et al*, 2020).

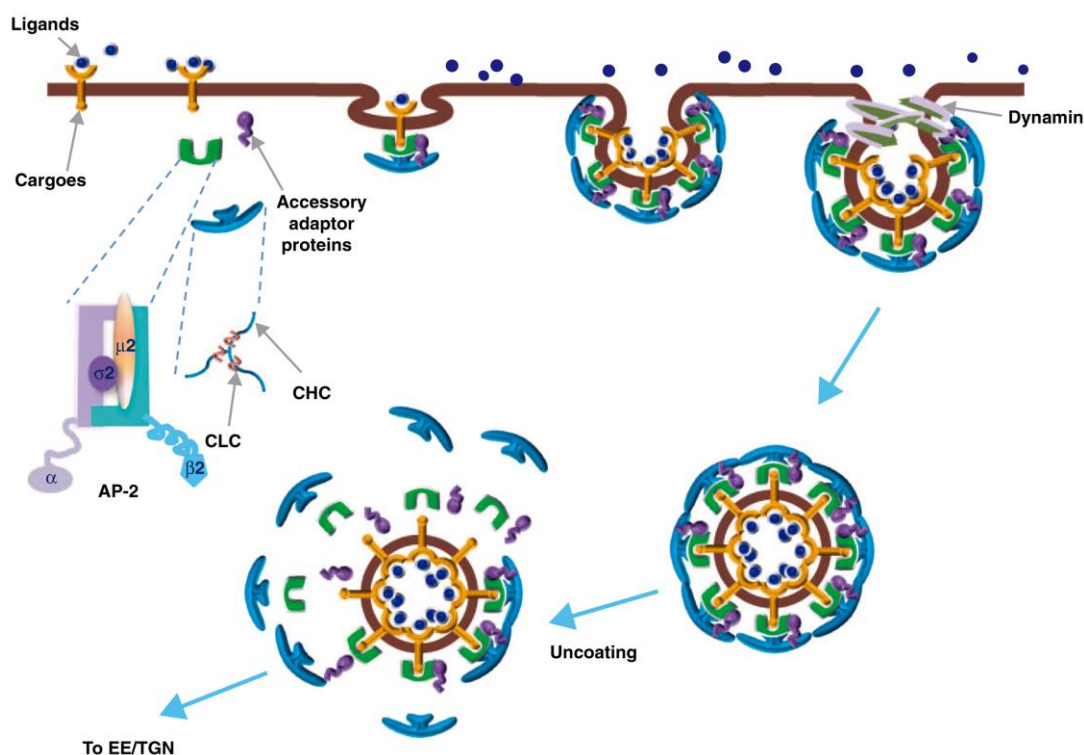


Figure 8. AP-2 complex and CME. Representation of the AP-2 heterodimer with its binding subunits (α and β) and its core (σ and μ). AP-2 binds directly to the receptors in the plasma membrane to recruit clathrin for the internalization of these receptors. This will start the invagination of the membrane into a CCP which will be eventually closed and become a vesicle coated on clathrin. AP-2 and clathrin are recycled to be reused in endocytosis and the uncoated vesicles will be targeted to lysosomes for its degradation. Image is taken from (Chen et al, 2011)

1.3.3 Endocytosis functions in the brain, cell cycle, and neurogenesis

Endocytosis is required for the cell's vital functions, such as communication with the extracellular environment, nutrient uptake, and signaling by the cell surface receptors. In the brain, CME internalizes transmembrane receptors together with their extracellular ligands (Yamashita & Kuruvilla, 2016), propagate signals between axon and soma (Cosker & Segal, 2014; Harrington & Ginty, 2013; Yamashita & Kuruvilla, 2016), contributes to synaptic plasticity (Wilkinson & Lin, 2004) and regulates guidance receptors and adhesion molecules, crucial for neural development (Yap & Winckler, 2012, 2015). Additionally, membrane retrieval by endocytosis is a crucial tool for neurons and other cells in the brain to maintain the membrane pool in neuronal activity by recycling synaptic vesicles (SV) (Kononenko & Haucke, 2015). There is a large body of evidence that endocytosis is the mechanism that ensures the asymmetric distribution of PM-localized

receptors and ligands (cell determinants) during division, ensuring a temporal and spatial regulation of neurogenesis (Yap & Winckler, 2015).

NUMB is an endocytic protein (Santolini *et al*, 2000), which is also a cell fate determinant. NUMB was discovered to bind directly to AP-2 subunit α and endocytic protein EPS15, as an endocytosis adaptor (Salcini *et al*, 1997; Santolini *et al.*, 2000; Yap & Winckler, 2012). NUMB endocytic activity can also be regulated by the kinase AAK1, which, when overexpressed, induces NUMB redistribution to perinuclear endosomes (Sorensen & Conner, 2008). During mitosis, NUMB will interact with the Golgi component ACBD3 (Zhou *et al*, 2007b) for asymmetric distribution to the apical membrane of the only one daughter cell that remains a progenitor (Shen *et al*, 2002). Interestingly, this distribution changes during corticogenesis, and while NUMB-containing daughter cell will remain a progenitor at embryonic mouse day 10 (E10), at E13, NUMB-containing daughter cells will undergo differentiation (Shen & Temple, 2002; Yap & Winckler, 2015; Zilian *et al*, 2001). Hence, NUMB different roles during development will modulate the balance between proliferation and differentiation. Additionally, via endocytosis, NUMB will internalize Notch (Berdnik *et al*, 2002), integrin (Nishimura & Kaibuchi, 2007), and RTK (Zhou *et al*, 2011) receptors. These receptors are involved in signaling pathways crucial for development, such as Notch, which promotes neural differentiation when PM receptor levels are reduced by NUMB internalization (Koch *et al*, 2013). Moreover, NUMB controls the asymmetric localization of AP-2 α during cell division, which is believed to modulate Notch signaling (Berdnik *et al.*, 2002). In line with this evidence, NUMB knockout (KO) mice display premature neuronal differentiation in the cortex (Shen *et al.*, 2002) and cerebellum (Klein *et al*, 2004).

WNT signaling is an essential pathway for neurodevelopment (Houart *et al*, 2002) and adult neurogenesis (Kuwabara *et al*, 2009). This pathway is also modulated by CME (Blitzer & Nusse, 2006), although it has not been proven that CME WNT regulation is essential in NPCs. Clathrin and AP-2 have been proposed as regulators of Frizzled co-receptor LRP6 signalosome assembly, and AAK1 promotes the clearance of LRP6 from the PM (Agajanian *et al*, 2019). WNT signaling and proliferation of NPCs might also be regulated by formin-dependent CIE endocytosis (Soykan *et al*, 2017). Actin-nucleating protein formin-2 and another actin-binding protein FlnA mediate LRP6 endocytosis, hence regulating the GSK3 β and β -catenin signaling (Lian *et al*, 2016).

Macropinocytosis machinery is also crucial for the NPCs proliferation and differentiation. RAC1 is vital in the learning-induced increase in the proliferation of NPCs in the adult hippocampus (Haditsch *et al*, 2013), and CDC42 activation is required for the proliferation and differentiation of

SVZ NSCs (Chavali *et al*, 2018; Keung *et al*, 2011). PI kinases are also crucial for neurodevelopment (Cosker & Eickholt, 2007; Waite & Eickholt, 2010). PI3K and its downstream effectors (mTOR and AKT) promote neuronal differentiation when they are upregulated (Zhang *et al*, 2017). Downregulation results in critical differentiation delays (Le Belle *et al*, 2011; Zucco *et al*, 2018).

Endocytosis is also indispensable for the migration, and internalization of surface guidance receptors (e.g., N-cadherin, β 1-integrin) in migrating neuroblasts (Chao & Kunz, 2009; Ezratty *et al*, 2009), hence modulating, cell adhesion and detachment. CCP are enriched to adhesive contacts with matrix substrates in migratory neuroblasts, while inhibition of dynamin and clathrin impairs neuronal migration because of impaired sorting of adhesion proteins (Shieh *et al.*, 2011). NUMB binds to several adhesion proteins (E-cadherin, N-cadherin, and β -catenin), and its inactivation in RG cells causes progenitor dispersion and disorganized cortical lamination (Rasin *et al*, 2007). It also regulates the endocytosis of BDNF-activated TRKB receptors at leading processes of the cell, regulating the migration of granule cell precursors in the cerebellum (Zhou *et al.*, 2011; Zhou *et al*, 2007a).

Endocytic protein disabled-2 (DAB2, also known as DOC-2) is known to interact with clathrin (Mishra *et al*, 2002a; Morris & Cooper, 2001) and AP-2 (Gertler *et al*, 1989; Mishra *et al.*, 2002a; Morris & Cooper, 2001). DAB1, a close homolog of DAB2, is enriched in the brain (Howell *et al*, 1997a; Howell *et al*, 1997b), and mutation results in defective brain development (Sweet *et al*, 1996; Yoneshima *et al*, 1997). DAB1 KO results in cortical lamination defects and aberrant cerebellum development (Howell *et al.*, 1997b). Interestingly, the phenotype is identical to mice lacking reelin or its receptors (Rice & Curran, 2001). This similarity is because of DAB1 importance for reelin signaling. DAB1 phosphorylated is increased via ApoE receptor 2 (ApoER2) and very-low-density lipoprotein receptor (VLDLR) regulating neuroblast migration (Howell *et al.*, 1997a; Howell *et al.*, 1997b; Rice & Curran, 2001). However, mice lacking the C-terminal region of DAB1, with AP-2- and SH3-binding sites, are born normal with no severe defects in cortical lamination (Herrick & Cooper, 2002). Intersectin 1 (ITSN1), part of the CME machinery (Koh *et al*, 2004; Pechstein *et al*, 2015; Sakaba *et al*, 2013), was shown to regulate CA1 splitting by interactions with VLDLR and DAB1.

Doublecortin (Dcx) is a microtubule-binding protein linked to X-linked lissencephaly syndrome in humans (des Portes *et al*, 1998; Friocourt *et al*, 2001; Taylor *et al*, 2000), typically expressed in migrating newborn neurons, and it is essential for an array of function crucial for migration, such

as regulation of microtubule dynamics, dynein-mediated nucleus centrosome coupling, and internalization of cell adhesion L1-CAM family member neurofascin (Tanaka *et al*, 2004; Yap *et al*, 2012). Neurofascin endocytosis requires its interaction with AP-2, as shown by AP-2 binding-deficient doublecortin mutant (Yap *et al*, 2018). Last but not least, EGF receptor, important for neuronal migration (Burrows *et al*, 2000; Puehringer *et al*, 2013), is internalized and degraded via CME (Le Roy & Wrana, 2005).

Endocytosis is vital during G0 to maintain primary cilium structure and function. The basal body of the cilia is a hotspot of CCV and endocytosis, which are required to maintain membrane delivery and retrieval and to modulate signaling (Pedersen *et al*, 2016). PI(4,5)P2 is maintained close to the cilia by OCRL (Prosseda *et al*, 2017), an inositol polyphosphate 5-phosphatase crucial for clathrin-coated pits dynamics and uncoating (Nandez *et al*, 2014). This importance for cilia structure is supported by CME defects in *Caenorhabditis elegans* resulting in the expansion of the ciliary membrane (Kaplan *et al*, 2012); while the gain of function results in cilia shortening (van der Vaart *et al*, 2015). CME at the cilia controls signaling necessary for maintaining a quiescent state by internalizing Sonic Hedgehog (Shh) and TGF- β pathway receptors (Ghossoub *et al*, 2016; Molla-Herman *et al*, 2010; Pedersen *et al*, 2016). CIE has been reported to happen at the basal body (Schreiber *et al*, 2000); Cav1 was described to mediate internalization and lysosomal delivery of PTCH1 (Yue *et al*, 2014).

Endocytosis is also essential in mitosis regulation. Autosomal recessive hypercholesterolemia (ARH), a CME adaptor protein (He *et al*, 2002; Mishra *et al*, 2002b), mediates centrosomal microtubule nucleation by interacting with components of γ -tubulin ring complex (Lehtonen *et al*, 2008). Cytokinesis requires of endocytosis for the correct separation of the two daughter cells. CME and caveolae-mediated endocytosis are crucial for zebrafish embryo cytokinesis (Feng *et al*, 2002). Formins also participate in cytokinesis, in *Drosophila diaphanous* (*dia*), protein deletion causes lethality at the onset of pupation (Castrillon & Wasserman, 1994).

Interestingly, CME has been shown to be strongly downregulated during mitosis (Berlin & Oliver, 1980; Boucrot & Kirchhausen, 2007; Fielding & Royle, 2013; Fielding *et al*, 2012; Koppel *et al*, 1982; Sager *et al*, 1984), and endocytic proteins such as clathrin, caveolin-1, and several ESCRT complex components, change their normal distribution in different stages of mitosis have been shown to be present at the centrosome, the mitotic spindle, or the mid-body (Boucrot *et al*, 2011; Lee *et al*, 2008; Maro *et al*, 1985; Okamoto *et al*, 2000; Olmos *et al*, 2015), which suggest that endocytic proteins could have alternative roles in mitosis. This phenomenon is called moonlighting

(or gene sharing) and is a phenomenon by which a protein can perform more than one function (Jeffery, 2003). Moonlighting is a common phenomenon in endocytic proteins, especially in cell division (Royle, 2011; Yu *et al.*, 2021).

Clathrin and epsin regulate kinetochore stability at the mitotic spindle (Booth *et al.*, 2011; Liu & Zheng, 2009; Maro *et al.*, 1985; Royle, 2012; Royle *et al.*, 2005). Clathrin presence at the mitotic spindle is well documented in the literature (Maro *et al.*, 1985; Okamoto *et al.*, 2000) and its mitotic functions have been shown to be independent of its interphase endocytic function (Hood & Royle, 2009; Royle, 2012; Royle & Lagnado, 2006). Clathrin characteristic triskelion structure is crucial for spindle-related functions since mutants abolish trimerization and cannot rescue the mitotic defects caused by clathrin depletion (Royle & Lagnado, 2006). Clathrin forms a complex with TACC3 (transforming acidic coiled-coil containing protein 3) and ch-TOG (colonic and hepatic tumor overexpressed gene), two microtubule-binding proteins implicated in mitotic spindle assembly (Fu *et al.*, 2010; Lin *et al.*, 2010). Aurora A kinase phosphorylates TACC3 to produce the formation of this complex. Mutations of serine residues of TACC3 confirm this hypothesis abolishes its association with clathrin, as well as the mitotic spindle (Fu *et al.*, 2010; Lin *et al.*, 2010). Intermicrotubule bridges are structures containing clathrin, which bundle mitotic spindle microtubules together. Depletion of clathrin or TACC3 leads to a loss of short intermicrotubule bridges (Booth *et al.*, 2011). Knocksideways acute removal of the clathrin-TACC3-ch-TOG complex from the mitotic spindle also results in a loss of intermicrotubule bridges (Cheeseman *et al.*, 2013). Further confirmation of the importance of clathrin at the spindle comes from RNA interference (RNAi)-mediated knockdown of CHC, resulting in many mitotic defects, including the instability of kinetochore fibers, continuous activation of the SAC, and errors in chromosome segregation (Royle *et al.*, 2005). Molecular inhibition of clathrin by PitStop2 resulted also in a similar mitotic phenotype (Smith *et al.*, 2013). RNAi-dependent KD of CHC results in multipolar spindles, and chemical inactivation of clathrin induces dimerization fragments of metaphase centrosomes (Boucrot & Kirchhausen, 2007).

Clathrin has been found to be localized to astral microtubules recruiting the microtubule-stabilizing protein GTSE1 using the clathrin adaptor interaction sites, repurposed during mitosis to recruit GTSE1 (Rondelet *et al.*, 2020). GTSE1 inhibits microtubule depolymerase MCAK to stabilize the microtubules (Rondelet *et al.*, 2020). Clathrin has been reported to participate in maintenance of centrosome structure and integrity (Foraker *et al.*, 2012). Depletion of CHC by RNAi and acute inactivation of clathrin by chemically induced dimerization fragments metaphase centrosomes.

Additionally, GAK's CHC phosphorylation at T606 site targets phosphorylated CHC to the centrosome, both in interphase and mitosis (Yabuno *et al*, 2019).

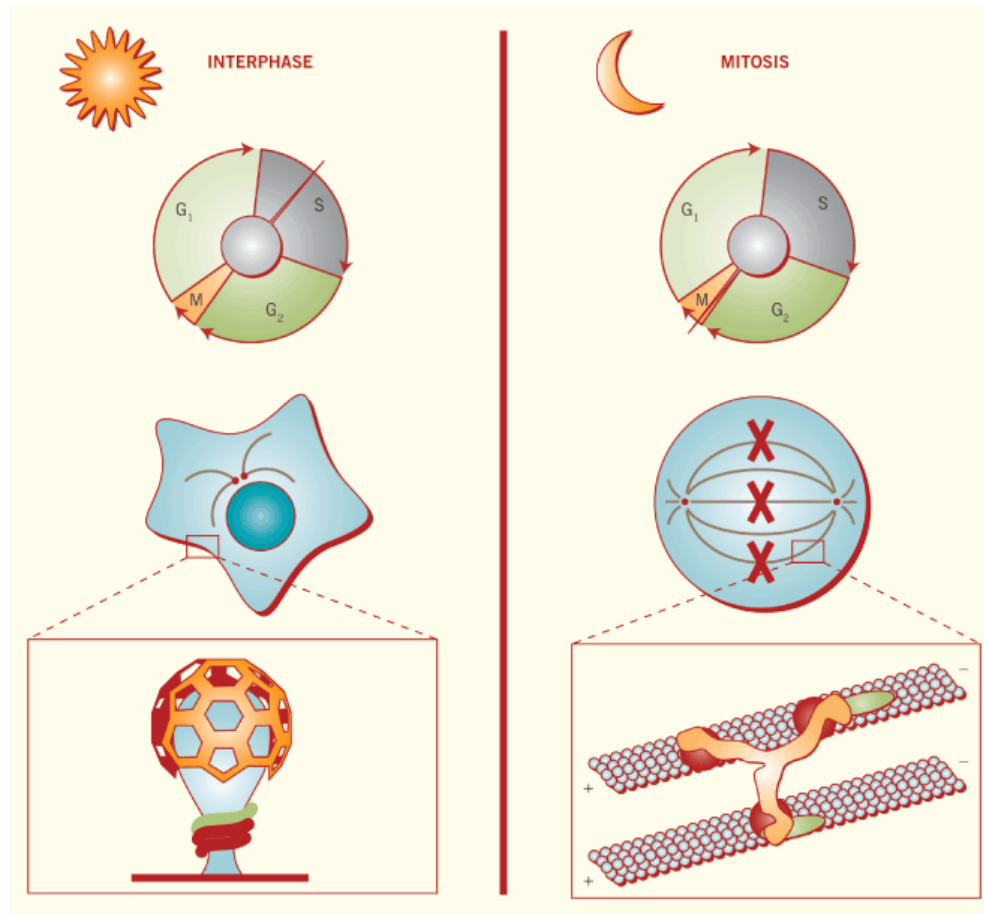


Figure 9. Duality of endocytic proteins. Example of different clathrin roles. On the left panel, clathrin is located to the plasma membrane as part of the clathrin-coated pits for CME. In contrast, on the right is localized to the mitotic spindle during mitosis to stabilize the microtubules forming it. This is a clear example of repurposing of endocytic machinery during the cell cycle. The image is taken from (Royle, 2011)

AP-2 β interacts with the mitotic checkpoint kinase BubR1 (Cayrol *et al*, 2002), although the mechanism of action is not yet understood. Dynamin2 is localized at the centrosome, modulating cytokinesis completion (Joshi *et al*, 2010; Konopka *et al*, 2006; Thompson *et al*, 2004). Moreover, dynamin importance in development is highlighted by the lethal congenital syndrome resulting from DNM2 homozygous mutation (Koutsopoulos *et al*, 2013) and early embryonic lethality of dynamin 2 KO mice (Ferguson *et al*, 2009).

Cell fate determinants and spindle orientation condition mode of cell division (Lancaster & Knoblich, 2012) and endocytic proteins have been shown to be crucial for these processes. Deletion of endocytic machinery likely will result in defective brain development and disbalance in NPCs proliferation and differentiation. Decreased survival embryonic or early postnatal lethality is a common characteristic of most mouse models with deleted CME components. Mice lacking the clathrin light chain (CLC) α , but not the CLC isoform, have shown a 50% decrease in survival rate during the first postnatal week (Redlingshofer *et al*, 2020; Wu *et al*, 2016).

Mutations of different AP-2 subunits, such as AP-2 μ deletion (Mitsunari *et al*, 2005), deletion of AP-2 β (Li *et al*, 2010), and AP-2 σ mutation (Gorvin *et al*, 2017) results in embryonic lethality. AP-2 μ brain-confined KO did not result in embryonic lethality, but mice did not survive past postnatal day 21 (P21) (Kononenko *et al*, 2017). Additionally, similar phenotypes have been found in KO models for Endophilins, CALM, EPS15L1, Epsin, and dynamin 1 (Chen *et al*, 2009; Ferguson *et al.*, 2007; Ishikawa *et al*, 2015; Milesi *et al*, 2019; Milosevic *et al*, 2011; Raimondi *et al*, 2011). Mutation of CLTCL1, encoding clathrin heavy-chain isoform 22, resulting in loss-of-function, develop early precursor differentiation due to increased secretion of neuropeptide cargo (Nahorski *et al*, 2015; Nahorski *et al*, 2018). Curiously, this is independent of clathrin mitotic functions, highlighting the possibility of several roles for the same protein in neurogenesis.

ESCRT-III is a protein crucial for membrane remodeling during endocytosis, but alternatively, it also participates in mitotic events such as the sealing of nuclear envelope (NE) and cytokinesis (Yu *et al.*, 2021). The NE starts to reassemble at the end of mitosis after encapsulating the chromatin (Güttinger *et al*, 2009). Removing remaining microtubule interactions with chromatin and closing of the NE are ESCRT-III dependent (Olmos *et al.*, 2015; Vietri *et al*, 2015). Recruitment of ESCRT-III relies on the binding of CHMP7 to the inner nuclear membrane protein LEM2 (Gu *et al*, 2017). Additionally, LEM2 has microtubule-binding affinity, allowing to phase separation of clustering microtubules to promote NE sealing (von Appen *et al*, 2020). LEM2-dependent activation of CHMP7 recruits CHMP4B, CHMP3, and CHMP2A, which are components that form the ESCRT-III spiral filament with the help of VPS4. Phosphorylation is tightly regulated by CC2D1B (Ventimiglia *et al*, 2018). Afterward, via IST1, AAA-ATPase spastin will be recruited, which will cleave any remaining microtubules. This function of ESCRT-III is reported to be conserved in migrating cells, where it will repair NE ruptures accumulated during cell migration in interphase (Raab *et al*, 2016).

ESCRT subunits are vital for cytokinesis. ESCRT-I subunit TSG101 and its associated protein ALIX are recruited to the midbody by centrosomal protein CEP55 (Lee *et al.*, 2008), which will trigger the recruitment of component of the ESCRT-III (Christ *et al.*, 2016). Similarly that in the NE, septins will be recruited to serve microtubules (Schöneberg *et al.*, 2018), forming a ring on each side of the midbody (Karasmanis *et al.*, 2019). ALIX will bind to the membrane protein complex Syntenin-Syndecan-4 to allow efficient scission (Addi *et al.*, 2020).

Cytokinesis with the presence of chromatin bridges has severe consequences for the cell, generating DNA damage (Warecki *et al.*, 2020). This is controlled by the abscission checkpoint modulated by the chromosome passenger complex (CPC). ESCRT-III component CHMP4C controls this checkpoint by interacting with Borealin (one of the components of the CPC), inhibiting the abscission process when phosphorylated by Aurora B (Capalbo *et al.*, 2016; Carlton *et al.*, 2012). Additionally, CHMP4C localizes at the kinetochore in prometaphase participating in the SAC (Petsalaki *et al.*, 2018).

CIE proteins have also been linked to cell cycle regulation. Overexpression of caveolin-1 induces G0/G1 cell cycle arrest in endothelial cells (Fang *et al.*, 2007). Moreover, caveolae increase in mitosis is believed to contribute to mitotic rounding (Boucrot *et al.*, 2011). In mitosis, caveolae are shown to be linked to mitotic spindle orientation (Matsumura *et al.*, 2016). Integrin prevents the internalization of caveolae (del Pozo *et al.*, 2004). Hence cholesterol-enriched microdomains and caveolin-1 can be selectively localized at the retracting edge of the cell by integrin signaling (Matsumura *et al.*, 2016), where they will recruit Gai, an anchoring component crucial for spindle orientation (Bergstrahl & St Johnston, 2014). Gai will form a complex together with LGN, NuMA, and Dynein/Dynactin which will bind to the microtubules towards the spindle pole so they can orient the spindle (Yu *et al.*, 2021).

Interestingly, there is strong evidence of several alternative roles of endocytic proteins in the brain. In neurons, BDNF receptor TRKB is internalized by CME (Beattie *et al.*, 2000; Cosker & Segal, 2014; Howe *et al.*, 2001; Zheng *et al.*, 2008), although, independently of CME, AP-2 will not only internalize activated TRK to signaling endosomes but will also regulate intracellular trafficking (Kononenko *et al.*, 2017). Additionally, AP-2 non-canonical function is essential for post-endocytic regulation and degradation of BACE1 to prevent the amyloidogenic processing of APP (Bera *et al.*, 2020). Endophilin A is a well-studied protein for its role in synaptic vesicle endocytosis (Farsad *et al.*, 2001; Gallop *et al.*, 2006; Milosevic *et al.*, 2011; Verstreken *et al.*, 2002), however, additional alternative function, independent of endocytosis, at the synapses include regulation of autophagy

(Murdoch *et al*, 2016; Soukup *et al*, 2016). Additionally, CALM can also regulate autophagy independently of endocytosis (Moreau *et al*, 2014).

2. AIMS OF THE STUDY

Knockout of AP-2 μ and AP-2 σ in mice causes early embryonic lethality (Gorvin *et al.*, 2017; Mitsunari *et al.*, 2005), while disruption of the AP-2 β subunit in developmental defects and perinatal mortality (Li *et al.*, 2010). Additionally, it has been shown to be important for the cell cycle by evidence in KD models of mitotic defects (Boucrot & Kirchhausen, 2007), centrosome overduplication, and cell cycle arrest in G1-S transition (Olszewski *et al.*, 2014). CME downregulation during mitosis (Berlin & Oliver, 1980; Boucrot & Kirchhausen, 2007; Fielding & Royle, 2013; Fielding *et al.*, 2012; Koppel *et al.*, 1982; Sager *et al.*, 1984), and presence of endocytic proteins in different organelles crucial for the cell cycle such as the centrosome, the mitotic spindle, or the mid-body (Boucrot *et al.*, 2011; Lee *et al.*, 2008; Maro *et al.*, 1985; Okamoto *et al.*, 2000; Olmos *et al.*, 2015), provides strong evidence of repurposing of endocytic proteins during the cell cycle. Interestingly, despite the close relation of endocytic machinery and AP-2 with development and cell cycle, the exact mechanism and contribution of this complex has never been studied, rising the following central question:

“What is AP-2 role in the cell cycle and how does affect development?”

Primary NPCs, astrocytes, and MEFs were obtained from tamoxifen-inducible AP-2 μ KO (*AP2- μ flox:CAG-CreTmx*) to investigate by a combination of different microscopy techniques, label-free quantitative proteomics, flow-cytometry analysis, biochemical analysis of protein interaction by co-immunoprecipitation, and live-cell imaging approaches to achieve three specific goals that would answer the central question:

1. What is the contribution of AP-2 to the cell cycle?
2. Is this function dependent or independent of clathrin?
3. Has AP-2 a critical role not only in the cell cycle but in other processes involve in neurodevelopment (e.g., migration)?

3. RESULTS

3.1 AP-2 deletion has severe consequences for NPCs proliferation and mitosis.

Firstly, a new in vitro model for the study of AP-2 deletion was established. For this purpose, telencephalic vesicles were extracted from E12-E13 embryos floxed for AP-2 μ under a tamoxifen-inducible Cre (*AP2- μ flox:CAG-Cre^{Tmx}*) to obtain primary NPCs. AP-2 μ is the stabilizing subunit of the complex and targeting it we can delete the whole AP-2 complex. After 48-72h of Tamoxifen treatment (using EtOH treatment for control cells), protein levels of AP-2 subunit α were analyzed by western blotting, showing undetectable levels in KO cells, confirming a successful deletion of the complex (Figure 10). In addition, AP-2 was knocked out in other cell types (Astrocytes and MEFs) following the same procedure (data not shown).

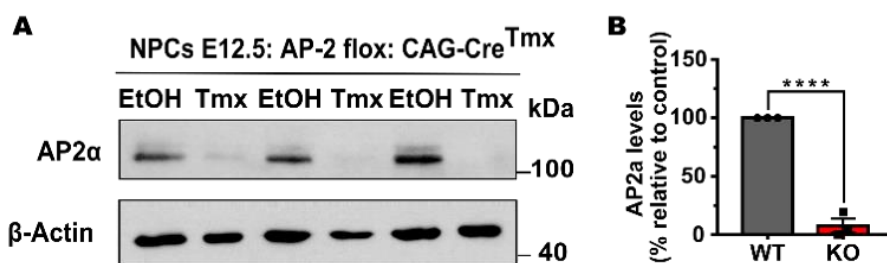


Figure 10. Tamoxifen treatment completely deletes AP-2 after 72 hours. (A) Western Blot of cell lysates of tamoxifen-treated NPCs compared with control cells (treated with EtOH) showing a significant reduction of AP-2 α levels after 48-72h of Tamoxifen treatment. (B) Protein levels are presented as relative levels (percentage to control). KO: 7.876 \pm 5.840, ****- p < 0.0001, N =3 in which each N is protein lysates obtained from independent cultures obtained from independent animals.

Live imaging of NPCs was performed to assess for 24h if the proliferation of neurospheres was affected after AP-2 deletion. Strikingly, there was an observable difference in the size of the neurospheres, with WT neurospheres growing exponentially while KO neurospheres did not increase their size (Figure 11A). Staining cells after 3 days in-vitro (DIV) and 7DIV confirmed this reduction of cell proliferation in the KO, but in addition, KO cells presented elongated morphology, a typical characteristic of cells undergoing a differentiation process (Figure 11B).

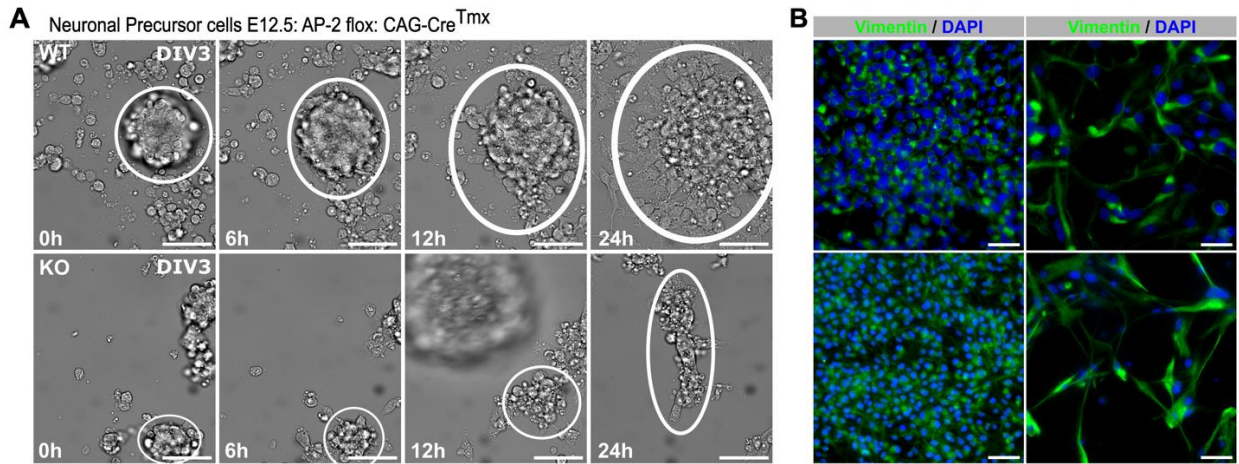


Figure 11. The proliferation of NPCs is compromised upon deletion of AP-2. (A) Timestamps from 24h live imaging in WT and KO neurospheres showing spheres growing (white circles) $N=3$ in which each N is an independent cell culture obtained from independent animals. Scale bar, $50\mu\text{m}$. **(B)** Representative images of NPCs cultured for 3 and 7 days after tamoxifen KO induction stained for DAPI and vimentin (green). Reduced cell numbers and enlarged morphology are observed in KO conditions. $N=3$ in which each N is an independent cell culture obtained from independent animals. Scalebar, $50\mu\text{M}$

Despite the evidence of a phenotype within 24h, most of the experiments were done between 48h and 72h to ensure a reliable deletion of AP-2. Mitosis is usually disrupted in proliferation defects, and its closely linked to endocytic machinery (Lin *et al.*, 2022; Royle, 2011); for this reason, the mitotic phases were analyzed in detail in KO NPCs. In line with the live imaging results, a decrease in mitotic cells in the KO condition was observed after 3DIV (Figure 12B), and within the mitotic cells, a significant decrease in metaphase (Figure 12B). This reduction of mitotic cells was exacerbated after 7DIV, with almost not mitotic cells in the KO condition (Figure 12C).

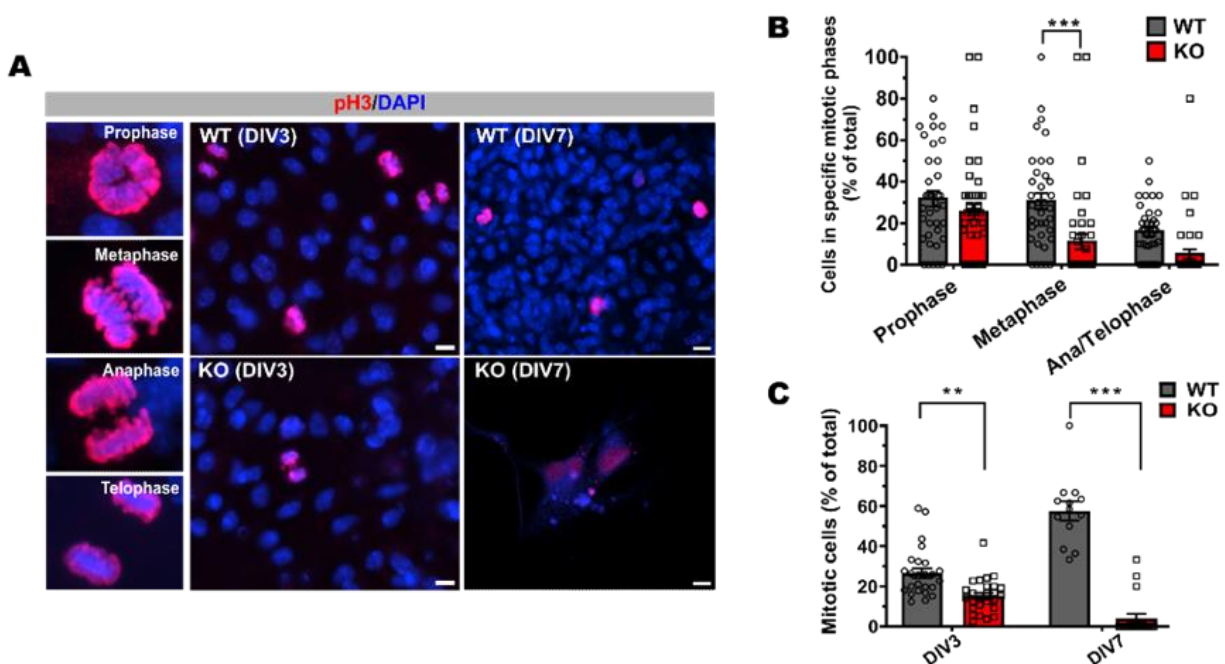


Figure 12. Mitotic cells are reduced with time upon AP-2 deletion. (A) Representative images of mitotic cells, stained with pH3 (red), in primary NPCs at DIV3 and DIV7. **(B)** Quantification of mitotic phases out of total mitotic cells in WT and KO cells (DIV3). $WT^{Prophase}=31.82$ $KO^{Prophase}=25.45$ $WT^{Metaphase}=30.64$ $KO^{Metaphase}=11.03$ $WT^{Ana/Telophase}=15.95$ $KO^{Ana/Telophase}=5.108$. In total 37 WT and 42 KO from $N=3$, in which each N is an independent cell culture obtained from independent animals. **(C)** Quantification of mitotic cells out of total cells in WT and KO cells. $WT^{DIV3}=29.32\pm 3.615$ $KO^{DIV3}=15.27\pm 1.653$ $WT^{DIV7}=57.48\pm 4.745$ $KO^{DIV7}=4.123\pm 2.303$. In total 26 WT and 26 KO, with at least 20 mitotic and 100 total cells per condition, from $N=3$, in which each N is an independent cell culture obtained from independent animals. Scale bars: $10\mu M$. **- $p<0.01$; ***- $p<0.001$. The data shown represent the mean \pm SEM.

Detailed analysis of AP-2 KO mitotic cells highlighted the presence of mitotic spindle aberrations with monopolar, apolar, and multiple spindles, which were not present in WT cells (Figure 13B). In addition, chromatin bridges appeared in late mitotic cells (Figure 13D), indicating that mitosis is reduced and severely affected by AP-2 deletion.

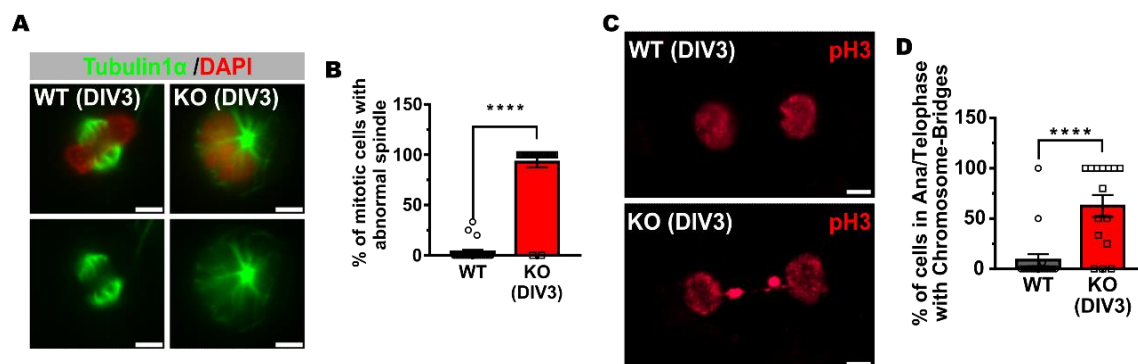


Figure 13. AP-2 KO NPCs present mitotic spindle anomalies and lagging chromosomes. (A) Representative images of mitotic cells with bipolar (WT) and abnormal spindles (monopolar spindle in KO) 3 days after tamoxifen treatment stained for Tubulin1α (green) and pH3 (red). (B) Quantification of mitotic cells with abnormal spindles in WT and KO cells. WT=3.406±1.922 KO=92.59±5.136. In total 23 WT and 27 KO, with at least 10 mitotic cells counted per condition, from N=3, in which each N is an independent cell culture obtained from independent animals. Scale bars: 5μM. (C) Representative images of mitotic cells without (WT) and with chromosome bridges (KO) 3 days after tamoxifen treatment. (D) Quantification of late mitosis cells with chromosome bridges in WT and KO cells. WT=8.681±6.045 KO=62.56±10.79. In total 18 WT and 15 KO, with at least 10 mitotic cells counted per condition, from N=3, in which each N is an independent cell culture obtained from independent animals. Scale bars: 5μM. ****-p<0.0001.

To fully confirm that AP-2 deletion is the cause of the phenotype, KO NPCs with an empty mCherry vector or an AP-2-RFP tagged plasmid were transfected (Figure 14A). The reintroduction of AP-2 increased the number of mitotic cells (Figure 14B) and rescued the chromatin bridges formed in late mitosis (Figure 14A).

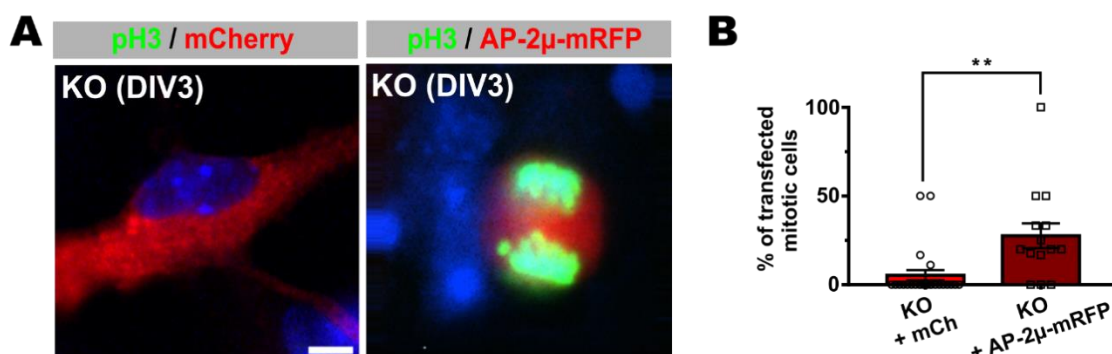


Figure 14. Reintroduction of AP-2μ rescues the mitotic phenotypes of AP-2 KO cells. (A) Representative images of mitotic cells transfected with mCherry and AP-2μ-RFP in primary NPCs (DIV3). (B) Quantification of mitotic cells out of total transfected cells. mCh=5.324±2.924 AP-2m-RFP=27.57±

7.030. In total 24 mCh and 14 AP-2m-RFP, with at least 20 transfected cells counted per condition, from $N=3$, in which each N is an independent cell culture obtained from independent animals. Scale bars: $5\mu\text{M}$.

** $p < 0.01$

In summary, AP-2 is crucial for correct mitosis in NPCs, and AP-2 deletion results in severe mitotic defects. However, what happens in the rest of the cell cycle? Is AP-2 involved only in mitosis or in other phases of the cell cycle?

3.2 AP-2 is required for cell cycle entry in the G1-S transition

Looking for a mechanism behind the phenotype previously observed proteomics analysis was done to compare pathways changed in the KO NPCs compared with the WT cell. Upregulation of Caspase-2 (CASP2) in AP-2 KO cells indicates possible senescence-related cell death (Figure 15A), which is linked with different types of cell cycle arrest. Moreover, among the downregulated pathways, some essential for the cell cycle were found (Figure 15B) proteins participating in G1-S transition, DNA replication, and protein translation. Furthermore, the downregulation of kinases and transcription factors critical for cell cycle progression was detected in KO cells (Figure 15C-D). Considering all previous statements, this data will indicate that the reduction of mitotic cells in the KO was probable a consequence of a cell cycle arrest before this process, either before or during DNA replication.

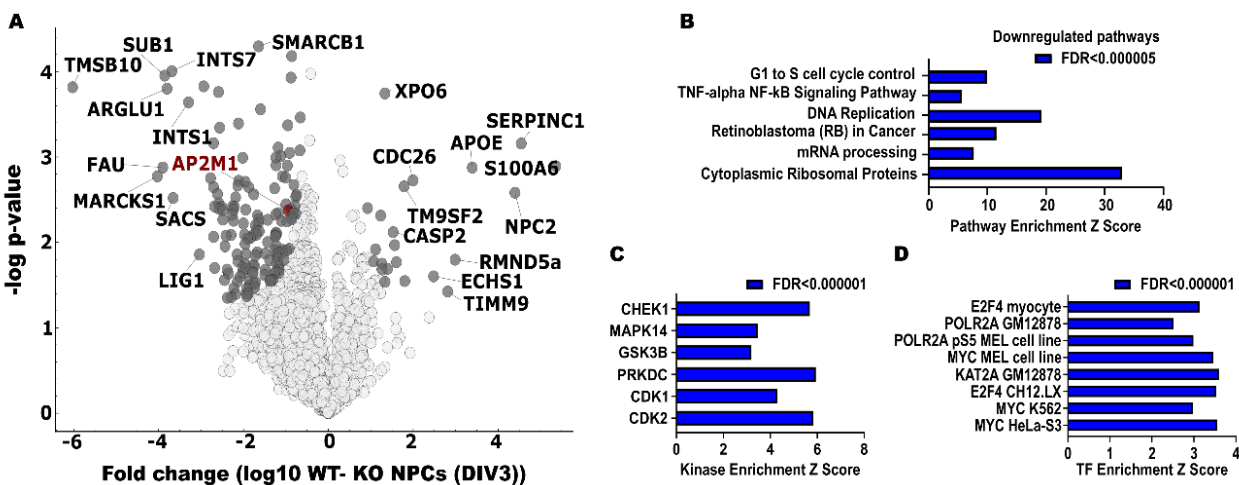


Figure 15. Proteins and pathways essential for cell cycle progression are affected in KO cells. (A) Proteins changes in KO NPCs compared to WT. In the X the Fold Change \log_{10} between WT and KO is plotted in the X-axis against $-\log q$ -value in the Y-axis. **(B)** Downregulated pathways essential for the cell cycle in KO cells are represented in the X-axis by the Enrichment Z score. FDR < 0.000005 **(C)**

Downregulated kinases essential for the cell cycle in KO cells represented in the X-axis by Enrichment Z score. $FDR < 0.000001$. **(D)** Downregulated transcription factors essential for the cell cycle in KO cells are represented in the X-axis by the Enrichment Z score. $FDR < 0.000001$. $N=3$ in which each N is protein lysates obtained from independent cell cultures from independent animals

A 24h EdU pulse combined with pH3 immunostaining was further performed in WT and KO NPCs to confirm the reduction in cycling cells before mitosis. For this experiment, mitotic cells were quantified within cycling cells. Even considering only cycling cells, a reduction of mitotic cells was observed in KO NPCs (Figure 16B) in line with previous results. When considering proliferating cells regarding total cell numbers, a reduction in the number of EdU-positive cells could be observed after 24 hours (Figure 16C).

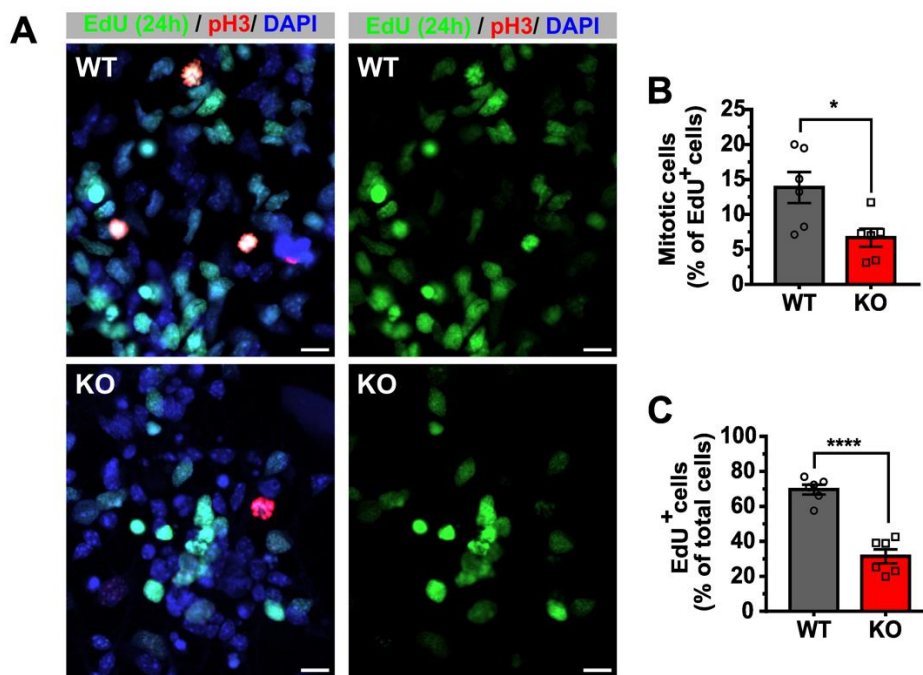


Figure 16. The proliferation of NPCs is reduced when AP-2 KO is induced. **(A)** Representative images of NPCs after 24h EdU pulse (green) and co-stained with pH3 (red). **(B)** Quantification of mitotic cells out of proliferating cells (EdU⁺ cells). $WT=13.25\pm 1.786$ $KO=7.684\pm 1.194$. In total 10 WT and 10 KO from $N=3$. **(C)** Quantification of proliferating cells (EdU⁺ cells) out of total cells. $WT=63.93\pm 4.556$ $KO=29.1\pm 2.727$. In total 11 WT and 11 KO, with at least 30 mitotic cells, 300 EdU cell and 1500 total cell per condition, from $N=3$, in which each N is an independent cell culture obtained from independent animals. Scale bars: $10\mu M$. *- $p\leq 0.05$; ****- $p< 0.0001$

Finally, to determine the exact moment of the arrest, NPCs were fixed in EtOH and stained with propidium iodide to analyze cell numbers in specific phases and dead cell numbers using flow cytometry. A reduction in phases G2/M and S was detected in KO NPCs with an increase in dead cells. Despite total G1 cells were reduced, less events were detected in KO condition, hence the percentage of G1 cells is not significantly reduced (Figure 17).

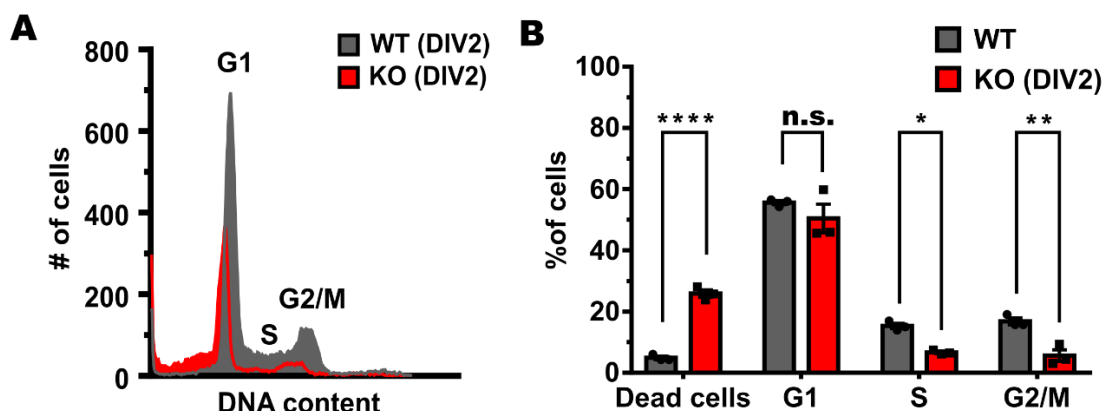


Figure 17. AP-2 KO arrest cells in the G1-S phase transition with increased dead cells. (A) Graphic representation of flow cytometry results 48 hours after KO induction. The first peak of the graph are cells in the G1 phase, followed by a plateau which are the S-phase cells, and the last peak are the G2 and mitosis cells. Dead cells are before the G1 peak. **(B)** Quantification of dead and cycling cells out of total cells. $WT^{DeadCells}=4.88$ $KO^{DeadCells}=25.89$ $WT^{G1}=55.58$ $KO^{G1}=50.46$ $WT^S=15.28$ $KO^S=6.663$ $WT^{G2/M}=16.83$ $KO^{G2/M}=5.604$. In total, each experiment measured $WT=20000$ events $KO\geq 5500$ events in three independent experiments ($N=3$) obtained from independent animals. n.s. -non-significant; *- $p\leq 0.05$; **- $p<0.01$; ****- $p<0.0001$

Taken together, these data provide stark evidence of a cell cycle disruption due to the loss of AP-2, which also results in cell death. In the next section, the mechanisms behind cell cycle arrest and cell death will be described.

3.3 AP-2 KO induces senescence-associated cell death and DNA-damage p53-dependent

The increase in cell death and upregulation of Caspase-2, reported in the previous section, are events associated with senescence, an irreversible state in which a cell stops division and eventually dies (Lim *et al.*, 2021). Senescence-associated β -galactosidase (SA- β -gal) assay was

used in order to detect senescent cells. SA- β -gal positive cells were increased in KO NPCs (Figure 18), indicating a senescent process when AP-2 is removed.

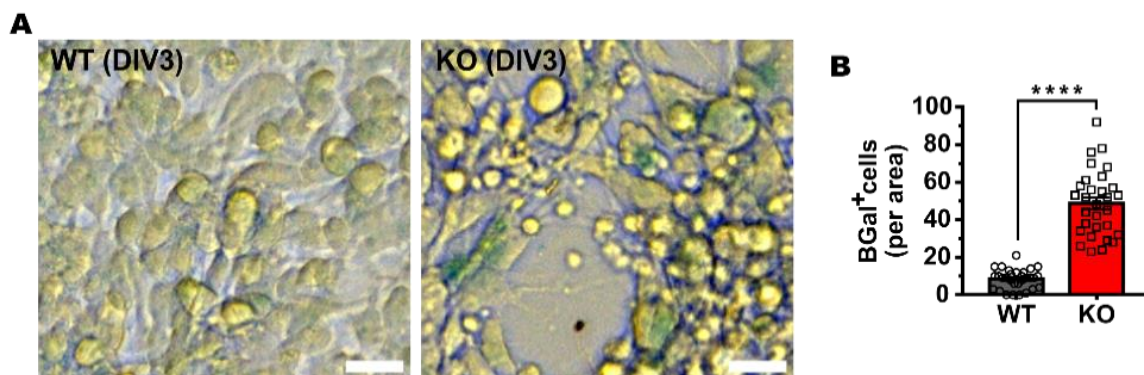


Figure 18. Senescence is increased in AP-2 KO cells. (A) Representative images of NPCs showing SA- β -gal detection (blue staining). **(B)** Quantification of SA- β -gal positive cells per area. WT=8.467 \pm 0.949 KO=48.70 \pm 3.193. In total 30 WT and 30 KO from N=3, in which each N is an independent cell culture obtained from independent animals. Scale bars: 10 μ M. ****-p<0.0001

Senescence-related cell death can be activated by caspase-2 downstream of p53, a tumor suppressor protein crucial for the G1-S checkpoint. Staining of p53 was done for detection of p53 activation in NPCs. A significant increase of p53 in KO NPCs was observed (Figure 19).

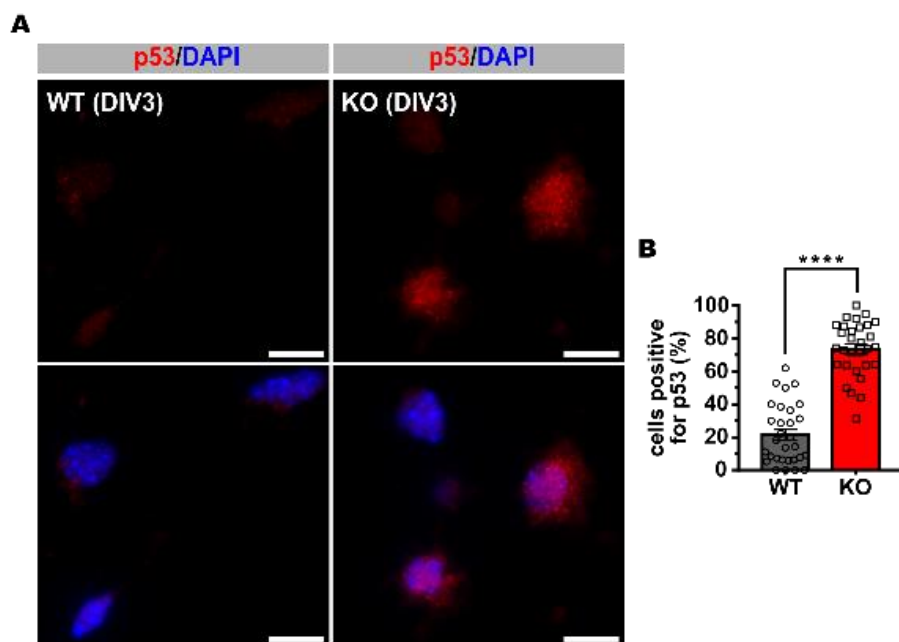


Figure 19. p53 is activated in AP-2 deleted NPCs. (A) Representative images of NPCs, stained for p53 (red). (B) Quantification of p53 positive cells out of total cells. WT=21.53±3.327 KO=73.60±3.052. In total 30 WT and 30 KO, with at least 100 cells counted per condition from N=3, in which each N is an independent cell culture obtained from independent animals. Scale bars: 10µM. ****-p<0.0001

DNA damage is tightly associated with cell cycle defects and is usually present in most cases of cell cycle arrest and p53 is usually activated in response to DNA defects. Immunostaining of γH2AX, a well-known marker of DNA damage showed a significant increase in cells with DNA damage (Figure 20).

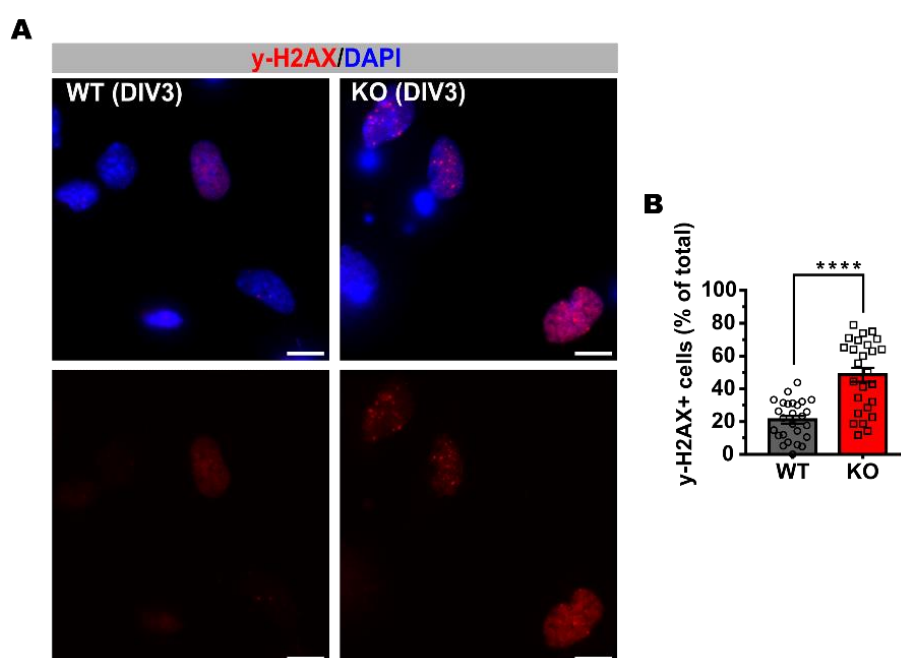


Figure 20. DNA damage is increased in AP-2 KO cells. (A) Representative images of NPCs, stained for γ-H2AX (red). (B) Quantification of γ-H2AX positive cells out of total cells. WT=21.14± 2.306 KO=48.54± 4.236. In total 26 WT and 26 KO, with at least 100 cells counted per condition from N=3, in which each N is an independent cell culture obtained from independent animals. Scale bars: 10µM. ****-p<0.0001

Together, these results showed that cell death is due to p53 activation and DNA damage resulting in cellular senescence activation. This is mechanism conserved in all the cell types, so it will be interested to test if other cells have the same phenotype when we delete AP-2, for that experiments with mouse embryonic fibroblasts (MEFs) were done to see not only if this statement is true, but also because these cells can be immortalize, hence bypassing the p53-dependent cell cycle arrest.

3.4 Disturbance of p53 signaling rescues the AP-2 KO phenotype

Since p53 is an essential protein in cell cycle modulation and looking at the significant increase when AP-2 is deleted, it was an excellent candidate to focus on the mechanisms behind cell cycle arrest. However, this is a conserved mechanisms and the question rise if AP-2 role in cell cycle is maintain in other cells. For this purpose, MEFs were obtained from embryos, and experiments were done to see if they could recapitulate the AP-2 KO phenotype as in NPCs.

Mitotic analysis was performed in MEFs in the same way as previously reported in section 3.1. As in NPCs, AP-2 deletion in MEFs reduced mitotic cells (Figure 21A-C) and mitotic spindle defects with lagging chromosomal bridges (Figure 21D-F). Hence, it was confirmed that the AP-2 role in the cell cycle is conserved in different cell types.

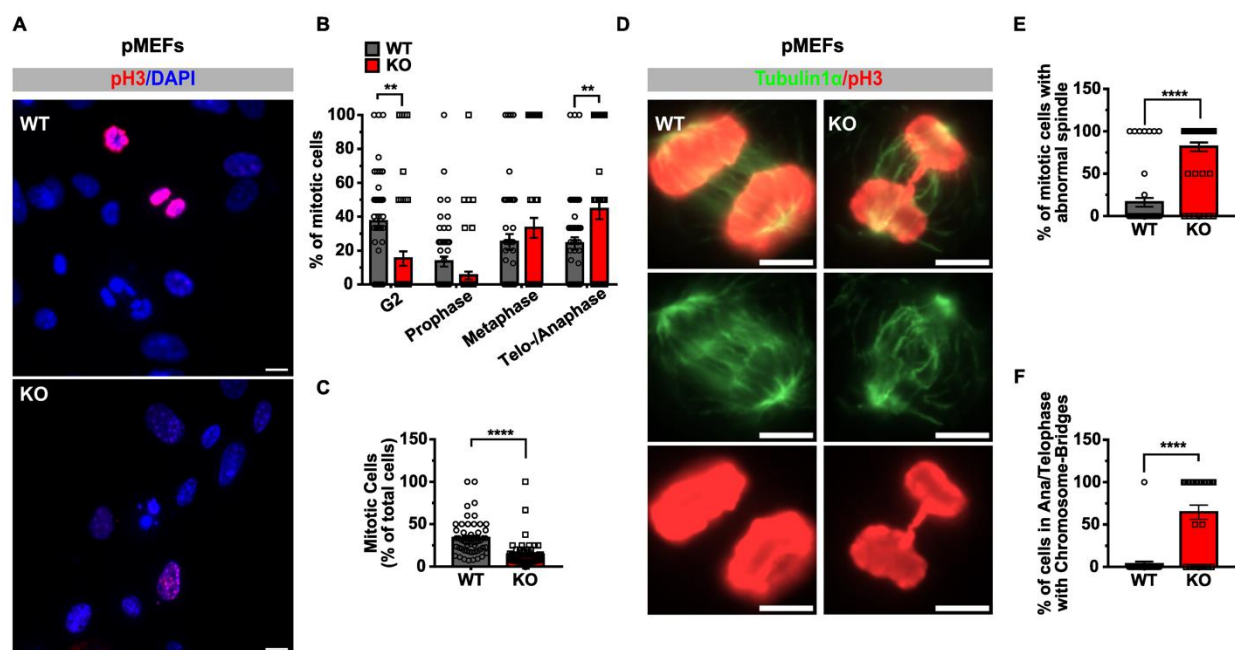


Figure 21. Mitosis is reduced and abnormal in MEFs upon AP-2 depletion. (A) Representative images of mitotic cells, stained with pH3 (red), in primary MEFs (DIV3). (B) Quantification of mitotic phases out of total mitotic cells in WT and KO cells. $WT^{G2}=37.28$ $KO^{G2}=15.28$ $WT^{Prophase}=13.48$ $KO^{Prophase}=5.278$ $WT^{Metaphase}=25.00$ $KO^{Metaphase}=33.33$ $WT^{Ana/Telophase}=24.23$ $KO^{Ana/Telophase}=44.44$. In total 52 WT and 60 KO from $N=3$, in which each N is an independent cell culture obtained from independent animals. (C) Quantification of mitotic cells out of total cells in WT and KO cells. $WT=33.43 \pm 2.896$ $KO=13.83 \pm 1.961$. In total 52 WT and 60 KO from $N=3$, in which each N is an independent cell culture obtained from independent animals. Scale bars: $10\mu M$. (D) Representative images of mitotic cells with bipolar (WT) and abnormal spindles (monopolar spindle in KO) 3 days after tamoxifen treatment stained for Tubulin1 α (green) and pH3

(red). **(E)** Quantification of mitotic cells with abnormal spindles in WT and KO cells. WT=16.15±5.183 KO=81.63±5.195. In total 49 WT and 49 KO from N=3, in which each N is an independent cell culture obtained from independent animals. Scale bars: 5µM. **(F)** Quantification of late mitosis cells with chromosome bridges in WT and KO cells. WT=3.125±3.125 KO=64.52±8.422. In total 32 WT and 31 KO from N=3, in which each N is an independent cell culture obtained from independent animals. Scale bars: 5µM. **- $p < 0.01$; ****- $p < 0.0001$.

Since MEFs recapitulate the mitotic defects of NPCs, it was decided to be used for p53 inhibitions experiments. There are several p53 inhibitors commercially available, although they interfere with other pathways. Equally, there are p53 RNAi that will knock-down p53, although there is no warranty that it will be an effective target to circumvent the G1-S checkpoint. Finally, the immortalization of MEFs by SV40 virus was used since SV40 transduction inactivates pRB, p53, and SEN6, which are crucial for G1-S transition (Hubbard & Ozer, 1999). Immortalized MEFs (iMEFs) experiments were performed in the same ways as previously with primary MEFs. A decrease in the mitotic cells was not observed in iMEFs (Figure 22A-C). Moreover, mitosis analysis showed that defects in the mitotic spindle and chromosome lagging were absent in AP-2 KO iMEFS (Figure 22D-F).

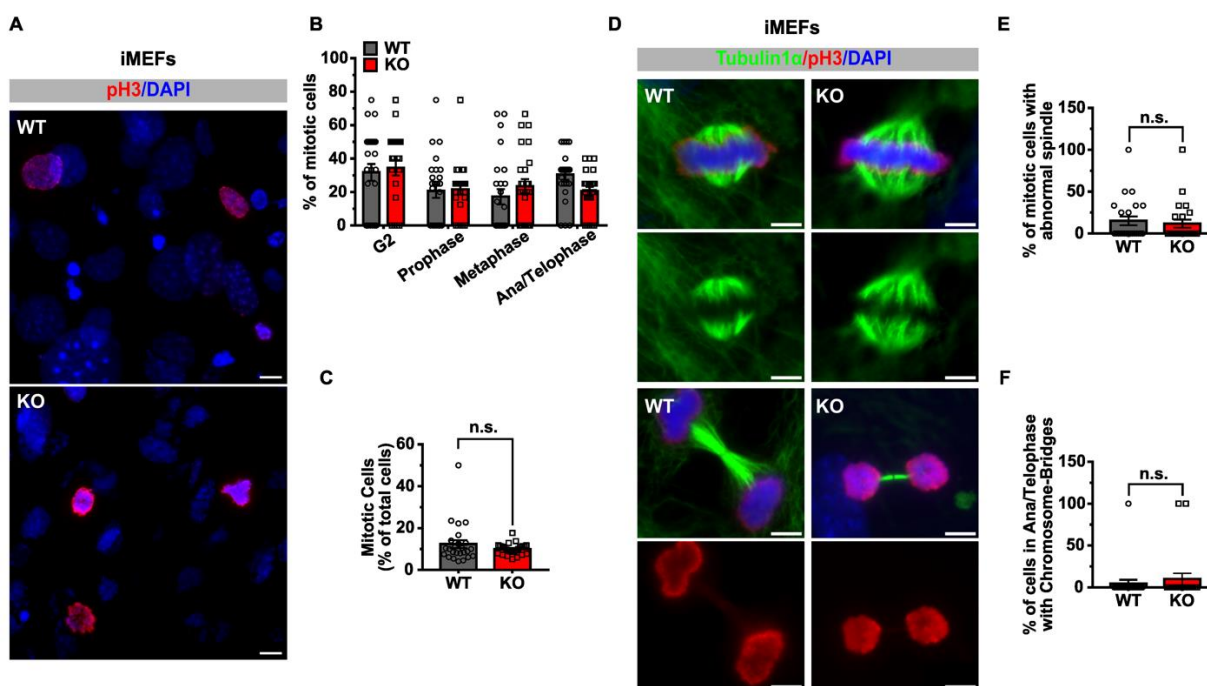


Figure 22. Mitosis phenotypes are rescued upon p53-pathway inhibition in iMEFs. **(A)** Representative images of mitotic cells, stained with pH3 (red), in immortalized MEFs (DIV3). **(B)** Quantification of mitotic

phases out of total mitotic cells in WT and KO cells. $WT^{G2}=31.76$ $KO^{G2}=34.40$ $WT^{Prophase}=20.57$ $KO^{Prophase}=21.57$ $WT^{Metaphase}=17.22$ $KO^{Metaphase}=23.50$ $WT^{Ana/Telphase}=30.45$ $KO^{Ana/Telphase}=20.53$. In total 25 WT and 25 KO, with at least 25 mitotic cells and 200 total cells counted per condition, from $N=3$, in which each N is an independent cell culture obtained from independent animals. **(C)** Quantification of mitotic cells out of total cells in WT and KO cells. $WT=12.35\pm 1.906$ $KO=9.900\pm 0.5416$. In total 25 WT and 25 KO from $N=3$, in which each N is an independent cell culture obtained from independent animals. Scale bars: $10\mu M$. **(D)** Representative images of mitotic cells with bipolar (WT) and abnormal spindles (monopolar spindle in KO) 3 days after tamoxifen treatment for Tubulin1 α (green) and pH3 (red). **(E)** Quantification of mitotic cells with abnormal spindles in WT and KO cells. $WT=15.22\pm 5.308$ $KO=11.74\pm 4.823$. In total 23 WT and 24 KO, with at least 25 mitotic cells counted per condition, from $N=3$, in which each N is an independent cell culture obtained from independent animals. Scale bars: $5\mu M$. **(F)** Quantification of late mitosis cells with chromosome bridges in WT and KO cells. $WT=4.545\pm 4.545$ $KO=10.00\pm 6.882$. In total 22 WT and 20 KO, with at least 25 mitotic cells counted per condition, from $N=3$, in which each N is an independent cell culture obtained from independent animals. Scale bars: $5\mu M$. n.s. -non-significant.

These results confirmed that p53 activation is the cause of cell cycle arrest in AP-2 KO cells and that inhibition of this pathway is enough to rescue the observed phenotype.

3.5 AP-2 interacts with centrosomal proteins and stabilizes centrosome structure

For the search of a possible mechanism which will explain what modulated p53-activated arrest, mass spectrometry pull-down for AP-2 subunit α was performed in WT embryonic brains to find potential interaction partners with the complex. Interestingly, among the proteins enriched, several components of the γ -tubulin complex were found, a complex of proteins crucial for centrosome structure and microtubule nucleation (Figure 23A). Moreover, the interaction was as strong as traditional interactors of AP-2 involved in CME. The formation of the complex was confirmed by the Co-immunoprecipitation pull-down in both E14-E16 and 8 weeks adult brains. In both cases, the formation of a complex between AP-2 α and several proteins of the γ -tubulin complex was detected (Figure 23B-D).

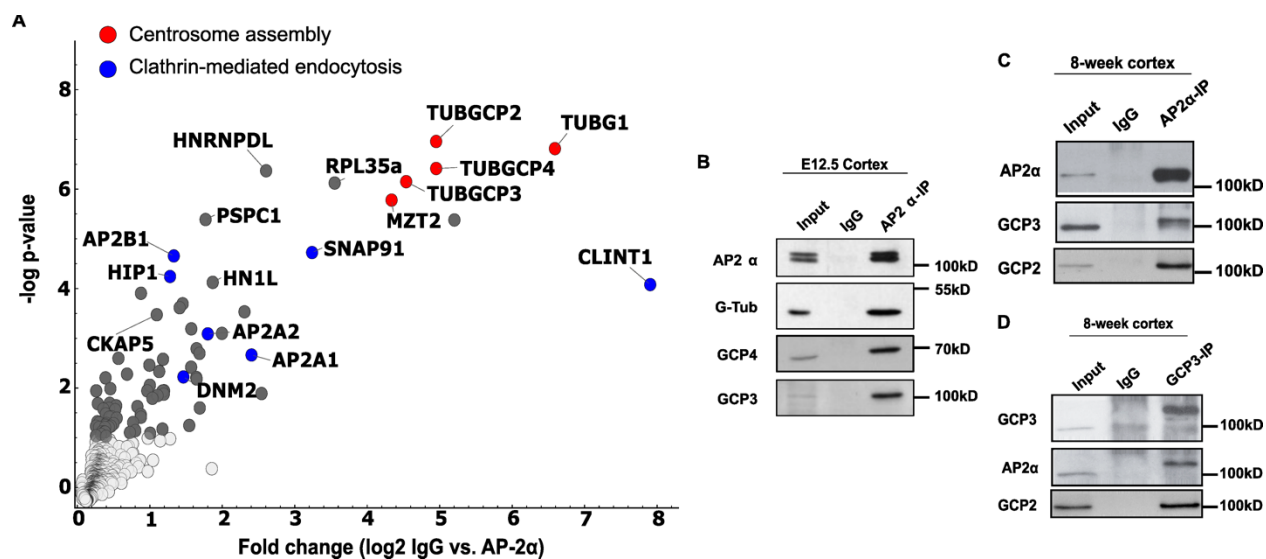


Figure 23. AP-2 subunit α interacts with components of the γ -tubulin complex, essential for centrosome structure and function (A) Proteins enriched in the AP-2 α IP compared to IgG control. Highlighted in gray are proteins with significant FDR values. Highlighted in blue / red are proteins associated with clathrin-mediated endocytosis / centrosome assembly. Fold Change log₂ between IgG and AP-2 α was plotted on the X-axis against -log p-value on the Y-axis. N=5 (B) Representative blots of Co-Immunoprecipitation of WT embryo lysates of AP-2 α with different components of γ -tubulin complex proteins for proteomic analysis validation. N=3, in which each N is protein lysates obtained from independent animals. (C-D) Representative blots of Co-Immunoprecipitation of WT cortex lysates of AP-2 α (C) with different components of γ -tubulin complex proteins and GCP3 (D) with AP-2 α and GCP2. N=3, in which each N is protein lysates obtained from independent animals.

In addition, immunostaining for AP-2 α and AP-2 μ with GCP3 showed a strong colocalization between AP-2 and GCP3 (Figure 24).

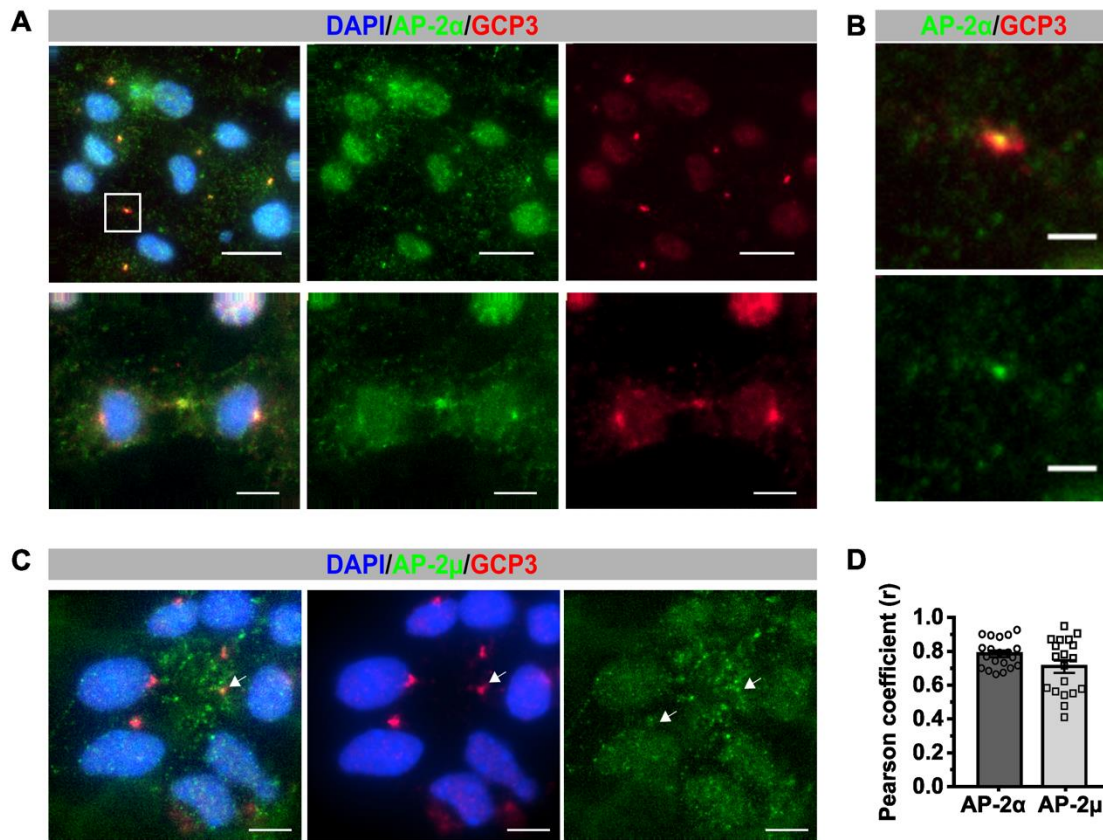


Figure 24. AP-2 subunits α and μ interact physically with GCP3 (A). Representative images of co-immunostaining of NPCs for AP-2 α (Green) with GCP3 (Red) and DAPI (Blue). **(B)** Zoom-in is showing strong colocalization of AP-2 α (Green) with GCP3 (Red). **(C)** Representative images of co-immunostaining of NPCs for AP-2 μ (Green) with GCP3 (Red) and DAPI (Blue). **(D)** Quantification of average Pearson Coefficient (r) of AP-2 α (panels A-B) and AP-2 μ (panel C) with GCP3. AP-2 α =0.7846 \pm 0.01869 AP-2 μ =0.7100 \pm 0.03724. In total, AP-2 α =20 AP-2 μ =19 from N=3, in which each N is an independent cell culture obtained from independent animals. Scale bars: 5 μ M.

For co-staining proteins from the different γ -tubulin complexes, NPCs were transfected with a γ -tubulin-GFP tagged plasmid to perform immunostaining for GFP (γ -Tubulin/centrosome), GCP3 (γ -TuSC) and GCP4 (γ -TuRC) (Figure 25A). Some of the KO NPCs presented a dispersed γ -Tubulin, an indicator of a defective centrosome assembly, and changes in the distribution of GCPs. There was a significant reduction in GCP4 (Figure 25C) and GCP3 (Figure 25D) levels with a loss of specific localization to the centrosomal area. In contrast, analysis of protein levels in KO cells detected a non-significant reduction of GCP3 and GCP4 (Figure 25D).

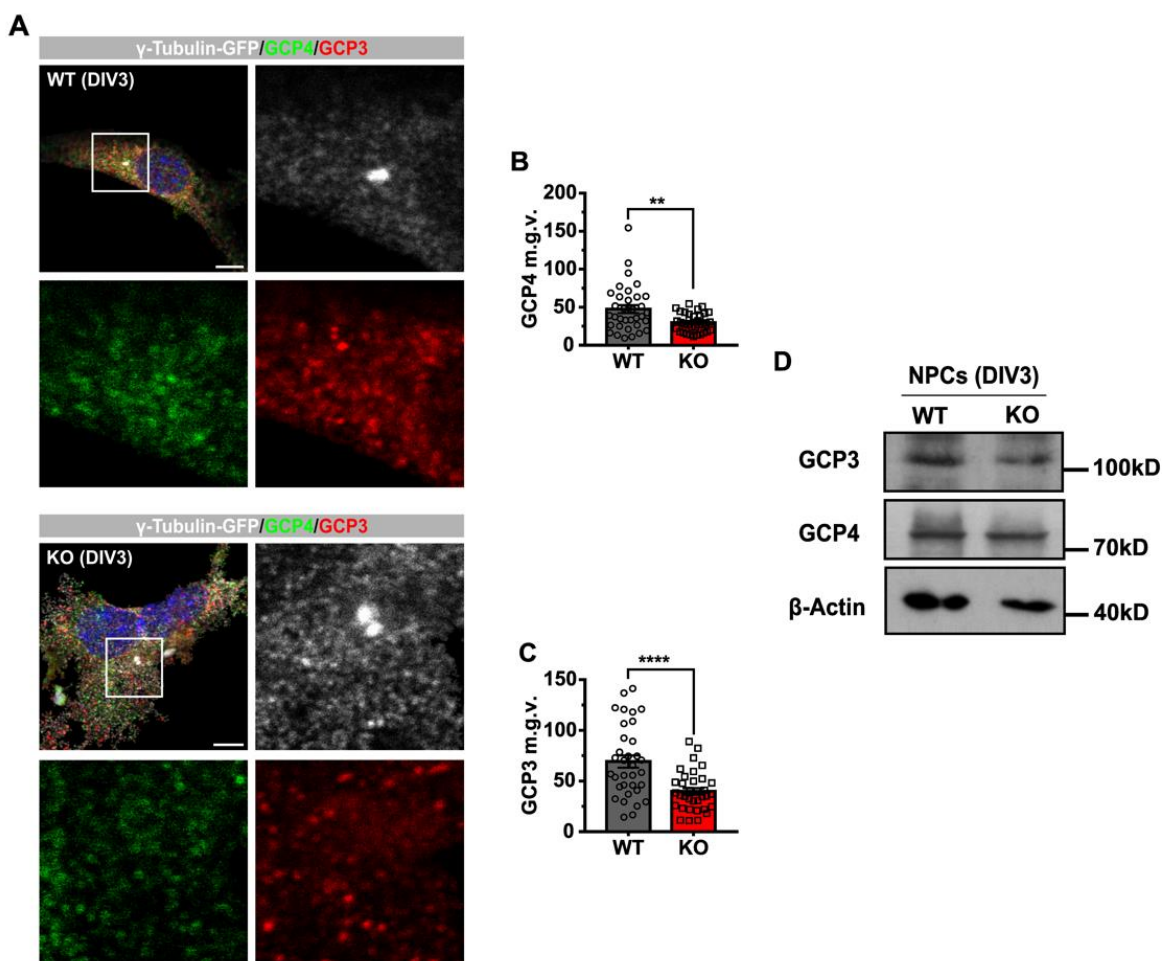


Figure 25. GCPs distribution and levels are altered upon AP-2 KO in NPCs. (A) Representative images of co-immunostaining of WT and KO NPCs for γ -tubulin-GFP transfected cells (white), GCP4 (green) and GCP3 (red). (B) Quantification of GCP4 mean grey value (m.g.v) relative to area in WT and KO NPCs. WT=47.47 \pm 5.293 KO=29.73 \pm 2.117 (C) Quantification of GCP3 mean grey value (m.g.v) relative to area in WT and KO NPCs. WT=69.20 \pm 6.085 KO=39.80 \pm 3.338. In total WT=34 KO=34 from N=3, in which each N is an independent cell culture obtained from independent animals. (D) Representative WBs show a non-significant decrease of GCP3 and GCP4 subunits. Scale bars: 5 μ M. **-p<0.01; ****-p<0.0001.

Since γ -TuSC looked more affected than γ -TuRC proteins, GCP2 (the other component of the γ -TuSC) was analyzed additionally by immunostaining. Like the previous experiment, GCP2 was significantly reduced, confirming the previously observed disruption (Figure 26).

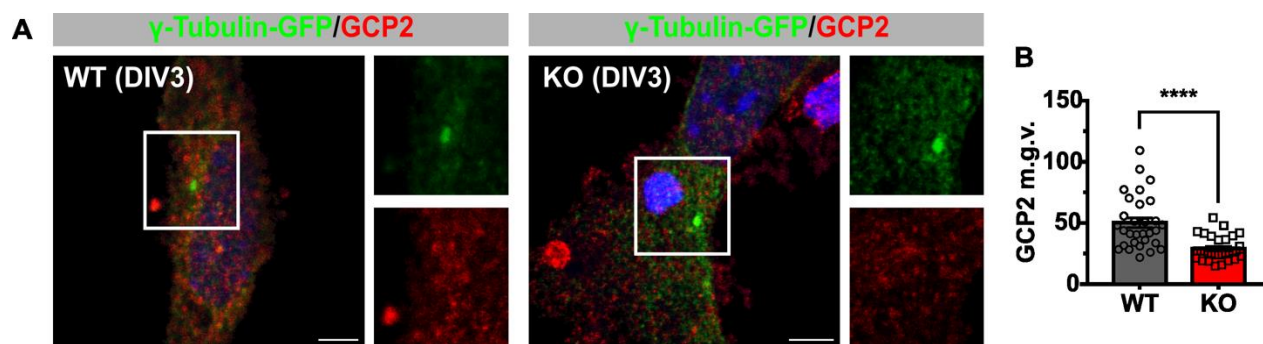


Figure 26. GCP2 distribution and levels are altered upon AP-2 KO in NPCs. (A) Representative images of co-immunostaining of WT and KO NPCs for γ -tubulin-GFP transfected cells (green) and GCP2 (red). (B) Quantification of GCP2 mean grey value (m.g.v) relative to area in WT and KO NPCs. $WT=50.14\pm 3.977$ $KO=29.03\pm 1.814$. In total, $WT=30$ $KO=30$ from $N=3$, in which each N is an independent cell culture obtained from independent animals. Scale bars: $5\mu M$. ****- $p<0.0001$.

Senescence-associated cell cycle arrest can occur for multiple reasons, but one of the leading causes is the centrosome since when its maturation or function is affected, it has severe implications at a cellular level. Moreover, aberrations of centrosome structure are the leading cause of proliferation defects. Staining of centrosomal proteins γ -tubulin and pericentrin (PCNT) showed that AP-2 KO NPCs present either cells without centrosomes or multiple centrosomes (Figure 27).

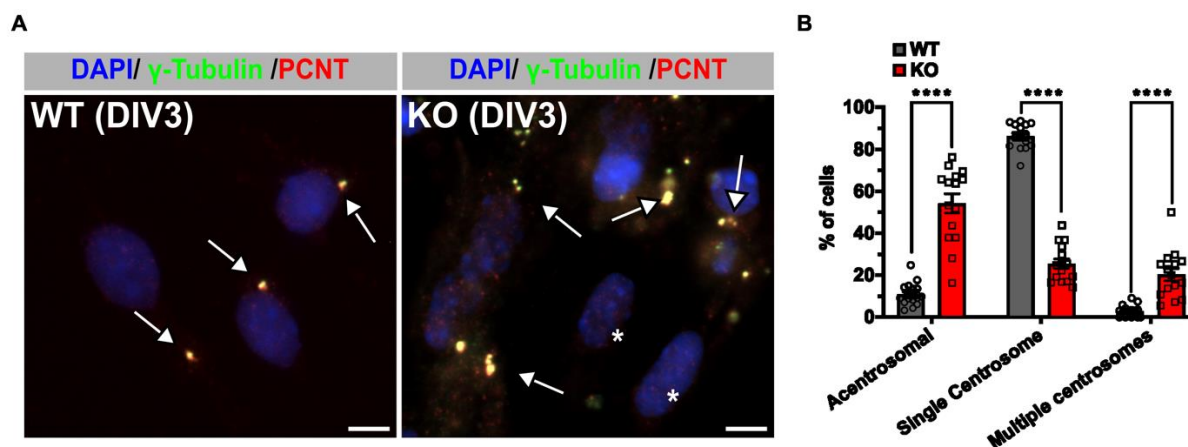


Figure 27. AP-2 KO NPCs present abnormal centrosomes. (A) Representative images of WT and KO NPCs co-stained with γ -tubulin (green) and PCNT (red). (B) Quantification of Acentrosomal, Single centrosome, and Multiple centrosomes cells out of total cells. $WT_{Acentrosomal}=14.23$ $KO_{Acentrosomal}=60.88$ $WT_{SingleCentrosome}=79.97$ $KO_{SingleCentrosome}=19.54$ $WT_{MultipleCentrosomes}=5.796$ $KO_{MultipleCentrosomes}=19.58$. In total 5

WT and 5 KO, with more than 100 cells counted per condition, from $N=3$, in which each N is an independent cell culture obtained from independent animals. Scale bars: $5\mu\text{M}$. $**p<0.01$; $****p<0.0001$.

In addition, PCNT was observed to be less localized in the KO, with a significant percentage of cells presenting a dispersed distribution of Pcnt (Figure 28A-B). However, since PCNT and γ -tubulin do not have a specific localization in the centrosome, staining of a specific marker of the centriole (Centrin) and a marker of the pericentriolar matrix (PCM1) was done and analyzed using super-resolution microscopy (STED). PCM is a cloud of puncta surrounding the centriole in cycling cells. However, in AP-2 KO NPCs PCM completely disappeared compared with WT cells (Figure 28C-D). This data is consistent with previous proteomics data in which PCM1 was downregulated in KO cells. In addition, when the WT group was analyzed, we can see two populations of cells; 1) cells with higher PCM1 intensity than KO (cycling cells) and 2) cells with the same PCM1 intensity as KO cells (non-cycling cells). Hence, arrested cells have no PCM around the centriole, as seen in KO cells.

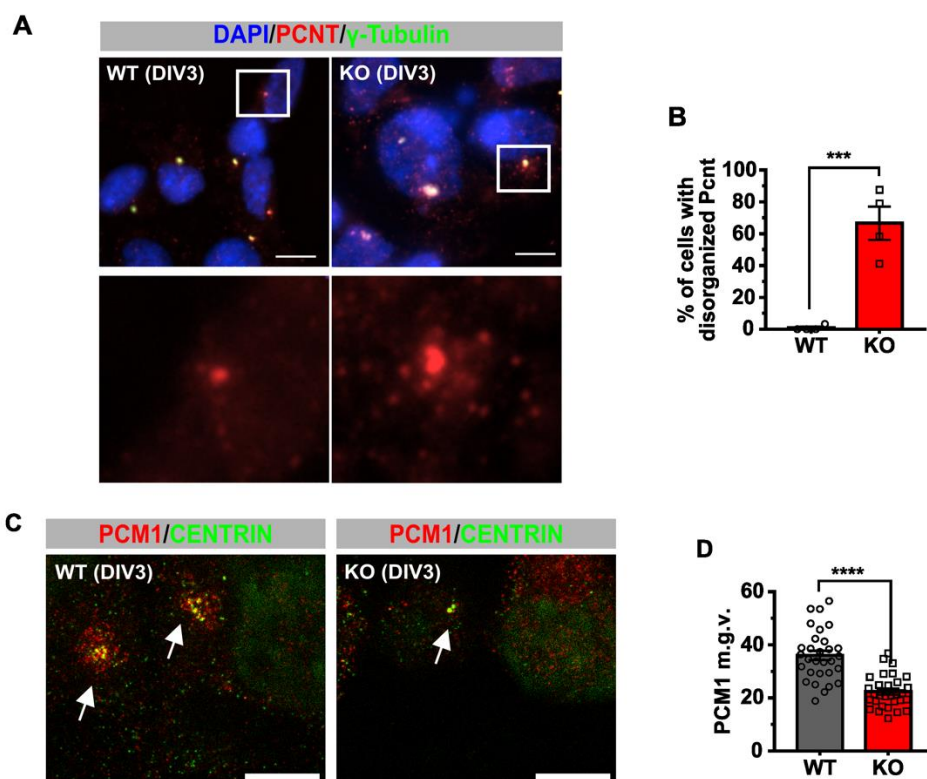


Figure 28. AP-2 KO cells have normal centrioles but abnormal pericentriolar matrix. (A) Representative images of WT and KO NPCs co-stained with γ -tubulin (green) and PCNT (red). (B) Quantification of cells with disorganized Pcnt out of total cells. $WT=0.8333\pm 0.8333$ $KO=66.52\pm 10.44$. In

total 4 WT and 4 KO, with at least 30 cells counted per condition, from $N=3$, in which each N is an independent cell culture obtained from independent animals. **(C)** Representative images of WT and KO NPCs co-stained with Centrin (green) and PCM1 (red). **(D)** Quantification of PCM1 mean grey value (m.g.v) relative to area in WT and KO NPCs. $WT=36.03\pm 1.745$ $KO=22.31\pm 1.128$. In total, $WT=30$ $KO=30$ from $N=3$, in which each N is an independent cell culture obtained from independent animals. Scale bars: $5\mu M$. $***-p<0.001$; $****-p<0.0001$.

In conclusion, centrosome maturation required for cell cycle progression is affected when AP-2 is deleted, highlighting a potential role of AP-2 in centrosome structure. Still the question whether this is dependent of clathrin, or no is open, the next section will determine if that is the case.

3.6 AP-2 role in cell cycle and centrosome is independent of Clathrin-Mediated Endocytosis

Since AP-2 is mainly associated with CME, it must be proved whether this new role of AP-2 in cell division is because of endocytosis or a new moonlight role. For that purpose, WT NPCs were treated with the drug PitStop2, which competitively inhibits the clathrin terminal domain and binds to AP-2 to inhibit CME selectively. PitStop2-treated cells did not present a reduction of mitotic cells (Figure 29B) nor spindle anomalies (Figure 29C). In addition, propidium iodide staining of cells treated with PitStop2 did not show any cell cycle arrest. However, there was a significant increase in dead cells, most likely by endocytosis inhibition (Figure 29D-E).

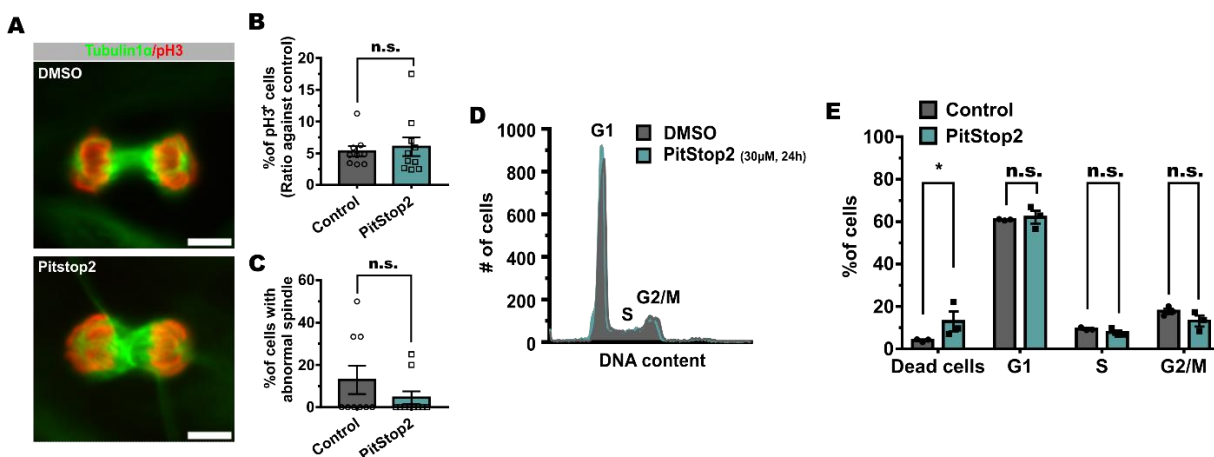


Figure 29. CME-inhibited cells do not present any mitotic defect or cell cycle arrest. **(A)** Representative images of mitotic cells, co-stained with pH3 (red) and tubulin1 α (green), in primary NPCs treated with PitStop2 (DIV3). **(B)** Quantification of mitotic cells out of total cells in Control and PitStop2 treated cells. $Control=5.301\pm 0.8264$ $PitStop2=6.022\pm 1.469$. In total 9 WT and 10 KO, at least 20 mitotic

cells and 200 total cells per condition, from $N=3$, in which each N is an independent cell culture obtained from independent animals. **(C)** Quantification of mitotic cells with abnormal spindles in Control and PitStop2 treated cells. Control= 12.96 ± 6.677 PitStop2= 4.500 ± 3.023 . In total 9 WT and 10 KO, at least 20 mitotic cells per condition, from $N=3$, in which each N is an independent cell culture obtained from independent animals. Scale bars: $5\mu\text{M}$. **(D)** Graphic representation of flow cytometry results 24 hours after PitStop2 treatment. The first peak of the graph are cells in G1 phase, followed by a plateau which are the S-phase cells, and the last peak are the G2 and mitosis cells. Dead cells are before the G1 peak. **(E)** Quantification of dead and cycling cells out of total cells. Control^{DeadCells}=4.012 PitStop2^{DeadCells}=12.94 Control^{G1}=60.89 PitStop2^{G1}=62.10 Control^S=9.368 \pm 3.176 PitStop2^S=7.738 Control^{G2/M}=17.77 PitStop2^{G2/M}=13.11. In total, each experiment measured 20000 events per condition in three independent experiments ($N=3$) obtained from independent animals. n.s. -non-significant; * $-p \leq 0.05$.

In addition to cell cycle analysis, centrosome analysis was performed. In line with the cell cycle results, centrosomes were not affected by PitStop2 treatment (Figure 30).

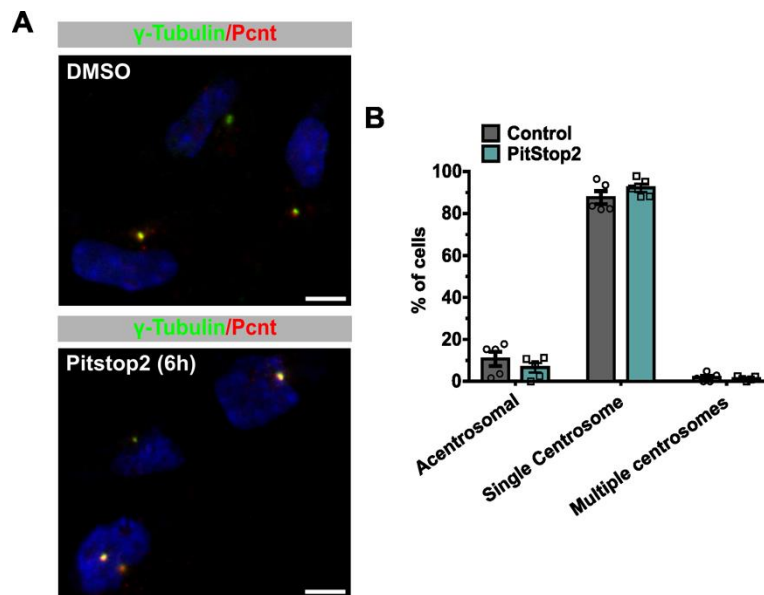


Figure 30. AP-2 KO NPCs present abnormal centrosomes. **(A)** Representative images of WT and KO NPCs co-stained with γ -tubulin (green) and PCNT (red). **(B)** Quantification of Acentrosomal, Single centrosome, and Multiple centrosomes cells out of total cells. Control^{Acentrosomal}=10.68 PitStop2^{Acentrosomal}=6.509 Control^{SingleCentrosome}=87.54 PitStop2^{SingleCentrosome}=92.14 Control^{MultipleCentrosomes}=1.776 PitStop2^{MultipleCentrosomes}=1.347. In total 5 Control and 5 PitStop2, at least 100 cells per condition, from $N=3$, in which each N is an independent cell culture obtained from independent animals. Scale bars: $5\mu\text{M}$.

Since these cells have functional AP-2, and PitStop2 treatment did not replicate the phenotype, it was confirmed that AP-2 has a novel role in the cell cycle independently of CME.

3.7 AP-2 KO increases ciliation, but cilia removal does not rescue the phenotype in astrocytes

The centrosome is tightly associated with another cellular structure, the primary cilium, which is present before the cycle starts. Cycle defects could be because of cilia problems since it is required to disassemble to form the centrosome and modulates signaling. Immunostaining for ARL13b, a primary cilia marker, showed increased cilia length (Figure 31B) and ciliated cells in AP-2 KO cells (Figure 31C).

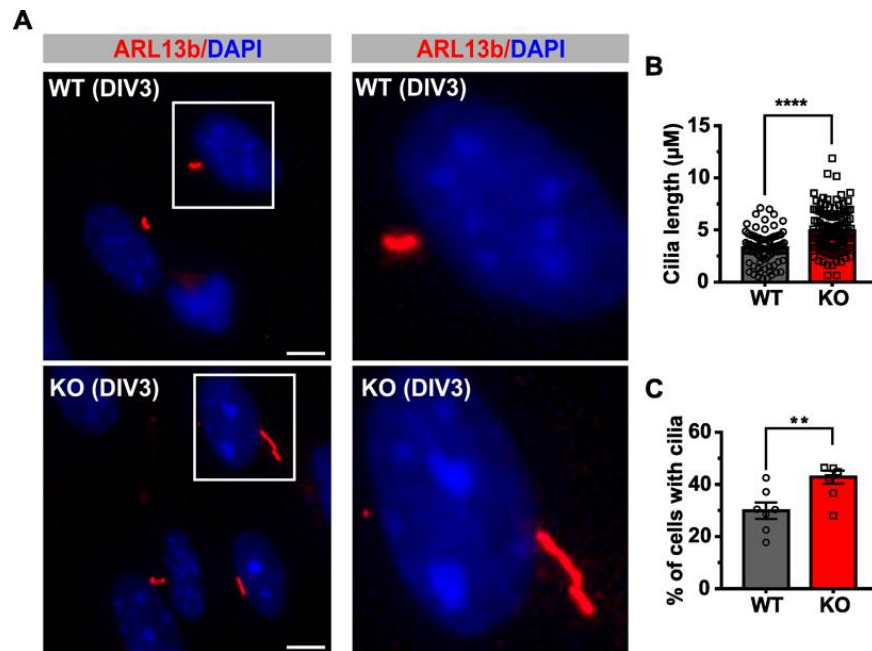


Figure 31. *AP-2 KO NPCs have increased ciliation and elongated cilia. (A) Representative images of WT and KO NPCs stained with ARL13b (red). (B) Quantification of cilia length in μM . WT=3.282 \pm 0.1586 KO=4.904 \pm 0.1900. In total 90 WT and 118 KO from N=3, in which each N is an independent cell culture obtained from independent animals. (C) Quantification of ciliated cells out of total cells. WT=29.89 \pm 3.144 KO=42.78 \pm 2.534. In total 7 WT and 8 KO, at least 100 cells per condition, from N=3, in which each N is an independent cell culture obtained from independent animals. Scale bars: 5 μM . **- p <0.01; ****- p <0.0001.*

In the same case as with the centrosomal and mitotic phenotypes, this cilia phenotype was not present upon clathrin inhibition using PitStop2 for 6h (Figure 32).

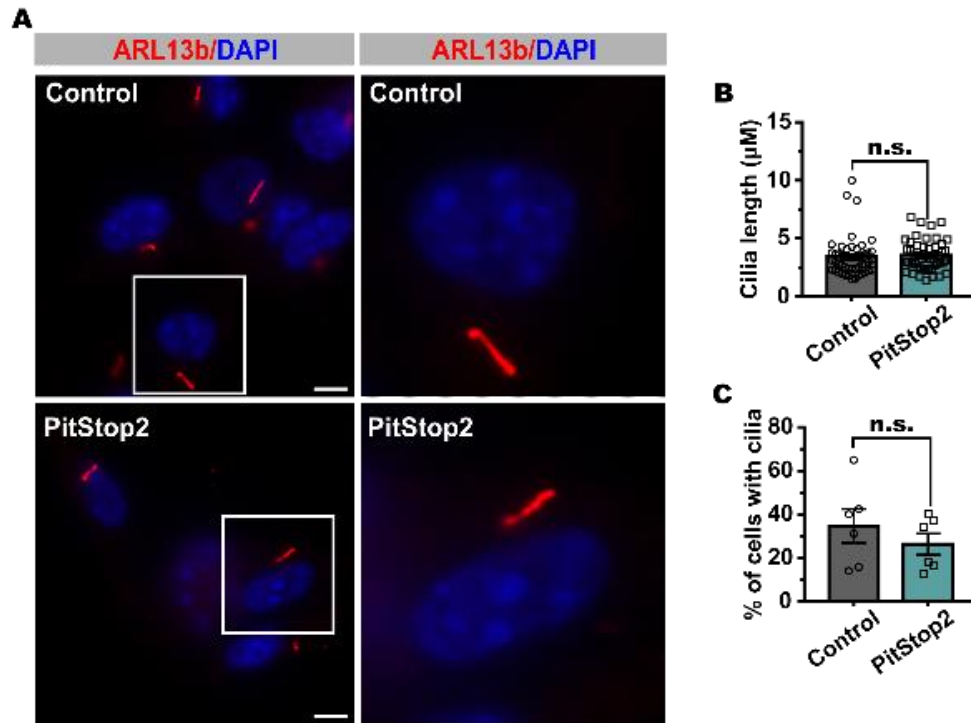


Figure 32. Disrupted CME NPCs do not present increased ciliation nor increased cilia length. (A) Representative images of Control and PitStop2 NPCs stained with ARL13b (red). **(B)** Quantification of cilia length in μM . Control= $3.282 \pm 3.402 \pm 0.2446$ PitStop2= 3.534 ± 0.1930 . In total 49 Control and 48 Pitstop2 from N=3, in which each N is an independent cell culture obtained from independent animals. **(C)** Quantification of ciliated cells out of total cells. Control = 34.73 ± 7.755 PitStop2= 26.37 ± 4.903 . In total 6 Control and 6 PitStop2, at least 100 cells per condition from N=3, in which each N is an independent cell culture obtained from independent animals. Scale bars: $5\mu\text{M}$. n.s. -non-significant

Rescue experiments were attempted in double KO for Ift88 (a protein required for cilia formation) and AP-2 μ in astrocytes. Astrocytes, same as NPCs and MEFs, have a decreased proliferation when AP-2 is depleted, shown by a reduction of Ki67, a well-known proliferation marker (Figure 33B). However, there were no significant differences between AP-2 KO and AP-2 Ift88 KO astrocytes (Figure 33D).

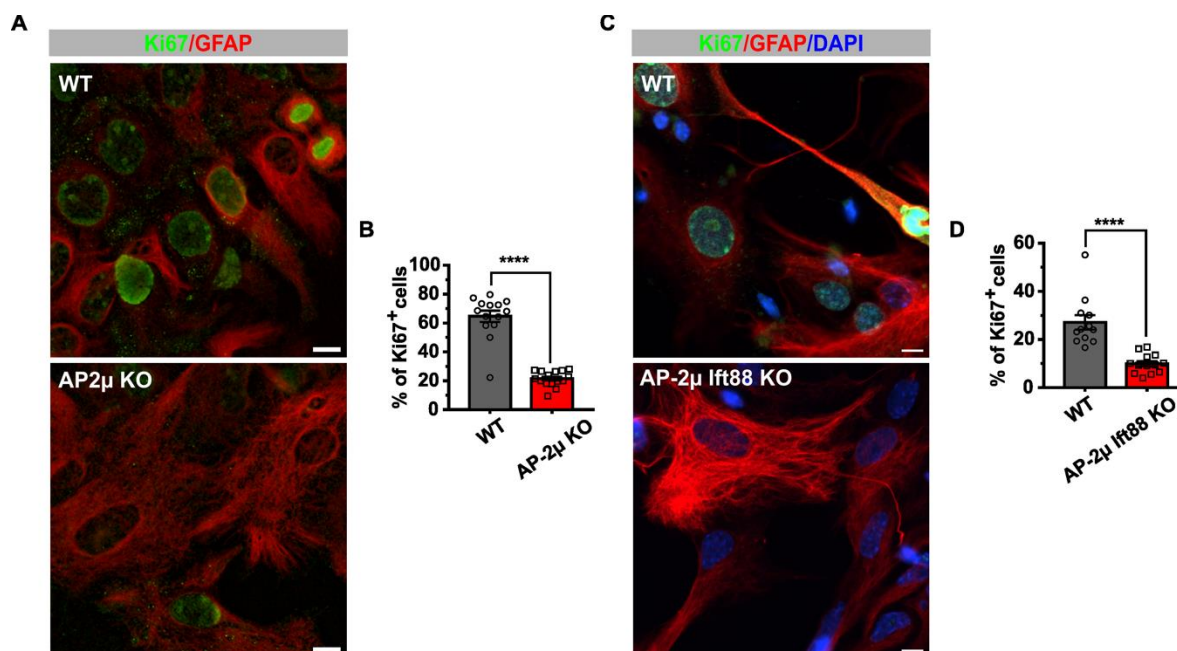


Figure 33. Astrocytes have proliferation defects that are not rescued by cilia KO. (A) Representative images of WT and KO NPCs co-stained with Ki67 (green) and GFAP (red). (B) Quantification of proliferating cells out of total cells. WT=64.63±3.928 AP2μ KO=21.53±1.370. In total 14 WT and 15 KO, at least 75 cells per condition, from N=3, in which each N is an independent cell culture obtained from independent animals. (C) Representative images of WT and double-KO NPCs co-stained with Ki67 (green) and GFAP (red). (D) Quantification of proliferating cells out of total cells. WT=27.13±3.022 AP2μ lft88 KO=9.933±1.108. In total 12 WT and 13 KO, at least 150 cells per condition, from N=3, in which each N is an independent cell culture obtained from independent animals. Scale bars: 5μM. ****-p<0.0001.

Considering these results, the possibility of a direct role of AP-2 in cilia disassembly was discarded; hence, the phenotype's cause must be at the centrosome. These results confirmed that AP-2 is strictly restricted to the centrosome and that cilia defects are a consequence rather than the reason for the cell cycle arrest. Considering the centrosome is affected, and its important role in microtubule nucleation, centrosomal disruptions should have physiological effects, the next section will describe how microtubules are affected upon AP-2 KO.

3.8 AP-2 is essential for MTOC activity and new-born neurons migration

Since AP-2 has been shown to have trafficking roles in other cells and processes, it was hypothesized the possibility of a role in trafficking γ-Tubulin complex components to the centrosome during the G1 to S transition. The logic behind this hypothesis is that we expect AP-2 to be localized at the plasma membrane when cells are not cycling. However, when the cell

cycle is activated, and endocytosis is downregulated, AP-2 will transport γ -Tubulin proteins from the basal body of the primary cilia at the plasma membrane to the centrosome. Live imaging of WT NPCs transfected with AP-2 μ -mCherry and γ -Tubulin-GFP was performed in order to observe the trafficking of these proteins. AP-2 was detected in the plasma membrane but also some particles were detected moving towards the centrosome area (Figure 34A).

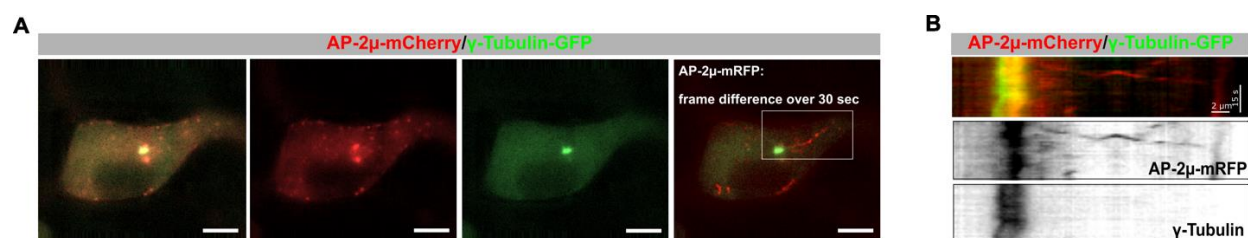


Figure 34. Evidence of possible AP-2 trafficking to the centrosome. (A) Maximum Intensity Projection of representative live-imaging videos of AP-2 trafficking in KO cells (10 minutes videos). **(B)** Representative figure of NPCs co-stained for Ki67 (white), GFP (green) and AP-2 α (red). Scale bars: 5 μ M.

AP-2 trafficking then will be important in microtubule nucleation from the centrosome, which requires γ -tubulin. To study de-novo microtubule nucleation, NPCs were treated with nocodazole to induce microtubule catastrophe followed by none or 5 min recovery. In control conditions, KO NPCs showed a decrease in microtubule intensity compared with WT (Figure 35), indicating a compromised microtubule structure of the KO cells. However, microtubule recovery was achieved after 5 minutes in both WT and KO at the same levels as control conditions (Figure 35). It was confirmed that KO NPCs could nucleate microtubules.

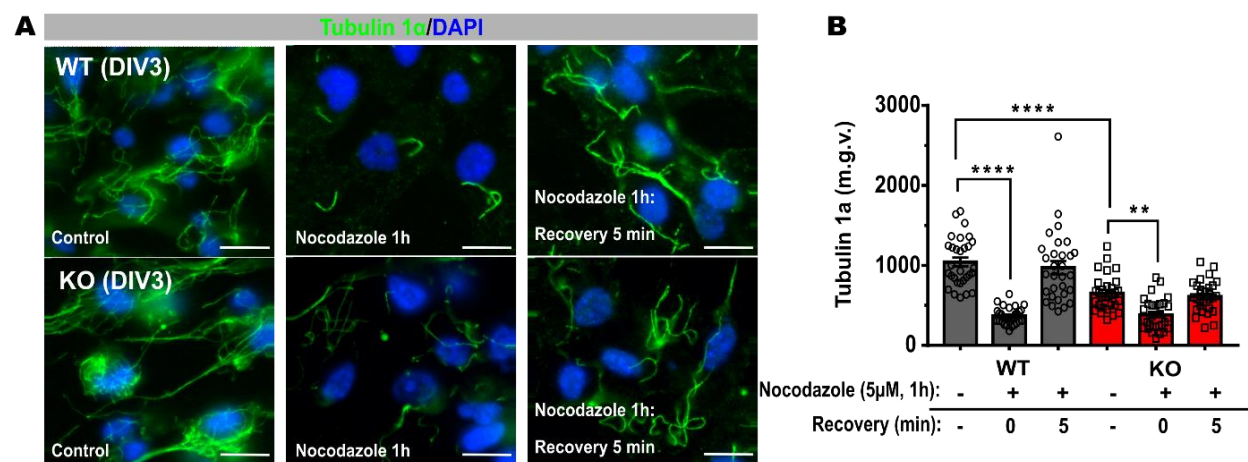


Figure 35. Microtubules are affected in AP-2 KO NPCs, but microtubule nucleation is not disrupted. (A) Representative figures of NPCs stained for Tubulin1 α (green). **(B)** Quantification of Tubulin1 α mean

grey value (m.g.v) relative to area in WT and KO NPCs. $WT^{Control}=1042$ $KO^{Control}=651.4\pm 68.98$ $WT^0=368.7$ $KO^0=381.0$ $WT^5=971.5$ $KO^5=608.3$. In total 30 per condition from $N=3$, in which each N is an independent cell culture obtained from independent animals. Scale bars: $5\mu M$. $**p<0.01$; $****p<0.0001$.

However, microtubule nucleation can happen independently of the centrosome, and a new method to study microtubule activity was required. To visualize its movement, NPCs were transfected with tdTomato-EB3, a protein that binds to microtubule caps. Strikingly, among KO NPCs, a population of cells presented a disorganized MTOC without any observable microtubule activity (Figure 36A-B), while other KO cells had regular MT activity (Figure 36C).

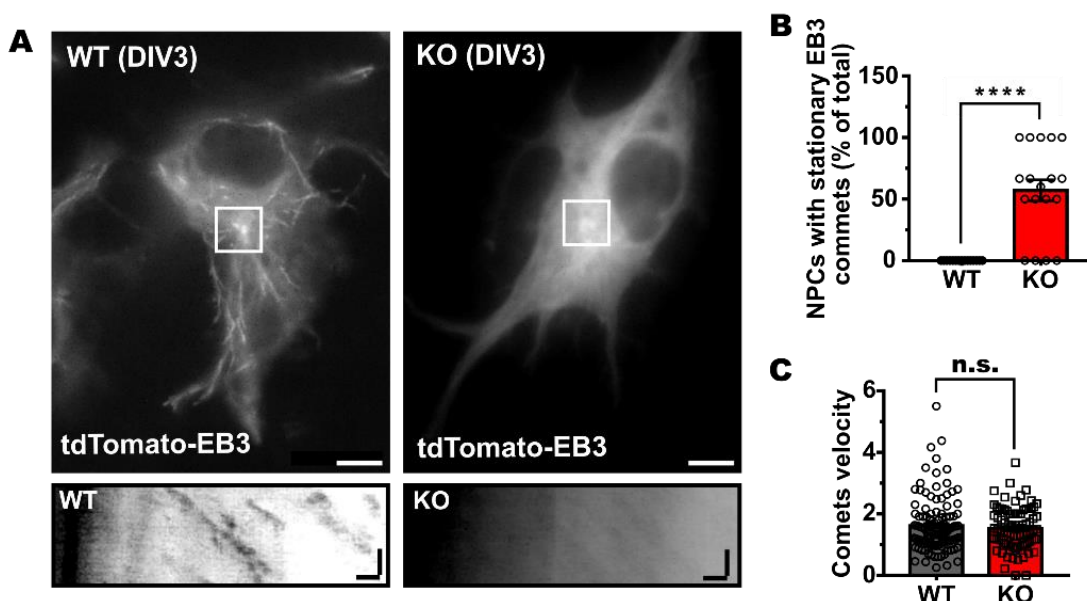


Figure 36. Microtubule activity is affected in AP-2 KO NPCs. (A) Maximum Intensity Projection of representative live-imaging videos of WT and KO NPCs transfected with Eb3TdTomoato (1-second frames in total 60 seconds). (B) Quantification of NPCs without microtubule activity out of total transfected cells. $WT=0.000\pm 0.000$ $KO=57.04\pm 8.636$. In total 15 WT and 18 KO, at least 10 cells per condition, from $N=3$, in which each N is an independent cell culture obtained from independent animals. (C) Quantification of comet velocity. $WT=1.614\pm 0.08126$ $KO=1.523\pm 0.07327$. In total 117 WT and 86 KO from $N=3$, in which each N is an independent cell culture obtained from independent animals. Scale bars: $5\mu M$. n.s. -non-significant; $****p<0.0001$.

In order to confirm if this phenotype was a centrosome-related function of AP-2 and to discard any primary cilia signaling role, experiments with astrocytes were performed to compare WT, AP-2 KO, and double KO (Ift88 and AP-2) effects in microtubule activity. As AP-2 KO NPCs, KO astrocytes present cells without microtubule activity (Figure 37A-B). Furthermore, as with the

proliferation defects, AP-2 lft88 KO astrocytes still present microtubule activity problems (Figure 37C-D).

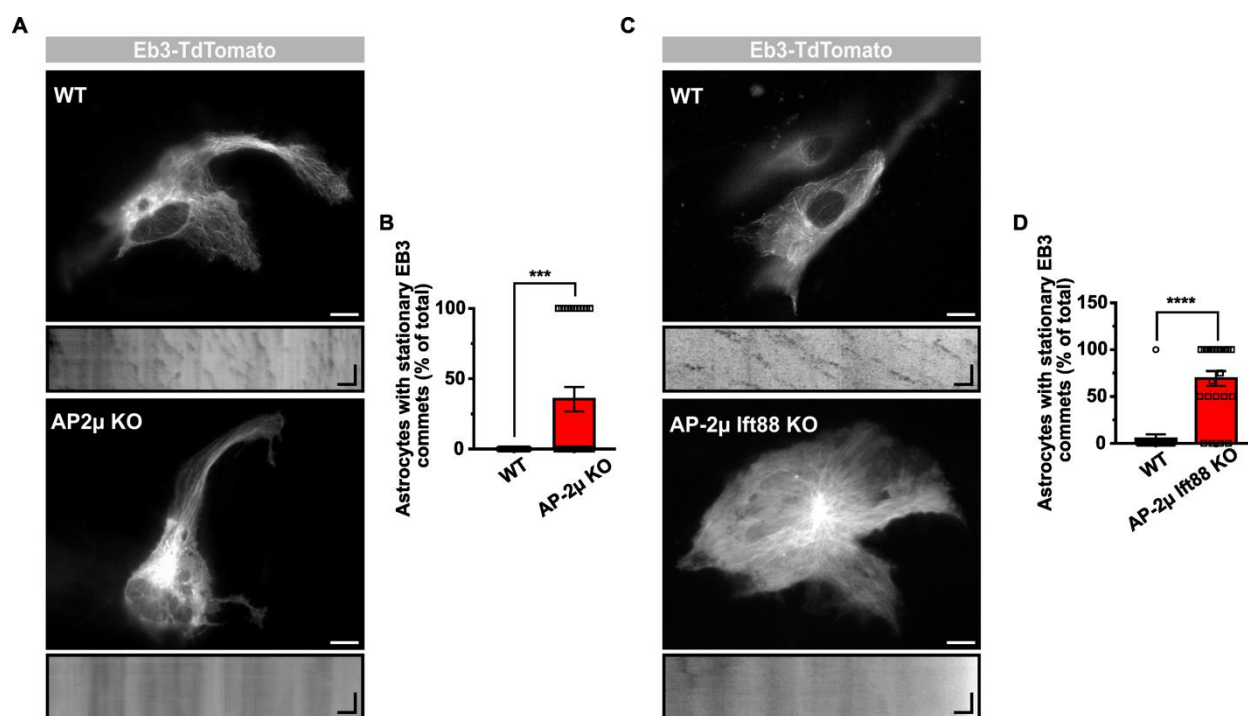
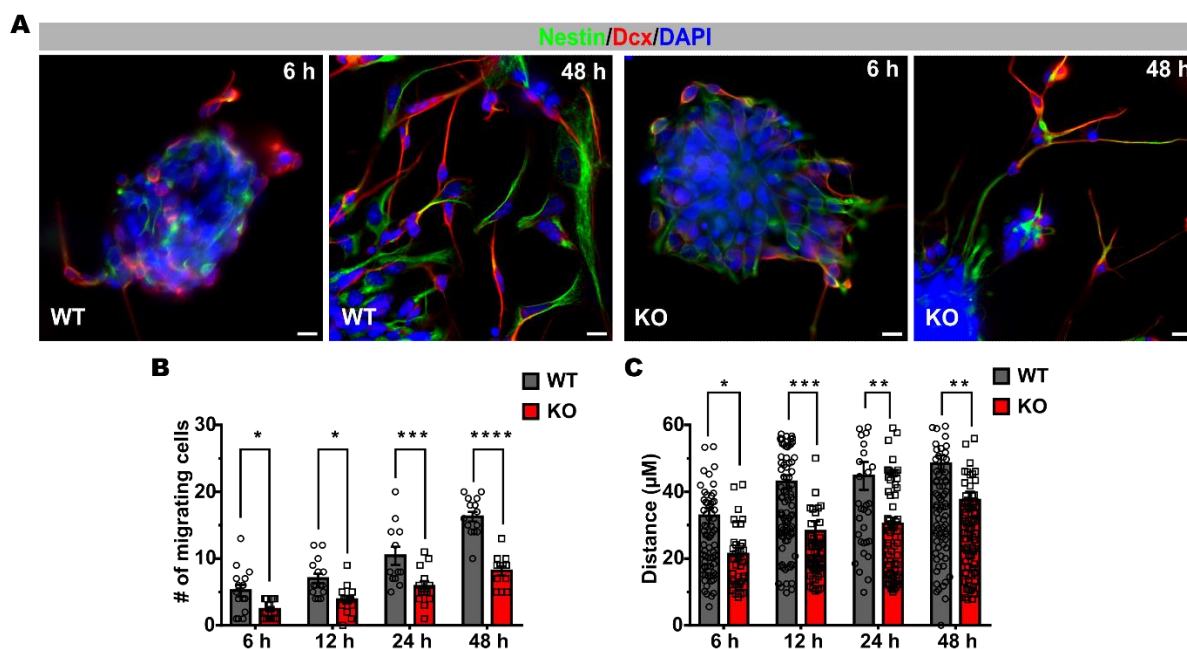


Figure 37. Microtubule activity is not rescued in AP-2+lft88 KO astrocytes. (A) Maximum Intensity Projection of representative live-imaging videos of WT and KO astrocytes transfected with Eb3TdTomato (1-second frames in total 60 seconds). **(B)** Quantification of astrocytes without microtubule activity out of total transfected cells. WT=0.000±0.000 KO=35.48±8.736. In total 27 WT and 31 KO, at least 10 cells per condition, from N=3, in which each N is an independent cell culture obtained from independent animals. **(C)** Maximum Intensity Projection of representative live-imaging videos of WT and double-KO astrocytes transfected with Eb3TdTomato (1-second frames in total 60 seconds). **(D)** Quantification of astrocytes without microtubule activity out of total transfected cells. WT=4.762±4.762 Ap2μ lft88 KO=69.20±8.005. In total 21 WT and 23 KO, at least 10 cells per condition, from N=3, in which each N is an independent cell culture obtained from independent animals. Scale bars: 5μM. ***-p<0.001; ****-p<0.0001.

Finally, another essential function of the centrosome and microtubules in NPCs is the migration of newborn neurons, and changes in them could affect the neurogenic ability of the NPCs. To analyze migration, a well-established method is the neurosphere migration assay, in which neurospheres are plated in Matrigel-coated coverslips, and the migration of neuroblasts from the sphere is observed after the withdrawal of growth factors to induce neuronal differentiation. Immunostaining was performed for nestin for undifferentiated NPCs and doublecortin (Dcx) for

differentiated neuroblasts. Compared with WT NPCs, KO cells presented reduced migrating cells exacerbated with time (Figure 38B) and the distance the cells migrated (Figure 38C).



In conclusion, despite AP-2 KO cell can nucleate de-novo microtubules, AP-2 deletion has severe consequences for microtubule activity in cells.

4. DISCUSSION

Research in the following thesis has provided strong evidence of a new moonlight role of AP-2 in the cell cycle and migration in neurogenesis. Moonlighting functions of endocytic proteins in the cell cycle is a widespread phenomenon within endocytic proteins (Royle, 2011; Yu *et al.*, 2021), so it is not surprising to find AP-2 involved; moreover, there is evidence in the literature of potential cell cycle involvement of AP-2 (Berdnik *et al.*, 2002; Blitzer & Nusse, 2006; Boucrot & Kirchhausen, 2007; Cayrol *et al.*, 2002; Olszewski *et al.*, 2014), although it was never fully confirmed. The novel interaction between γ -tubulin and AP-2 and its contribution to the cell cycle, centrosome structure, microtubule nucleation, and cell migration have been an exciting novel discovery. Loss of AP-2 in NPCs results in cell cycle arrest in G1 to S transition, centrosome disruption, mitotic defects, microtubule nucleating defects, and delayed migration. This results in p53-dependent activation of cell cycle checkpoints which will eventually induce caspase-2 mediated cell death, a process that is a characteristic hallmark of senescence. This effect of AP-2 is conserved in different cell types, and the bypass of p53-dependent signaling resulted in a phenotype rescue. However, despite the data pointing to the p53 pathway as the mechanisms involved in the cell cycle arrest observed, the role of AP-2 in the cell cycle has not been thoroughly studied. In the following sections, the main discoveries of this thesis will be discussed together with the potential hypotheses as to which roles AP-2 could have in the cell cycle.

4.1 AP-2 is essential for G1 to S transition, and AP-2 deletion results in cell cycle arrest

AP-2 deletion has been reported to be incompatible with life since deletion of AP-2 μ (Mitsunari *et al.*, 2005), deletion of AP-2 β (Li *et al.*, 2010), and AP-2 σ mutation (Gorvin *et al.*, 2017) results in embryonic lethality. Interestingly, the deletion of AP-2 μ results in lethality at E3.5 (Mitsunari *et al.*, 2005), a point at which the blastocyst is formed, a mass of highly dividing cells. Considering that AP-2 is required for cell cycle entry, this phenotype could be explained by severe cell cycle arrest during development. Previous works reported cell cycle arrest, with reduced cells in S and G2/M phase and multiple centrosomes in AP-2 KD MEFs (Olszewski *et al.*, 2014) and mitotic alteration in AP-2 KD BS-C-1 cells (Boucrot & Kirchhausen, 2007). On the other hand, the data of this thesis reported additionally loss of centrosome, DNA damage, and senescence activation, not reported in previous studies. The main difference between the model used in this thesis and other models

is that it is a full AP-2 deletion, while previous works used a KD approach. Hence, a decrease in AP-2 levels could be enough to produce an effect, but not enough to induce cell death.

Caspase-2 activation is also newly reported in AP-2 KO models. Interestingly Caspase-2 has a close relation with the cell cycle and the p53 pathway (Lim *et al.*, 2021). Cyclin D3 regulates G1 to S transition modulating E2F activation and Rb repression (Kato, 1999), but additionally, it stabilizes Caspase-2, promoting cell death (Mendelsohn *et al.*, 2002). Moreover, Caspase-2 phosphorylation by CDK1-Cyclin B1 inhibits caspase-2 to avoid cell death during mitosis (Andersen *et al.*, 2009; Castedo *et al.*, 2004). Although caspase-2 can be activated by mitotic failure, this process is p53-independent (Castedo *et al.*, 2004; Sidi *et al.*, 2008), confirming that AP-2-dependent cell cycle arrest is at the G1 to S transition. Interestingly, centrosome signaling is crucial for caspase-2 modulation, and it has been shown that centrosomal anomalies result in the activation of PIDDosome, which limits cell proliferation via the caspase-2-p53 axis (Burigotto *et al.*, 2021; Evans *et al.*, 2021). AP-2 defective centrosome could cause a caspase-2 and p53 activation, hence the cycle arrest. Another significant difference is the use of primary cells in this thesis; cell lines are created by telomerase reverse transcriptase (TERT) expression, mutations in cell cycle checkpoint proteins, or oncogene introduction (Maqsood *et al.*, 2013). Previous studies used cell lines as models, which would have an abnormal regulation of cell cycle checkpoints, disturbing senescence-related pathways. Moreover, AP-2 KO immortalized MEFs by SV40 transformation did not present a phenotype compared with AP-2 KO primary MEFs. SV40 transduction inactivates pRB, p53, and SEN6, which are crucial for G1-S transition (Hubbard & Ozer, 1999). For the same reason, since most of the research on AP-2 has been done in cell lines or neurons, it explains why such a strong phenotype has not been reported in more studies.

Another possibility of caspase-2 mediated arrest is in response to DNA damage since caspase-2 cleaves MDM2 removing the C-terminal RING domain, which is required for p53 ubiquitination (Oliver *et al.*, 2011). Evidence in the literature has pointed out that γ -tubulin is closely related to DNA repair and has been found to be localized at S-phase in the nucleus forming a complex with Rad51 (Hořejší *et al.*, 2012; Lesca *et al.*, 2005; Zhang *et al.*, 2007), AP-2 interaction with γ -tubulin could be essential for DNA damage repair, and AP-2 loss will induce accumulation of DNA damage.

On the other hand, AP-2 subunits are downregulated in gliomas (Buser *et al.*, 2019) which is surprising considering the data supporting AP-2 KO cell cycle arrest. Although endocytosis is

altered in cancer cells and could be that endocytic machinery is repurposed for cell cycle-related function exclusively, or as seen before in cell lines, cancer cells have different cell cycle mechanics than primary cells, and hence AP-2 function in cell cycle could not be crucial for cancer cells. Finally, preliminary data not included in the thesis in which primary NPCs were transfected to overexpress AP-2 μ did not change proliferation rates compared with control conditions.

4.2 AP-2 novel interactions with centrosomal components are vital for a proper centrosome structure and function.

Presented data showed an intense interaction between γ -tubulin components and AP-2, defective centrosomes, and increased ciliation. The confirmation of novel interaction partners for AP-2 was a surprising discovery previously not documented. However, there have been clues of the link between AP-2 and centrosome in the literature. Evidence was shown of AP-2 α localization to the centrosome by (Balestra *et al*, 2013), and more recently, using CEP63 as a centrosomal bait, AP-2- μ and AP-2 σ were found at the centrosome of hNSCs (O'Neill *et al*, 2022). Moreover, endocytic trafficking of centrosomal components has been described to modulate centriole duplication (Xie *et al*, 2018). Additionally, other endocytic proteins like ARH have been found to mediate microtubule nucleation by interaction with components of the γ -tubulin ring complex (Lehtonen *et al.*, 2008).

Data from the thesis goes in line with these observations since AP-2 was localized close to centrosomal proteins and AP-2 deletion severely affected centrosome structure. Interestingly clathrin has been found to participate in centrosome structural integrity in a CME-independent mechanism (Foraker *et al.*, 2012) and has been found at the centrosome in both mitosis and interphase (Yabuno *et al.*, 2019). Moreover, it is known to repurpose clathrin adaptor interaction sites for cycle-related functions (Rondelet *et al.*, 2020), which could liberate AP-2 to perform CME-independent functions at the centrosome both in interphase and mitosis. Additionally, AP-2 deletion severely affected localization and levels of centrosomal proteins localized at the PCM. PCM integrity contributes to centriole cohesion (Barrera *et al*, 2010; Cabral *et al*, 2013) and is where microtubule nucleation happens at the centrosome (Moritz *et al*, 1995). Moreover, PCM size changes depending on the γ -tubulin levels recruited to the centrosome becoming larger to support microtubule nucleation during mitosis (Khodjakov & Rieder, 1999; Robbins *et al*, 1968), which could explain PCM reduction and mitotic defects by decreased γ -tubulin levels at the

centrosome by loss of AP-2. However, the question remains whether AP-2 is essential for centrosome maturation during interphase, centrosomal nucleation of the mitotic spindle, or both.

The centrosome cycle is crucial for division in development. In the case of centrosomal loss, p53 is activated by delayed mitosis resulting in cell death (Lambrus *et al*, 2016; Meitinger *et al*, 2016; Phan *et al*, 2021). A significant population of AP-2 KO cells lacked centrosomes, and p-53 activation upon AP-2 loss could be the cause behind the cell death of AP-2 KO cells. Interestingly, another population of cells presented centrosome amplification, which induces p53-activated cell death (Dionne *et al*, 2018; Lizarraga *et al*, 2010; Marthiens *et al*, 2013). The presence of these two phenotypes could be because tamoxifen-induced KO used in an asynchronous population of cells will not ensure AP-2 deletion at the same point in the cycle. Hence, AP-2 could have different functions while progressing through the cell cycle. Additionally, AP-2 KO cells present severe mitotic defects, possibly because of a defective centrosome. This will be discussed in detail in section 4.3.

Future studies might benefit from using primary MEFs, which can be synchronized to have a homogenous population and a deletion of AP-2 at different point of the cycle to find what AP-2 does at each point of the cell cycle.

The different hypotheses of AP-2 role at the centrosome will be discussed later in section 4.5.

4.3 AP-2 KO defective centrosomes have physiological effects on microtubule activity and cell migration.

It has been previously established that a link between AP-2 and microtubules exist, with alpha-tubulin acetyltransferase (α TAT), localized to CCP by direct interaction with AP-2 α , and KD of either α TAT or AP-2 α is enough to reduce cell migration. However, KD of CHC is not enough for migration reduction (Montagnac *et al*, 2013). As previously discussed, the interaction of AP-2 with components of the γ -tubulin ring complex is essential for centrosome structure and microtubule nucleation activity. However, several cases have been reported that in the absence of centrosomes or specific centrosomal proteins, several components of the PCM can cluster together to perform acentrosomal microtubule nucleation (Balestra *et al*, 2021; Chen *et al*, 2022; Chinen *et al*, 2021; Gartenmann *et al*, 2020; Meitinger *et al*, 2020; Watanabe *et al*, 2020; Yeow *et al*, 2020); however, microtubule density is significantly reduced and is sensitive to rearrangement of the cytoskeleton. This spontaneous clustering of PCM components could

explain why AP-2 KO cells can nucleate microtubules de novo after nocodazole treatment and why the mitotic spindle is formed despite being severely affected. Interestingly this is a common phenomenon in differentiated cells (Muroyama & Lechler, 2017; Muroyama *et al.*, 2016; Sallee & Feldman, 2021) which could mean that the AP-2 effect in microtubule nucleation could be more robust in undifferentiated than in fully differentiated cells, although similar disruption of microtubule activity was observed in AP-2 KO NPCs and Astrocytes. Further research should be done to confirm or reject this hypothesis.

Microtubule activity is crucial during mitosis, especially the formation of a bipolar mitotic spindle to ensure the correct division into two daughter cells (Vicente & Wordeman, 2015). As we discussed before, defective centrosome-dependent microtubule activity could be the cause behind the mitotic phenotypes observed in AP-2 KO NPCs. Microtubule nucleation can happen in the absence of centrosomes, as discussed above (Balestra *et al.*, 2021; Chen *et al.*, 2022; Chinen *et al.*, 2021; Gartenmann *et al.*, 2020; Meitinger *et al.*, 2020; Watanabe *et al.*, 2020; Yeow *et al.*, 2020), moreover, even mitotic spindle formation can happen without centrosomes involvement (Carazo-Salas *et al.*, 1999; Meunier & Vernos, 2012, 2016; Moutinho-Pereira *et al.*, 2013). However, mitosis in the absence of a centrosome will not ensure an error less division and hence could result from higher chromosomal instability (Sir *et al.*, 2013). AP-2 KO cells can form spindles, which could be formed acentrosomally, and these spindles show defects such as non-characteristic polar morphology or unstable microtubules. Moreover, the presence of chromatin bridges could cause the DNA-damage increase observed. These results support centrosome importance for a correct mitosis, but also that mitotic spindle formation can happen without centrosomes.

The endocytic role of migration has been previously reported by modulating cell adhesion proteins (Chao & Kunz, 2009; Ezratty *et al.*, 2009; Shieh *et al.*, 2011). Specifically, endocytosis by AP-2 of other proteins necessary for cell adhesion was shown to be crucial for migration (Kamiguchi & Yoshihara, 2001). Moreover, AP-2 binds directly with NUMB (Berdnik *et al.*, 2002; Santolini *et al.*, 2000), a protein crucial in cell adhesion and migration, and Integrin turnover, a cell adhesion molecule important for microtubule-mediated migration, was founded to be modulated by AP-2 α (De Franceschi *et al.*, 2016). Additionally, AP-2 has been found to bind to Dcx (Yap *et al.*, 2018), an essential microtubule-associated protein required for newborn neuron migration. This adds complexity to the already potential roles of AP-2 since it is not only crucial for the cell cycle but also for migration, possible by endocytic-dependent mechanism (such availability of adhesion

proteins) or independent of CME (centrosomal/microtubule-related functions. Preliminary data in vivo (not included in this thesis) have shown that the AP-2 KO effect in the centrosome, microtubules, and migration is conserved in vivo by an accumulation of Dcx positive cells in the lateral ventricle of the sub-ventricular zone and cortex layering disruption. However, AP-2 in vivo contribution has not been studied in detail. In vivo experiments using a more suitable model or ex-vivo 3D cultures (such as organotypic cultures or organoids) could shed light on the AP-2 effect in the brain structure or adult neurogenesis.

Centrosomal microtubules are necessary for proper centrosome-nucleus coupling, which is essential for nuclear migration and neuronal migration (Tanaka *et al.*, 2004; Tsai & Gleeson, 2005). Although some studies showed that migration could happen via centrosome-unattached microtubules (Schaar & McConnell, 2005; Umeshima *et al.*, 2007), microtubule-centrosome attachment is the main contributor to neuronal migration (Rao *et al.*, 2016). AP-2 defective centrosome could severely impact microtubule-centrosome coupling and results in migration delays.

Finally, it is worth mentioning that primary cilia have been linked to the modulation of migration of neuroblasts and neurons, and ciliary gene depletion resulted in altered migration (Anvarian *et al.*, 2019; Baudoin *et al.*, 2012; Guo *et al.*, 2015; Higginbotham *et al.*, 2012; Matsumoto *et al.*, 2019; R Ferreira *et al.*, 2019; Stoufflet *et al.*, 2020; Wheway *et al.*, 2018). Even though increased ciliogenesis is not the cause of cell cycle arrest, it could be possible that these altered cilia will affect signaling to direct neuronal migration.

4.4 AP-2 role in centrosome and cell division is independent of CME.

PitStop2 inhibition of CME showed mitotic alterations, apoptosis, and centrosome fragmentation (Boucrot & Kirchhausen, 2007; Smith *et al.*, 2013); a similar phenotype was found by RNAi KD of CHC resulting in many mitotic defects, including the instability of kinetochore fibers, continuous activation of the SAC, and errors in chromosome segregation (Royle *et al.*, 2005). Strikingly, PitStop2 treatment in primary NPCs did not reproduce any phenotype reported in the literature nor from AP-2 KO NPCs. Interestingly, mutations of CHC in *Drosophila* result in lethality in larval stages and infertility (Bazinet *et al.*, 1993), which contrast with the severe developmental embryonic phenotypes of AP-2 subunits KOs (Gorvin *et al.*, 2017; Li *et al.*, 2010; Mitsunari *et al.*, 2005).

On the other hand, the phenotypes reported in the literature are completely different from the AP-2 KO phenotype of this thesis. Firstly, this thesis reported a cell cycle arrest at the G1/S transition showing a reduction of mitotic cells, while PitStop2 treatment in the literature increases the proportion of mitotic cells due to mitotic arrest by SAC activation. Another difference between the literature and the thesis results is that PitStop2 treatment induces Caspase-3 mediated cell death, which is not upregulated in this thesis KO, which has Caspase-2-dependent cell death. CME downregulation on mitosis has been widely reported in the literature (Berlin & Oliver, 1980; Boucrot & Kirchhausen, 2007; Fielding & Royle, 2013; Fielding *et al.*, 2012; Koppel *et al.*, 1982; Sager *et al.*, 1984), and, as discussed in previous sections, clathrin adaptor interaction sites are repurposed for clathrin cell cycle functions (Rondelet *et al.*, 2020). This supports that AP-2 role in the cell cycle is independent of clathrin, and each molecule will have its own functions. Moreover, the clathrin role seems to be restricted exclusively to centrosomal microtubule nucleation, and while AP-2 is also crucial for microtubule nucleation, its role seems to be more critical for centrosome structure and stability.

However, it is challenging to study CME machinery since KO for clathrin or AP-2 resulted in lethal phenotypes. Additionally, because AP-2 is indispensable for CME, it is complicated to determine whether functions are dependent on AP-2 or because of clathrin loss. For this purpose, a new *in vivo* model was developed in our lab by deleting the AP-2 α subunit via Crispr-Cas9. Unfortunately, there was no observable KO phenotype in development nor in primary cell cultures obtained from this animal. There is the possibility that when AP-2 subunits are deleted, compensatory mechanisms arise from other complex subunits to maintain such an essential function, in contrast with the complete deletion of the AP-2 complex by AP-2 μ deletion. Further studies have to be done to determine such a phenotypical difference.

4.5 Possible hypothesis

Despite the strong evidence of AP-2 implication in the centrosome assembly, the question of what AP-2 does in cell division and how does affects neurogenesis and other cycling cells is still open. Additionally, as we see before, endocytic proteins such as clathrin have different functions at different cycle stages, the same case could be for AP-2, and some of these hypotheses could coexist.

Several hypotheses explaining how the observed phenotype could be produced will be discussed in detail, supported by the experimental data and the literature.

4.5.1 AP-2 traffics γ -Tubulin components to the centrosome from the basal body in the plasma membrane.

Cilia KO experiments did not rescue the centrosomal and cell cycle phenotype of AP-2 KO cells, which was a clear indication that there was no effect in signaling from the cilia. However, even without cilia, if AP-2 is not present, there will still not be a proper centrosome maturation and cell cycle progression. AP-2 is localized to the plasma membrane during CME (Kirchhausen, 1999; Owen *et al.*, 2004), and it has been shown to be able to traffic different proteins either capitalizing on endocytic machinery or independent of clathrin. In addition, there is strong evidence in the literature that endocytosis is inhibited during cell division (Berlin & Oliver, 1980; Boucrot & Kirchhausen, 2007; Fielding & Royle, 2013; Fielding *et al.*, 2012; Koppel *et al.*, 1982; Sager *et al.*, 1984) which explains why moonlighting is so common in endocytic protein during the cell cycle (Royle, 2011; Yu *et al.*, 2021). With endocytosis reduced, AP-2 will be free to do other functions independent of clathrin. γ -tubulin proteins are present at the basal body of the cilia, and, with cilia disassembly, these proteins will bind to AP-2 and transport to the centrosome to commence centrosome formation. Despite evidence of movement of AP-2 μ puncta towards the centrosome, it is not sufficient to fully claim this hypothesis, and technical limitations did not allow the visualization of AP-2 trafficking. Further experiments should be done to corroborate this hypothesis.

4.5.2 AP-2 helps stabilize the centrosome structure binding to γ -Tubulin components

Another possible hypothesis, considering evidence from the previous section, is that AP-2 is a stabilizing complex that keeps the centrosomal structure stable. The literature showed that AP-2 KD is enough for centrosome overamplification (Balestra *et al.*, 2013; Olszewski *et al.*, 2014). Moreover, clathrin is already required at the S-phase at the centrosome for microtubule stabilization (Cheeseman *et al.*, 2013; Foraker *et al.*, 2012), and clathrin-dependent microtubule stabilization requires to repurpose of the adaptor binding sites of clathrin (Rondelet *et al.*, 2020). This hypothesis is compatible with the previous one since it will happen in a sequential mode; firstly AP-2 will traffic components to the centrosome and afterwards it will help to keep the cohesion between these proteins. For this reason, without AP-2 not only proteins do not reach the centrosome, even with a compensatory mechanism, centrosome structure will be unstable and hence compromised, as observed in the results.

4.5.3 AP-2 binding to γ -Tubulin components at the centrosome is necessary for spindle formation

Clathrin localization at the mitotic spindle was reported two decades ago (Okamoto *et al.*, 2000), and since then, several papers have studied the depth of its contribution to mitosis (Booth *et al.*, 2011; Cheeseman *et al.*, 2013; Foraker *et al.*, 2012; Fu *et al.*, 2010; Hood & Royle, 2009; Lin *et al.*, 2010; Rondelet *et al.*, 2020; Royle, 2012; Royle *et al.*, 2005; Royle & Lagnado, 2006; Smith *et al.*, 2013; Yabuno *et al.*, 2019). In addition, several endocytic proteins are linked to centrosome and microtubule activity (Lehtonen *et al.*, 2008; Thompson *et al.*, 2004). Finally, also considering that endocytosis is downregulated during mitosis (Berlin & Oliver, 1980; Boucrot & Kirchhausen, 2007; Fielding & Royle, 2013; Fielding *et al.*, 2012; Koppel *et al.*, 1982; Sager *et al.*, 1984), and repurposing of clathrin adaptor binding sites (Rondelet *et al.*, 2020) opens the possibility that AP-2 interaction with the γ -tubulin complex proteins will be the basis for the nucleation of the mitotic spindle and microtubule cohesion to the kinetochore. Mitotic failure will result in senescence-associated cell death and the loss of cycling cells that was observed. This phenotype could also complement the two previous one suggesting several functions of AP-2 which will change in different cycle phases.

4.5.4 AP-2 mediates local protein translation at the centrosome

Although the interaction between AP-2 and γ -Tubulin components is solid, evidence in the literature shows that microtubule-related functions are not enough to explain such a stark effect in the cycle (Insolera *et al.*, 2014). Traditionally, the centrosome has been considered a microtubule organizing center, but in the last decades, evidence points to a much more exciting function of the centrosome, instead as a signaling hub and control center of the cell cycle (Arquint *et al.*, 2014; Doxsey *et al.*, 2005). Different RNA-binding proteins, ribosomes, and translation initiation factors are localized to the centrosome and implicated in PCM maintenance or other centrosome functions (Zein-Sabatto & Lerit, 2021). Moreover, some have been found even to segregate asymmetrically, conditioning cell fate determination (Kusek *et al.*, 2012). Taking this all together, it could be hypothesized that RNAs are responsible for the centrosome's complex role in the cell cycle outside of its MTOC-related roles. Interestingly, within the proteomics results in section 3.2 and the mass spectrometry results in section 3.5, several affected pathways necessary for RNA binding and metabolism and some enriched RNA-binding proteins or ribosomal proteins what could be potential interaction partners of AP-2. However, this is not enough evidence and further research should be done. This hypothesis despite not been due to

γ -tubulin complex proteins interaction could still overlap with these functions, suggesting that apart from γ -tubulin complex proteins transport to the centrosome, it could be local protein synthesis that will be RNA-dependent, proteins that will need to be stabilize in order to keep a centrosomal structure which will be required for microtubule nucleation.

4.5.5 AP-2 acts at the transcriptional level in the nucleus

Evidence in the literature has pointed to the roles of γ -tubulin in gene expression at the nucleus important for the G1 to S transition (Ehlén *et al*, 2012; Höög *et al*, 2011). Additionally, it has been reported that γ -tubulin is closely related to DNA repair and has been found to be localized at S-phase in the nucleus forming a complex with Rad51 (Hořejší *et al.*, 2012; Lesca *et al.*, 2005; Zhang *et al.*, 2007). AP-2 interaction with γ -tubulin might be crucial to modulate DNA repair mechanisms and gene expression in the early phases of the cell cycle. Despite the lack of evidence of AP-2 having a NLS in the literature still could act in two ways to modulate nuclear activity, firstly, shuttling γ -tubulin from the plasma membrane to the nuclear membrane enhancing gene expression or to activate DNA repair and secondly, inhibiting it by sequestering γ -tubulin in the cytoplasm. However, despite the literature evidence for that, no experimental data support the hypothesis, except the observed phenotype, and the increased DNA damage could be the cause of centrosomal defects rather than a consequence. Interestingly, this could also coexist with previous hypothesis since it is happening at the early onset of the cell cycle, even before centrosome formation.

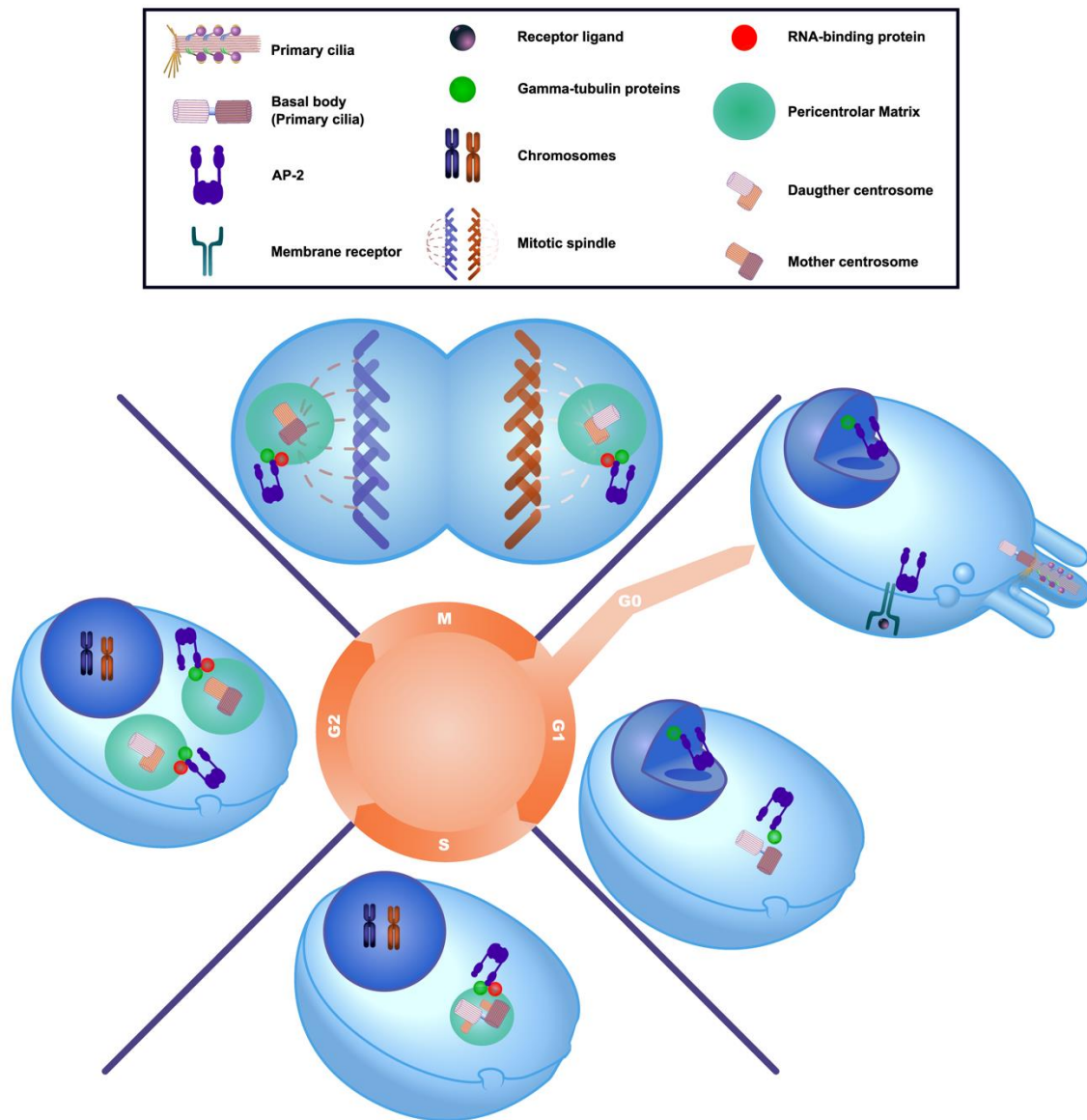


Figure 39. Graphic representation of potential AP-2 roles in cell cycle. AP-2 potential roles are tightly related to the centrosome cycle. At the onset of the cell cycle it will shuttle γ -tubulin complex proteins from the PM, which will allow the maturation of the centrosome. During this process they will support structure stability and/or local protein synthesis, which will ensure a correct microtubule activity during mitosis to form the bipolar mitotic spindle. Another possibility is the modulation of γ -tubulin activity in gene expression at the nucleus at the beginning of the cycle.

5. CONCLUDING REMARKS AND DIRECTIONS FOR FUTURE WORK

The work performed in the frame of this doctoral dissertation aimed: (I) what is the contribution of AP-2 to the cell cycle; (II) is this function dependent or independent of clathrin; (III) has AP-2 a critical role not only in the cell cycle but in other processes involved in neurodevelopment. During the development of this thesis, the following key findings have been revealed:

1. AP-2 deletion results in cell cycle arrest at the G1 to S transition. This result is supported by previously observed arrest by (Olszewski *et al.*, 2014) and could be the cause of severe embryonic lethality in AP-2 KO models (Gorvin *et al.*, 2017; Li *et al.*, 2010; Mitsunari *et al.*, 2005). In contrast with the literature, AP-2 KO also presented an increase in senescence-associated cell death by activating the caspase2-p53 axis and DNA-damage. This contrasts with previous works; however, AP-2 studies have been done in cell lines, which usually have mutations in cell cycle checkpoints (Maqsood *et al.*, 2013). In line with this, immortalization of MEFs by SV40 transformation rescue the AP-2 KO phenotype, interestingly SV40 transduction inactivates pRB, p53, and SEN6, which are crucial for G1-S transition (Hubbard & Ozer, 1999). These observations invite us to reconsider the use of cell lines in cell cycle studies and to study why oncogenes expression or tumorigenesis can bypass AP-2 role in cell cycle control quality.
2. AP-2 α interacts strongly with γ -tubulin complex proteins. Despite the novelty of the discovery, AP-2 localization at the centrosome was previously reported (Balestra *et al.*, 2013; O'Neill *et al.*, 2022), and ARH, and endocytic protein, have been found to bind to components of the γ -tubulin ring complex (Lehtonen *et al.*, 2008). AP-2 deletion resulted in severe centrosome structural defects, centrosome amplification, and centrosome loss, confirming an essential contribution of AP-2 to centrosome functioning. Specifically, loss of PCM integrity could be the consequence of mitotic phenotypes observed, but how AP-2 contributes to PCM, either in its assembly during interphase or during microtubule nucleation in mitosis, has still to be elucidated. Previously reported p53-caspase-2 axis activation could be because of defective centrosomes since centrosome anomalies, either by amplification or deletion, result in different pathways, which both end in p53-dependent activation of caspase-2 (Dionne *et al.*, 2018; Lambrus *et al.*, 2016; Lizarraga *et al.*, 2010; Marthiens *et al.*, 2013; Meitinger *et al.*, 2016; Phan *et al.*, 2021). Finally, it is worth mentioning that tamoxifen treatment for and induced KO in a population of asynchronous cells could result in AP-2 loss at different cell cycle points, which could explain the

heterogeneous phenotype. Future studies could benefit from the use of cells that can be synchronized, such as MEFs.

3. AP-2 KO defective centrosomes result in impaired microtubule activity. and cell migration. This thesis reported defects in mitotic spindle and microtubule activity in AP-2 KO cells and previous observations of disruption of centrosomal structures important for microtubule activity. However, microtubule nucleation can happen independently of centrosomes by PCM components assembly (Balestra *et al.*, 2021; Chen *et al.*, 2022; Chinen *et al.*, 2021; Gartenmann *et al.*, 2020; Meitinger *et al.*, 2020; Watanabe *et al.*, 2020; Yeow *et al.*, 2020), what could explain why microtubule activity is affected, but not de novo microtubule nucleation. Additionally, acentrosomal microtubule nucleation could explain why spindles are formed in AP-2 KO cells during mitosis (Carazo-Salas *et al.*, 1999; Meunier & Vernos, 2012, 2016; Moutinho-Pereira *et al.*, 2013), however mitosis in the absence of centrosome is prone to genomic instability (Sir *et al.*, 2013). Finally, migration has been found to be impacted by a decrease in migrating cells and migrating distance. However, the involvement of AP-2 in several processes important for migration opens the question if this effect is because of centrosomal-defective microtubule dynamics reported in this thesis or previous functions, pointing to several potential functions of AP-2 along the cell cycle and neurogenesis progress.
4. AP-2 role in centrosome and cell division was founded to be independent of CME. PitStop2 did not produce and observable phenotype in comparison with AP-2 KO cells. This contrast with the literature since PitStop2 treatment produces a phenotype in previous works (Boucrot & Kirchhausen, 2007; Royle *et al.*, 2005; Smith *et al.*, 2013). This thesis hypothesis is supported by the fact that phenotypes reported in the literature are completely different from the AP-2 KO phenotype of this thesis, with PitStop2 phenotypes being mostly mitotic related and cell death via caspase-3, and AP-2 KO having an impact additionally in centrosomes and arrest in G1 to S transition (rather than the SAC arrest of PitStop2 treated cells) and has caspase-2-dependent cell death. Moreover repurpose of clathrin adaptor binding sites during mitosis (Rondelet *et al.*, 2020) and CME downregulation on mitosis (Berlin & Oliver, 1980; Boucrot & Kirchhausen, 2007; Fielding & Royle, 2013; Fielding *et al.*, 2012; Koppel *et al.*, 1982; Sager *et al.*, 1984), further support this hypothesis, suggesting a repurpose of endocytic machinery during the cell cycle with different and overlapping functions.

5. Finally, several hypotheses have been proposed for the role of AP-2 during the cycle. The strong interaction with components of the γ -tubulin ring complex suggests a role of AP-2 in centrosome recruitment of proteins, centrosomal stabilization, and mitotic microtubule nucleation. This function could coexist since they will happen at different cycle phases. Another interesting hypothesis is that AP-2 binding with components of the γ -tubulin ring complex will mediate its location to the centrosome to mediate local protein translation since it has been founded that interaction partners important for RNA binding and several pathways related to RNA metabolism affected in AP-2 KO NPCs. Finally, another likely hypothesis is that AP-2 modulates γ -tubulin presence in the nucleus at the onset of the cell cycle to enhance gene expression or to activate DNA repair.

6. MATERIALS AND METHODS

6.1 Materials

6.1.1 General laboratory equipment

<i>Instrument</i>	<i>Manufacturer</i>	<i>Identifier</i>
<i>Cabinet, Horizontal laminar flow</i>	Thermo Fisher Scientific	Heraguard ECO
<i>Cabinet, vertical laminar flow (primary cells)</i>	Thermo Fisher Scientific	Safe 2020
<i>Centrifuges</i>	Eppendorf Hettich VWR	5702R 320R MicroSTAR 17R
<i>Electrophoresis Power Source</i>	VWR	300V
<i>Electrophoresis chamber (PCR)</i>	VWR	700-0569
<i>Electrophoresis chamber (WB)</i>	Bio-Rad	Mini-Protean Tetra Cell
<i>Dissection tools</i> <i>Forceps</i> <i>Scissors</i> <i>Scalpel</i>	FST	11253-27 16020-14 11270-20 14090-09 13002-10 14002-13 10073-14
<i>Freezer (-20°C)</i>	LIEBHERR	9988187-12
<i>Fridge (4°C)</i>	LIEBHERR	9983491-10
<i>Gel imager system (PCRs)</i>	Bio-Rad	Gel Doc™ XR+
<i>Incubator CO₂</i>	Eppendorf	Galaxy 1705
<i>Incubator Shaker</i>	Eppendorf	M1335-0002
<i>Microscope, inverted (cell culture)</i>	Leica	Leica DMI1
<i>Microscope, inverted fluorescence</i> Camera Temperature module LED Light source Software	Zeiss Hamamatsu Zeiss CoolLED Micro-Manager	Axiovert 200M C11440 TempMoudleS pE-4000 MicroManager1.4

Objectives: 40x/1.4 oil DIC 63x/1.4 oil	Zeiss Zeiss	420762-9900 420780-9900
<i>Microscope, inverted confocal</i> Camera Detector Software Objectives: 40x/0.85 63x/1.20	Leica Leica Leica Leica Leica Leica	TCS SP8 HyVolution 2 4 HyD's, 1 PMT LAS X Apo CORR CS PL APO W motCORR CS2
<i>Microscope, stereo (dissection)</i>	Leica	Leica M80
<i>Microwave</i>	Inverter	Sharp
<i>Neubauer chamber</i>	Marienfeld	0640110
<i>Osmometer</i>	Gonotec	Osmomat 3000
<i>pH-meter</i>	Mettler Toledo	Seven Easy
<i>Photometer</i>	Eppendorf	Bio Photometer plus
<i>Sonicator</i>	BRANSON	Sonifier 250
<i>Scales</i>	OHAUS VWR	EX225D T1502746
<i>Thermocycler</i>	VWR	peqSTAR
<i>Thermoshaker</i>	CellMedia	Thermomixer basic
<i>Water bath</i>	VWR	VWB6
<i>Vortex</i>	Scientific Industries	Vortex-Genie 2

6.1.2 Chemicals

<i>Chemical</i>	<i>Manufacturer</i>	<i>Identifier</i>
<i>2-β-Mercaptoethanol</i>	Roth	4227.1
<i>2-Propanol</i>	Roth	CP41.3
<i>Acetic acid 100%</i>	Roth	3738.4
<i>Acetone</i>	Roth	5025.1
<i>Ammonium chloride</i>	Roth	K298.2
<i>Ammonium peroxodisulfate (APS)</i>	Merck	1.012.001.000

<i>Ampicillin sodium salt</i>	Roth	K029.2
<i>Boric acid</i>	VWR	J67202
<i>Bovine Serum Albumin</i>	Sigma	A7906
<i>Bromophenol blue</i>	Sigma	B5525
<i>Calcium chloride dihydrate</i>	Roth	5239.2
<i>Calcium chloride hexahydrate</i>	Roth	T886.1
<i>Cresyl violet acetate</i>	Sigma	C5042
<i>D-(+)-Glucose</i>	Sigma	G5767
<i>D-Mannitol</i>	Sigma	M4125
<i>Digitonin</i>	Roth	4005.1
<i>Dimethyl sulfoxide (DMSO)</i>	Roth	A994.2
<i>di-Potassium hydrogen phosphate</i>	Roth	6875.1
<i>di-Sodium hydrogen phosphate dihydrate</i>	Roth	4984.1
<i>di-Sodium hydrogen phosphate anhydrous</i>	Merck	106559
<i>EDTA</i>	AppliChem	A1104.1000
<i>EGTA</i>	Roth	3054.2
<i>Ethanol</i>	Omnilabs	A1613.2500PE
<i>Gelatin from porcine skin</i>	Sigma	G2500
<i>Glycerol</i>	Roth	7530.1
<i>Glycine</i>	Roth	3908.3
<i>HEPES</i>	Sigma	H4034
<i>Hydrochloric acid 32%</i>	Roth	X896.2
<i>IGEPAL</i>	Sigma	I8896
<i>Kanamycinsulfat</i>	Roth	T832
<i>LB-Agar (Lennox)</i>	Roth	X965.2
<i>LB-Medium (Lennox)</i>	Roth	X964.2
<i>Luminol</i>	Roth	4203.1
<i>Magnesium chloride hexahydrate</i>	Roth	2189.1
<i>Magnesium sulfate heptahydrate</i>	Roth	P027.2
<i>Methanol</i>	Roth	4627.5

<i>Milk powder</i>	Roth	T145.2
<i>Normal Goat Serum (NGS)</i>	Thermo Fisher Sci	16210064
<i>Paraformaldehyde (PFA)</i>	Merck	104.005.100
<i>p-coumaric acid</i>	Sigma	C9008
<i>Phenol red</i>	Sigma	P3532
<i>PIPES</i>	Sigma	P8203
<i>Ponceau S</i>	Roth	5938.1
<i>Potassium acetate</i>	Roth	T874.1
<i>Potassium chloride</i>	Roth	6781.1
<i>Potassium dihydrogen phosphate</i>	Roth	3904.1
<i>Potassium disulfite</i>	Sigma	60508
<i>Potassium hypochlorid</i>	Carl Roth	9062.3
<i>Saponin</i>	Serva	34655
<i>Sodium chloride</i>	Roth	3957.1
<i>Sodium hydrogen carbonate</i>	Roth	6885.1
<i>Sodium hydroxide</i>	Roth	6771.1
<i>Sodium dodecyl sulfate (SDS) ultra-pure</i>	Roth	2326.2
<i>Sodium tetraborate</i>	VWR	1303964
<i>Sucrose</i>	Sigma	S0389
<i>Tetramethylenediamine (TEMED)</i>	AppliChem	A1148.0028
<i>Tris (hydrogenmethyl) aminomethane (Tris-base)</i>	VWR	28.808.294
<i>Trizma hydrochloride (Tris-HCl)</i>	Sigma	T3253
<i>Trypan blue</i>	Roth	CN76.1
<i>Tween 20</i>	VWR	663684B

6.1.3 Reagents

6.1.3.1 Reagents for molecular biology

<i>Reagent</i>	<i>Manufacturer</i>	<i>Identifier</i>
<i>Acryl/BisTM solution (30%) 37.5:1</i>	VWR	E347
<i>Bradford Reagent</i>	Sigma	B6916
<i>Complete Mini Protease Inhibitor</i>	Roche	11836153001
<i>DNA ladder (100 bp/ 1 kb)</i>	Thermo Fisher Sci	SM0323/SM0311
<i>DNA Gel Loading Dye (6X)</i>	Thermo Fisher Sci	R0611
<i>DreamTaq DNA polymerase</i>	Thermo Fisher Sci	EP0703
<i>ECLTM WB detection reagents</i>	GE Healthcare	RPN2106
<i>Normal Goat Serum</i>	Gibco	16210064
<i>Nuclease-free water</i>	Ambion	AM9938
<i>PageRuler Plus Prestained Prot. Ladder</i>	Thermo Fisher Sci	26619
<i>PierceTM Protease and phosphatase inhibitor mini tablets</i>	Thermo Fisher Sci	A32959
<i>SYBR Safe DNA Gel Stain</i>	Thermo Fisher Sci	S33102

6.1.3.2 Cell culture media and reagents

<i>Reagent</i>	<i>Manufacturer</i>	<i>Identifier</i>
<i>Accutase</i>	Sigma	SCR005
<i>B-27 Supplement (50X)</i>	Thermo Fisher Sci	17504-044
<i>Recombinant Human Basic Fibroblast Growth Factor (FGF)</i>	Thermo Fischer Sci	13256-029
<i>Conconamycin A</i>	Sigma	C9705
<i>BDNF</i>	Almone	DE2457539
<i>Cytosine β-D-arabinofuranpsode hydrochloride</i>	Sigma	C6645
<i>DMEM (1X)+GlutaMAXTM</i>	Thermo Fisher Sci	31966-021
<i>DMEM/F-12(1.1) (1X)+GlutaMAXTM</i>	Thermo Fisher Sci	31331-028

<i>Deoxyribonuclease I from bovine pancreas</i>	Sigma	D5025
<i>EBSS</i>	Thermo Fisher Sci	14155-048
<i>Recombinant Human Epidermal Growth Factor (EGF)</i>	Thermo Fisher Sci	PHG0315
<i>Fetal Bovine Serum</i>	Merck	S0115
<i>Fetal Bovine Serum (sterile filtered) (FBS)</i>	Sigma	F7524
<i>GlutaMAX™</i>	Thermo Fisher Sci	35050-061
<i>HBSS (1X) [-] CaCl₂, [-] MgCl₂</i>	Thermo Fisher Sci	14175-053
<i>HEPES (1M)</i>	Thermo Fisher Sci	15630-080
<i>Insulin, human recombinant zinc</i>	Thermo Fisher Sci	12585-014
<i>Laminin</i>	Sigma	L2020-1MG
<i>MEM</i>	Thermo Fisher Sci	51200-046
<i>MG132</i>	Sigma	M7449
<i>Penicillin/Streptomycin (P/S)</i>	Thermo Fisher Sci	15140-122
<i>Poly-D-lysine (1mg/mL)</i>	Merck	A-003-E
<i>Sodium Pyruvate</i>	Thermo Fisher Sci	11360-039
<i>Soybean trypsin inhibitor</i>		
<i>Transferrin, Holo, Bovine Plasma</i>	Merck	616420
<i>Trypsin from bovine pancreas</i>	Sigma	T1005
<i>(Z)-4-Hydroxytamoxifen (Tamoxifen)</i>	Sigma	H7904-5MG

6.1.4 Kits and other equipment

<i>Reagent</i>	<i>Manufacturer</i>	<i>Identifier</i>
<i>β-Gal Senescence Assay</i>	Cell Signaling Technology	9860
<i>Molecular Probes™ Click-iT™ EdU Alexa Fluor™ 488 Bildgebungs-Kit</i>	Thermo Fisher Sci	C10337
<i>Lipofectamine 3000</i>	Thermo Fisher Sci	L3000-008
<i>Lipofectamine LTX</i>	Thermo Fisher Sci	

<i>ProFection Mammalian Transfection System- Calcium Phosphate</i>	Promega	E1200
--	---------	-------

6.1.5 Antibodies

<i>Antibody</i>	<i>Host</i>	<i>WB</i>	<i>ICC</i>	<i>Manufacturer</i>	<i>Identifier</i>
<i>anti-AP-2α</i>	Mouse monoclonal	-	1:500	Abcam	ab2730
<i>anti-AP-2α</i>	Mouse monoclonal	1:1000	-	BD	610501
<i>anti-AP-2-μ</i>	Mouse monoclonal	-	1:300	BD	611350
<i>anti-ARL13b</i>	Rabbit polyclonal	-	1:1000	Abcam	Ab153725
<i>anti-Centrin</i>	Mouse monoclonal	-	1:1000	Sigma	04-1624
<i>Anti-Dcx</i>	Guinea pig polyclonal	-	1:500	Merck	AB2253
<i>anti-GAPDH</i>	Mouse monoclonal	1:1000	-	Sigma-Aldrich	G8795
<i>anti-GCP2</i>	Rabbit polyclonal	1:1000	1:500	Millipore	MABT1322
<i>anti-GCP3</i>	Rabbit polyclonal	1:1000	1:500	Elabscience (Biomol GmbH)	E-AB-62346
<i>anti-GCP4</i>	Mouse monoclonal	1:100	1:50	Santa Cruz Biotechnology	sc-271876
<i>anti-GFAP</i>	Mouse monoclonal	-	1:500	Sigma	G3893
<i>anti-GFP</i>	Chicken polyclonal	-	1:2000	Abcam	ab13970
<i>anti-Ki67</i>	Rabbit polyclonal	-	1:1000		

<i>anti-mCherry</i>	Mouse monoclonal	-	1:200	Novus Biologicals	NBP1-96752
<i>anti-Nestin</i>	Chicken polyclonal	-	1:500	Novus	NB100-16074
<i>anti-p53</i>	Rabbit polyclonal	-	1:1000	CST	2524
<i>anti-PCM1</i>	Rabbit polyclonal	-	1:100	Sigma	HPA023370
<i>anti-PCNT</i>	Rabbit polyclonal	-	1:500	Abcam	ab4448
<i>anti-pH3</i>	Rabbit polyclonal	-	1:1000	Millipore	06-570
<i>anti-Vimentin</i>	Chicken polyclonal	-	1:500	Novus Biochemical	NB300-223SS
<i>anti-α-TUBULIN</i>	Mouse monoclonal	-	1:500	Synaptic Systems	302 211
<i>anti-β-actin</i>	Mouse monoclonal	1:1000	-	Sigma	A-5441
<i>anti-γ-H2AX</i>	Rabbit polyclonal	-	1:500	Cell Signaling	9718
<i>anti-γ-Tubulin</i>	Mouse monoclonal	1:1000	1:1000	Sigma	T6557
<i>Normal Mouse IgG</i>	Normal Mouse IgG	1:5000	-	Millipore	12-371
<i>Normal Rabbit IgG</i>	Normal Rabbit IgG	1:5000	-	Cell Signaling	2729
<i>Goat anti-Mouse IgG (H+L) peroxidase-conjugated</i>	Goat anti-Mouse IgG (H+L) peroxidase-conjugated	1:2000	-	Jackson ImmunoResearch	115-035-003

<i>Goat anti-Mouse IgG, light chain specific, peroxidase-conjugated</i>	Goat anti-Mouse IgG, light chain specific, peroxidase-conjugated	1:2000	-	Jackson ImmunoResearch	115-035-174
<i>Goat anti-Rabbit IgG (H+L) peroxidase-conjugated</i>	Goat anti-Rabbit IgG (H+L) peroxidase-conjugated	1:2000	-	Jackson ImmunoResearch	111-035-003
<i>Alexa Fluor 488 Goat anti-Chicken IgG</i>	Alexa Fluor 488 Goat anti-Chicken IgG	-	1:500	Thermo Fisher Sci	A-11039
<i>Alexa Fluor 488 Goat anti-Mouse IgG</i>	Alexa Fluor 488 Goat anti-Mouse IgG	-	1:500	Thermo Fisher Sci	A-11029
<i>Alexa Fluor 488 Goat anti-Rabbit IgG</i>	Alexa Fluor 488 Goat anti-Rabbit IgG	-	1:500	Thermo Fisher Sci	A-11034
<i>Alexa Fluor 568 Goat anti-Mouse IgG</i>	Alexa Fluor 568 Goat anti-Mouse IgG	-	1:500	Thermo Fisher Sci	A-11031
<i>Alexa Fluor 568 Goat anti-Rabbit IgG</i>	Alexa Fluor 568 Goat anti-Rabbit IgG	-	1:500	Thermo Fisher Sci	A-11036
<i>Alexa Fluor 568 Goat anti-Chicken IgG</i>	Alexa Fluor 568 Goat anti-Chicken IgG	-	1:500	Thermo Fisher Sci	A-11041

<i>Alexa Fluor 647 Goat anti-Mouse IgG</i>	Alexa Fluor 647 Goat anti-Mouse IgG	-	1:500	Thermo Fisher Sci	A-21236
<i>Alexa Fluor 647 Goat anti-Rabbit IgG</i>	Alexa Fluor 647 Goat anti-Rabbit IgG	-	1:500	Thermo Fisher Sci	A-21245
<i>ATTO647N Goat anti-Rabbit</i>	ATTO647N Goat anti-Rabbit	-	1:500	Sigma Aldrich	40839-1ML- F

6.1.6 Oligonucleotides and vectors

6.1.6.1 Genotyping primers

<i>Gene</i>	<i>Sequence (5'- 3')</i>	<i>Annealing temp (°C)</i>
<i>AP-2 1</i>	CTC ATA TAC GAG CTG CTG GAT G	65
<i>AP-2 2</i>	CCA AGG GAC CTA CAG GAC TTC	65
<i>General Cre 1</i>	GAA CCT GAT GGA CAT GTT CAG G	62
<i>General Cre 2</i>	AGT GCG TTC GAA CGC TAG AGC CTG T	62
<i>General Cre 3</i>	TTA CGT CCA TCG TGG ACA	62
<i>General Cre 4</i>	TGG GCT GGG TGT TAG CC	62
<i>lft88 reverse</i>	GCC TCC TGT TTC TTG ACA ACA GTG	58
<i>lft88 forward 1</i>	GGT CCT AAC AAG TAA GCC CAG TGT T	58
<i>lft88 forward 2</i>	CTG CAC CAG CCA TTT CCT CTA AGT CAT GTA	58

6.1.6.2 Plasmids

<i>Plasmid (source gene)</i>	<i>Manufacturer</i>	<i>Identifier</i>
<i>pmCherry-N1</i>	Clontech	632524
<i>AP-2μ-mRFP</i>	Prepared by Tanja Maritzen	N/A
<i>EB3-tdTomato (human)</i>	Addgene	#50708
<i>mEmerald-EB3-7</i>	Addgene	#54075
<i>AP-2μ2-mCherry</i>	Addgene	#27672
<i>γ-Tubulin-S65T-GFP</i>	Kind gift from Dr. H. Bazzi	N/A

6.1.7 Mouse models

<i>Mouse model</i>	<i>Manufacturer</i>	<i>Identifier</i>
<i>C57BL/6J</i>	CECAD <i>in vivo</i> facility	N/A
<i>Ap2m1lox/lox: tamoxifen inducible CAG-Cre</i>	Kononenko et al. (2017)	N/A
<i>Ap2m1lox/lox lft88lox/lox lft88: tamoxifen inducible CAG-Cre</i>	Kononenko et al. (2017) Bazzi	N/A

6.1.8 Solutions and Media

6.1.8.1 Routinely used solutions

If not mentioned, solutions were stored at room temperature (RT)

<i>Name</i>	<i>Composition</i>
<i>1.5M Tris pH 8.8</i>	<ul style="list-style-type: none"> • 181.65g Tris Base • 0.4% (w/v) SDS • 1L ddH₂O • pH 8.8
<i>0.5M Tris pH 6.8</i>	<ul style="list-style-type: none"> • 6g Tris Base • 0.4% (w/v) SDS • 100 mL ddH₂O • pH 6.8
<i>10% Acrylamide gel</i>	<ul style="list-style-type: none"> • 8.04 ml H₂O

	<ul style="list-style-type: none"> • 5ml 1.5M Tris pH 8.8 • 6.67ml 30% acrylamide/bis • 200µl 10% SDS • 100µl APS 10% • 10µL TEMED
<i>4% Acrylamide gel (Stacking)</i>	<ul style="list-style-type: none"> • 6mL ddH₂O • 2.52 mL 0.5 M Tris pH 6.8 • 1.32 mL acrylamide/bis • 100µL 10%SDS • 50µL 10% APS • 10µL TEMED
<i>2% agarose gel</i>	<ul style="list-style-type: none"> • 2% (w/v) agarose in TBE 1X
<i>B buffer</i>	<ul style="list-style-type: none"> • 35.6g Na₂HPO₄*2H₂O • 31.7g Na₂HPO₄, pH=7.4 • in 500mL H₂O
<i>Blocking solution WB (milk powder)</i>	<ul style="list-style-type: none"> • 5% (w/v) milk powder in TBS-T
<i>ICC blocking/permeabilizing solution</i>	<ul style="list-style-type: none"> • 5% (v/v) NGS • 0.2% (w/v) Saponin or 0.1% (v/v) Triton in PBS
<i>Imaging Buffer</i>	<ul style="list-style-type: none"> • 1mL B buffer • 100µL NaCl 5M • 4.9 µL MgCl₂ • 13µL CaCl₂ 1M • Total volume 10 mL
<i>Neutralization Buffer</i>	<ul style="list-style-type: none"> • 1.3g Tris-HCl in 200mL ddH₂O. pH=5
<i>Lammeli Buffer (4x)</i>	<ul style="list-style-type: none"> • 250mM Tris-HCL • 1% (w/v) SDS • 40% (v/v) Glycerol • 4% (v/v) β-mercaptoethanol • 0.02% Bromophenol
<i>PFA 4% (ICC fixation)</i>	<ul style="list-style-type: none"> • 4% (w/v) PFA, • 4% (w/v) Sucrose, • dissolved in PBS. pH 7.4
<i>PBS</i>	<ul style="list-style-type: none"> • 0.137M NaCl • 0.0027M KCl; • 0.01M Na₂HPO₄ • 1.8mM KH₂PO₄
<i>Proteinase K solution</i>	<ul style="list-style-type: none"> • 50mM Tris-HCl • 1mM CaCl₂

	<ul style="list-style-type: none"> • 50% Glycerol, in ddH₂O to generate dilution Buffer. + 20g Proteinase K for 1mL of dilution buffer.
<i>Ponceau staining solution</i>	<ul style="list-style-type: none"> • 1% (w/v) Ponceau S • 2% (v/v) acetic acid in ddH₂O
<i>RIPA buffer</i>	<ul style="list-style-type: none"> • 50mM Tris-Base • 150 mM NaCl • 1% (v/v) IGEPAL • 0.5% (w/v) Sodium deoxycholate • 0.1% (w/v) SDS dissolved in ddH₂O • 1 tablet of protease inhibitor and phosphatase inhibitor/10mL RIPA buffer
<i>Running Buffer 10X</i>	<ul style="list-style-type: none"> • 25mM Tris-Base • 192mM Glycine • 0.1% (w/v) SDS in ddH₂O
<i>Transfer Buffer 10X</i>	<ul style="list-style-type: none"> • 25mM Tris-Base • 192mM Glycine • 0.025% (w/v) SDS in ddH₂O
<i>Transfer Buffer 1X</i>	<ul style="list-style-type: none"> • 10% (v/v) Transfer Buffer 10X • 20% (v/v) methanol • 70% (v/v) ddH₂O
<i>Tail lysis buffer</i>	<ul style="list-style-type: none"> • 1M Tris-Base • 0.5M EDTA • 20% (w/w) SDS • 5M NaCl, in ddH₂O, pH 8.5
<i>TBE 10X</i>	<ul style="list-style-type: none"> • 108g Tris-Base • 55g Boric acid • 7.4g EDTA in 1L ddH₂O
<i>TBS-T</i>	<ul style="list-style-type: none"> • 20mM Tris • 137 Mm NaCl • 0.1% (v/v) Tween 20
<i>Lysis buffer for IP (Co-IP buffer)</i>	<ul style="list-style-type: none"> • 50 mM Tris-HCl • 1% IGEPAL • 100mM NaCl • 2mM MgCl₂ in ddH₂O • 1 tablet of protease and phosphatase inhibitors/10mL of lysis buffer

6.1.8.2 Cell culture media

All cell culture media was filtered through 0.2 µm pore size membranes and stored at 4°C

<i>Name</i>	<i>Composition</i>
<i>Basic Media</i>	<ul style="list-style-type: none"> • 1L MEM • 5g Glucose • 200mg NaHCO₃ • 100mg Transferrin
<i>Borate Buffer 0.1M</i>	<ul style="list-style-type: none"> • 1.24g boric acid • 1.9g sodium tetraborate • in 400ml autoclaved ddH₂O
<i>Digestion Solution</i>	<ul style="list-style-type: none"> • 137mM NaCl • 5mM KCl • 7mM Na₂HPO₄ • 25mM HEPES • dissolved in autoclaved ddH₂O. pH 7.2
<i>Dissociation Solution</i>	<ul style="list-style-type: none"> • Hank's • 12mM MgSO₄x7H₂O
<i>Growth / Differentiation Media</i>	<ul style="list-style-type: none"> • 100mL Basic Media • 5mL sterile filtered FBS • 0.25mL GlutaMAX • 2mL B-27 • 1mL P/S
<i>Hank's solution</i>	<ul style="list-style-type: none"> • 500 mL HBSS • 5mL Sodium pyruvate • 5mL HEPES • 5mL P/S
<i>Hank's FBS</i>	<ul style="list-style-type: none"> • Hank's + 20% (v/v) sterile filtered FBS
<i>MEF media</i>	<ul style="list-style-type: none"> • DMEM • 10% (v/v) FBS • 0.1% (v/v) P/S
<i>NPCs media</i>	<ul style="list-style-type: none"> • 50 mL DMEM/F12+GlutaMAX • 1 mL B27 • 0.5 mL P/S • 0.25 mL EGF • 0.125 mL b-FGF
<i>Plating Media</i>	<ul style="list-style-type: none"> • 100 mL Basic Media • 10 mL sterile filtered FBS • 1mL GlutaMAX

	<ul style="list-style-type: none">• 625µL Insulin• 1.1 mL P/S
--	--

6.2 Methods

6.2.1 Animals

C57/BL/6 mice were housed in polycarbonate cages at standard 12/12 day-night cycles, and water and food were provided *ad libitum*. All animal experiments were approved by the ethics committee of LANUV Cologne and were conducted according to the committee's guidelines. Conditional tamoxifen-inducible (Ap2m1lox/lox × inducible CAG-Cre) is described in (Kononenko *et al.*, 2017) and was used for in vitro experiments. C57BL6/NRj were used for WT experiments (Mass-spectrometry, Co-IPs, colocalization, and trafficking experiments).

6.2.2 Genotyping

DNA extraction. Newborn pups were tattooed after birth, and subsequently, 1mm of the tail from each pup was collected for genotyping. In the case of embryos, a tail cut was given to the genotype after extraction. DNA extraction from each tail sample was performed by incubating samples in 300 µL of tail lysis buffer plus 3 µL of proteinase K solution at 55°C overnight (ON). For the isolation of DNA, digested samples were centrifuged at 13 000 revolutions per minute (rpm) for 5 min. The supernatant was discarded, and the pellet was resuspended with 400 µL of isopropanol and gently mixed prior to centrifugation at 13 000 rpm for 15 min. Again, the supernatant was discarded, and DNA was washed once with 70% ethanol, followed by another centrifugation of 13 000 rpm for 10 min. Finally, the supernatant was discarded, the pellet dried out, and resuspended with 100 µL of autoclaved water.

PCR. DNA samples were diluted in PCR tubes following the master mix shown below. Note that working primers were diluted at 10pmols/µL.

<i>Ift88, AP-2, Cre</i>	<i>Volume (μL)</i>
<i>Sample</i>	1
<i>Dream Taq Buffer</i>	2
<i>MgCl₂ 25mM</i>	2
<i>Primer mix</i>	1 each primer
<i>DNTPs 2 mM</i>	1.5
<i>Dream Taq pol.</i>	0.2 μ L
<i>H2O till 20 μL total</i>	

PCR program:

<i>Step</i>	<i>AP-2 (30 cycles)</i>		<i>Cre (35 cycles)</i>		<i>Ift88 (35 cycles)</i>		
	<i>T ($^{\circ}$C)</i>	<i>Time</i>	<i>T ($^{\circ}$C)</i>	<i>Time</i>	<i>T ($^{\circ}$C)</i>	<i>Time</i>	
<i>Initial denaturation</i>	95	5min	95	5min	95	5min	
<i>cycles</i>	denaturation	94	30s	95	30s	95	30s
	Anneling	65	30s	62	30s	58	30s
	Elongation	72	30s	72	30s	72	30s
<i>Final extension</i>	72	5min	72	5min	72	5min	
<i>Hold</i>	4		4		4		

Electrophoresis. PCR results were subsequently mixed with a DNA loading sample and charged in a 2% Agarose gel with SYBR safe at a concentration indicated by the manufacturer's guideline. Finally, electrophoresis was done at 120V for 40 min, and results were visualized by the gel imager system (Bio-Rad).

6.2.3 Preparation of cell cultures and transfections

6.2.3.1 Coating

The coating was performed by dissolving PDL with borate buffer and adding it to the coverslips or dishes for at least 2 h at 37°C. Afterward, the coverslips were washed with autoclaved water.

For NPCs, and additional coating with laminin dissolved in PBS was done and incubated for 12 h and afterward washed with DMEM/F-12(1.1) (1X)+GlutaMAX™

6.2.3.2 Neural progenitor cell cultures and transfection

Embryos were obtained between stages E12-E14 of pregnancy, and the telencephalic vesicles were extracted and digested for 20 min in 0.05% Trypsin with DNase. The addition of Soybean Trypsin Inhibitor stopped trypsinization, and tissue was homogenized by pipetting gently ten times with a p1000 and ten times with a p200. Cells were centrifuged at 1.500 rpm for 1min and washed once before resuspending the pellet in proliferation media, to be then counted with a solution of trypan blue and a Neubauer chamber. 50µL solution containing 10.000 cells were plated in pre-coated 24mm diameter coverslips or 3 cm diameter dishes. The coating was performed the day before by dissolving the PDL with borate buffer 0.1M and adding it on the coverslips or dishes for 2 to 16 hours, which afterward were washed with autoclaved water and dried, to be coated with Laminin overnight and were washed with autoclaved water and air-dried before plating. Once cells were attached to the surface of the coverslip or dish (1-2 h), 2 mL of prewarmed proliferation media was added to each well, and cells were placed inside the incubator at 37°C, 5% CO₂. Cells were plated at a concentration of 50.000 cells/ml for stock and 10.000 cells/ml for experiments

Plasmid transfections of NPCs: Cells were transfected 1 hour after refreshing the medium using Lipofectamine LTX (Invitrogen). For this, it was mixed in the following order 1 µg plasmid DNA, 2,5 µL of Plus Reagent, and 1,5µL of Lipofectamine and resuspended in Opti-MEM medium (100 µl) (for each well of a 6-well plate), followed by incubation for 20 min allowing for lipo-complex formation. Lipo-complexes were added to the cells and incubated at 37 °C, 5% CO₂ for 24-48h, depending on plasmid expression.

6.2.3.3 Preparation of mouse embryonic fibroblasts cell cultures and SV40-mediated immortalization

Embryos were obtained between stages E12-E14 of pregnancy. Head, visceral tissues, and gonads were removed from the embryos, and the carcass was incubated in 0.25% Trypsin/1 mM EDTA for 20 min at 37°C. The trypsinization was stopped by adding MEF culture medium. The tissue was dissociated by pipetting up and down. Next, the samples were incubated for 5 min at RT, followed by centrifugation at 200 rcf for 5 min. The supernatant was discarded, the pellet was resuspended in MEF culture medium, and the cells were plated in 10 cm dishes. The cells were incubated at 37 °C with 5% CO₂ until they were confluent.

SV-40 immortalization of MEFs: an SV40 Virus with Polybrene (kindly provided by Dr. Frederik Tellkamp, AG Krüger) was added to the cells. The medium was changed 12 h after transduction.

This process was repeated several times to get a higher infection rate. Cells were cultured with MEF culture medium in 10 cm dishes and incubated at 37°C with 5% CO₂ until they were confluent. Cells are considered immortalized after passage 10.

6.2.3.5 Preparation of primary astrocytic cell cultures and transfections

Cortex and hippocampi were isolated from postnatal pups at P1–5, cut into small pieces, washed twice in Hank's+20%FBS and Hank's, and digested with 10 mg trypsin, and 10 µL DNase dissolved in 2 mL of digestion solution, which was then incubated at 37°C for 15 min. Trypsination was stopped by washing twice with Hank's+20%FBS and Hank's, prior addition of 2 mL of dissociation solution containing 10 µL of DNase. Samples were mechanically dissociated by pipetting 2-3 times with a fire-polished glass pipette, followed by the centrifugation of cells at 0.3 rcf, 8 min at 4°C. The supernatant was discarded, and the pellet of cells was re-suspended in plating media, which were then counted with a solution of trypan blue and a Neubauer chamber. 50µL solution containing 50 000 cells were plated in pre-coated 24mm diameter coverslips or 3 cm diameter dishes. Once cells were attached to the surface of the coverslip or dish (1-2 h), 2 mL of prewarmed plating media was added to each well, and cells were placed inside the incubator at 37°C/5% CO₂. After 24 h, half of the media was removed, and the same amount of Growth media was added. 48 h after the cell culture preparation, the same volume of media used after 24 h was added. No further media was added afterward.

Plasmid transfections of astrocytes: Astrocytes were transfected at DIV 7–9 using an optimized calcium phosphate protocol (Kononenko *et al*, 2013). 6µg plasmid DNA was added to 12.5µL of CaCl₂ 2M, and 81.5 µL of water (for each well of a 6-well plate, and mixed with an equal volume of 2x HEPES buffered saline (100µl) (ProFection Mammalian Transfection System- Calcium Phosphate) and incubated for 20 min, allowing for precipitate formation. Meanwhile, cells were incubated in NBA medium for the same time at 37°C, 5% CO₂. Subsequently, precipitates were added to the cells and incubated at 37°C, 5% CO₂, for 30 min. Finally, coverslips were washed twice with HBSS medium and transferred back to the medium. The osmolarity of NBA and HBSS media was adjusted to the original cellular media of the astrocytes with D-mannitol to avoid osmotic shock.

6.2.3.4 Induction of homologous recombination of AP-2 μ / Ift88 KO allele by tamoxifen

To initiate homologous recombination in cells from floxed animals expressing a tamoxifen-inducible Cre recombinase, they were treated with 0.4 μ M (Z)-4-hydroxytamoxifen immediately after plating. Ethanol was added to control neurons (WT) in an amount equal to tamoxifen.

6.2.5 EdU Pulse Labelling

NPCs were incubated for a 24h pulse in 0.2 μ M EdU (component A of Click-iT[®] EdU Imaging Kit, Invitrogen) at 37 °C, 5% CO₂. After EdU incubation, cells were fixed in 3.7% formaldehyde in PBS for 15 minutes at room temperature. Formaldehyde was removed, and cells were washed twice with 1 mL of 3% BSA in PBS and permeabilized for 20 minutes at RT in 0.5% Triton[®] X-100.

EdU detection was performed according to manufacturers' instructions, followed by immunostaining for other markers.

6.2.6 β -Gal Senescence Assay

NPCs were seeded in 6-well plates, and after 48 hours medium was removed, wells were rinsed with PBS before fixing with 1x fixative solution provided by senescence β -galactosidase staining kit (9860, Cell Signaling Technology) for 15 minutes. The fresh β -galactosidase staining solution was prepared according to the manufacturer's instructions. Cells in each well were stained with 0.5 mL staining solution after being washed with PBS twice. The staining process was accomplished after incubating at 37°C in a dry, ON incubator. The β -galactosidase positive cells were considered senescent cells and counted in ten randomly chosen fields per experiment and condition.

6.2.7 Neurosphere Migration Assay

Neurospheres were pipetted without dissociation and seeded in Matrigel-coated coverslips. After 6, 12, 24, and 48 hours, cells were observed and imaged in a Brightfield microscope before fixation. Immunostaining was performed in the fixed coverslips and imaged. Migrated distance and number of migrating cells were analyzed in ImageJ.

6.2.8 Immunocytochemistry of cultured cells

Depending on the protein of interest, cells were either fixed in 4% paraformaldehyde (PFA) in phosphate-buffered saline (PBS containing 137 mM NaCl, 2.7 mM KCl, 10 mM Na₂HPO₄, 1.8 mM, K₂HPO₄, pH 7.4) for 15 min at room temperature (RT) or 8 min in ice-cold Methanol at -

20°C. Afterward they were washed three times with PBS and blocked for 1 h at RT with a blocking buffer containing 0.3% saponin (SERVA Electrophoresis GmbH) or 0.2% TritonX-100 and 5% normal goat serum (NGS) in PBS. Neurons were then incubated with primary antibodies in the blocking buffer for 1 h at RT or ON at 4°C. Coverslips were rinsed three times with PBS (5 min each) and incubated with corresponding secondary antibodies for 30–60 min at RT in a blocking solution. Finally, coverslips were washed three times in PBS and mounted in Immu-Mount (Thermo Scientific).

6.2.9 Immunostaining of Tubulin1 α

NPCs were treated on DIV 2 either with 0.2 μ g/ml Nocodazole (Sigma) or with 0.2 μ g/ml DMSO for 1 h. Afterward, cells were fixed immediately, or media was exchanged, and cells were incubated for 5 minutes in the incubator to allow microtubule regrowth. Before fixation, cells were rinsed with warm PHEM buffer (60 mM PIPES, 25 mM HEPES, 10 mM EGTA, 4 mM MgCl₂), followed by an incubation step in PHEM buffer containing 0.05% Triton-X-100 at 37°C for 1.5 min to remove the soluble Tubulin. Then, fixation was done with cold methanol (–20 °C) for 8 min, permeabilized and blocked with PBS-S (PBS containing 0.2% saponin (Serva), and 2.5% BSA, Sigma) for 30 min at RT and incubated with primary antibodies diluted in PBS-S for 2 h. Coverslips were rinsed twice in PBS-S (2 min each) and incubated with corresponding secondary antibodies (diluted 1:500) in PBS-S for 30 min. Finally, coverslips were washed four times in PBS-S and mounted in Immu-Mount (Thermo Scientific).

6.2.10 Microscope picture analysis

Fixed cells were imaged using either using Zeiss Axiovert 200M microscope (Observer. Z1, Zeiss, USA) equipped with 40x/1.4 oil DIC objective and 63x/1.4 oil DIC objective and the Micro-Manager software or with Leica SP8 confocal microscope (Leica Microsystems) equipped with a 63x/1.32 oil DIC objective and a pulsed excitation white light laser (WLL; ~80-ps pulse width, 80-MHz repetition rate; NKT Photonics). For quantitative analysis of cell cycle percentage of cells, ciliated cells, and centrosome analysis, several pictures were considered until quantification of a significant number of cells per experiment (at least 100 total cells and 10 or more cells of interest). Fluorescent protein levels were analyzed by manually selecting the cell body using ImageJ selection tools (ROI), and the mean gray value was quantified within the ROI after the background subtraction. Coverslips were imaged using EVOS FL Auto 2 (Invitrogen, USA) to quantify the number of senescent cells.

6.2.11 STED imaging

STED imaging was done using a gSTED superresolution and confocal microscope (Leica Microsystems) equipped with 100x oil objective (HC PL APO 100x/1.4 Oil STED, Leica Microsystems) and a pulsed excitation white light laser (WLL; 80-MHz repetition rate; NKT Photonics) and two STED lasers (continuous wave at 592 nm, pulsed at 775 nm, MPBC). Within each independent experiment, samples were acquired with equal settings. Alexa Fluor 488 and ATTO 647N were excited using a pulsed WLL at 480 and 640 nm, respectively. Fluorescence signals were detected sequentially by hybrid detectors starting with the longer wavelength. Images were acquired with a scanning format of 1,024 × 1,024, eight-bit sampling, and 5 zoom. Analysis was done using ImageJ.

6.2.12 Live imaging of cultured neurons

NPCs were imaged at 37°C in an imaging buffer (see above) using Zeiss Axiovert 200M microscope (Observer. Z1, Zeiss, USA) equipped with 40X/1.40 Oil DIC objective; a pE-4000 LED light source (CoolLED) and a Hamamatsu Orca-Flash4.0 V2 CMOS digital camera. Time-lapse images of NPCs expressing EB3-Tdtomato plasmids were acquired every second using Micro-Manager software (Micro-Manager1.4, USA) for 60 s. Kymographs were generated using the software KymoMaker (Chiba *et al*, 2014) and analyzed by ImageJ.

6.2.13 Propidium Iodide Flow Cytometry

Cells were spined-down at 2500 rpm for 3 min, then washed with 1mL 1xPBS and centrifuged again. Half of the PBS was removed to add to the pellets dropwise 9.5mL of ice-cold 70% ethanol. Cells were spined down at 3000rpm before staining to remove ethanol and washed with PBS twice. The cell pellet was resuspended in Propidium iodide solution (PI 10ug/ml, RNase A 200 ug/ml, and 0.1% TritonX-100 in 1xPBS) and incubated 5 minutes at 37°C or 30 min at RT. Flow cytometry was performed using BD LSR Fortessa, gating the analysis to 20,000 events (or in the case of KO cells due to the low number till the sample was thoroughly analyzed) and analysed using Flowing software 2.

6.2.14 Western blotting

NPCs were allowed to proliferate after Ethanol or Tamoxifen treatment for 48 hours. Afterward, cells were lysed using radioimmunoprecipitation assay buffer (RIPA) containing 50 mM Tris (pH = 8.0), 150 mM NaCl, 1.0% IGEPAL, 0.5% sodium deoxycholate, 0.1% SDS, and 1x protease

inhibitor cocktail (Roche). Proteins were extracted for 45 min on ice, followed by the centrifugation of lysates at 14,000 g for 20 min, and protein concentration was measured by the Bradford assay. Samples were analyzed by SDS-PAGE on 10% Tris-Glycine gels, followed by blotting on the nitrocellulose membrane. The membranes were blocked for 1 h at RT in 5% skim milk in TBS buffer (20 mM Tris pH = 7.6, 150 mM NaCl) containing 0.1% Tween (TBS-T) and incubated with primary antibodies overnight at 4°C. Next, the membranes were washed two times (10 min each) with TBS-T and one time with TBS buffer and incubated with a secondary antibody for 1 h at RT in TBS-T buffer. Afterward, the membranes were washed and developed using an ECL-based autoradiography film system. Analysis was performed using ImageJ.

6.2.15 Co-immunoprecipitation assays

Embryos were obtained between stages E14-E16 of pregnancy, and the telencephalic vesicles were extracted and homogenized in Co-IP buffer containing 50 mM Tris-HCl pH = 7.4, 100 mM NaCl, 1% NP-40, 2 mM MgCl₂, and 1× protease inhibitor. Samples were sonicated and proteins were extracted for 45 min on ice, followed by the centrifugation of lysates at 17,000 g for 20 min at 4°C. An equivalent amount of mouse AP-2 antibody or non-specific mouse IgG was coupled to Protein G Dynabeads (Invitrogen). Antibody-coupled Dynabeads were incubated with the supernatant for overnight at 4°C on the shaker. Following the incubation, Dynabeads were washed three times with Co-IP buffer, and proteins were eluted using SDS-PAGE sample buffer and analyzed by Western blotting.

6.2.16 Mass Spectrometry analysis of AP-2 α binding partners

Embryos were obtained between stages E14-E16 of pregnancy, and the telencephalic vesicles were extracted and homogenized in Co-IP buffer, as described in the previous section. After boiling the samples at 95 °C for 5 min, the samples were loaded onto SDS-PAGE gels, reduced (DTT), and alkylated (CAA). Digestion was performed using trypsin at 37 °C overnight. Peptides were extracted and purified using Stagetips. Eluted peptides were dried in vacuo, resuspended in 1% formic acid/4% acetonitrile, and stored at -20 °C prior MS measurement.

All samples were analyzed by the CECAD proteomics facility on a Q Exactive Plus Orbitrap mass spectrometer that was coupled to an EASY nLC (both Thermo Scientific). Peptides were loaded with solvent A (0.1% formic acid in water) onto an in-house packed analytical column (50 cm, 75 μ m I.D., filled with 2.7 μ m Poroshell EC120 C18, Agilent). Peptides were chromatographically separated at a constant flow rate of 250 nL/min using the following gradient: 3-7% solvent B (0.1%

formic acid in 80 % acetonitrile) within 1.0 min, 7-23% solvent B within 35.0 min, 23-32% solvent B within 5.0 min, 32-85% solvent B within 5.0 min, followed by washing and column equilibration. The mass spectrometer was operated in data-dependent acquisition mode. The MS1 survey scan was acquired from 300-1750 m/z at a resolution of 70,000. The top 10 most abundant peptides were isolated within a 1.8 Th window and subjected to HCD fragmentation at a normalized collision energy of 27%. The AGC target was set to 5e5 charges, allowing a maximum injection time of 108 ms. Product ions were detected in the Orbitrap at a resolution of 35,000. Precursors were dynamically excluded for 20.0 s. All mass spectrometric raw data were processed with Maxquant (version 1.5.3.8, (Tyanova *et al*, 2016a)) using default parameters. Briefly, MS2 spectra were searched against the Uniprot mouse reference proteome containing isoforms (UP589, downloaded at 26.08.2020), including a list of common contaminants. False discovery rates on protein and PSM level were estimated by the target-decoy approach to 1% (Protein FDR) and 1% (PSM FDR) respectively. The minimal peptide length was set to 7 amino acids and carbamidomethylation at cysteine residues was considered as a fixed modification. Oxidation (M), Phospho (STY), and Acetyl (Protein N-term) were included as variable modifications. The match-between runs option was enabled between replicates. LFQ quantification was enabled using default settings. Follow-up analysis was done in Perseus 1.6.15 (Tyanova *et al*, 2016b).

6.2.17 Proteomics

NPCs were lysed in 8M Urea/50 mM TEAB buffer containing protease inhibitors. Samples were sonicated, followed by the centrifugation of lysates at 20,000 g for 15 min. Lysates were reduced (DTT), and alkylated (CAA). Digestion was performed using trypsin at 37 °C overnight. Peptides were extracted and purified using Stagetips.

All samples were analyzed by the CECAD proteomics facility on a Q Exactive Plus Orbitrap mass spectrometer that was coupled to an EASY nLC (both Thermo Scientific). Peptides were loaded with solvent A (0.1% formic acid in water) onto an in-house packed analytical column (50 cm — 75 µm I.D., filled with 2.7 µm Poroshell EC120 C18, Agilent). Peptides were chromatographically separated at a constant flow rate of 250 nL/min using the following gradient: 3-4% solvent B (0.1% formic acid in 80 % acetonitrile) within 1.0 min, 5-27% solvent B within 119.0 min, 27-50% solvent B within 19.0 min, 50-95% solvent B within 1.0 min, followed by washing and column equilibration. The mass spectrometer was operated in data-dependent acquisition mode. The MS1 survey scan

was acquired from 300-1750 m/z at a resolution of 70,000. The top 10 most abundant peptides were isolated within a 1.8 Th window and subjected to HCD fragmentation at a normalized collision energy of 27%. The AGC target was set to 5e5 charges, allowing a maximum injection time of 55 ms. Product ions were detected in the Orbitrap at a resolution of 17,500. Precursors were dynamically excluded for 30.0 s.

All mass spectrometric raw data were processed with Maxquant (version 1.5.3.8, (Tyanova *et al.*, 2016a)) using default parameters against the Uniprot canonical mouse database (UP589, downloaded 15.08.2019) with the match-between-runs option enabled between replicates. Follow-up analysis was done in Perseus 1.6.15 (Tyanova *et al.*, 2016b).

6.2.18 Statistical Analysis

Significant estimates were obtained from independent experiments (N) for analysis. MS Excel and GraphPad Prism version 7 were used to assess the statistical analysis. The statistical significance between the two groups for all normally distributed raw data was evaluated with a two-tailed unpaired t-test student. The statistical significance between more than two groups for all normally distributed raw data was evaluated using Two-Way ANOVA multiple comparison (Sidak multiple comparison test, with a single pooled variance, was used to determine the statistical significance between the groups). Significant differences were accepted at $p < 0.05$.

7. REFERENCES

- Addi C, Presle A, Frémont S, Cuvelier F, Rocancourt M, Milin F, Schmutz S, Chamot-Rooke J, Douché T, Duchateau M *et al* (2020) The Flemmingsome reveals an ESCRT-to-membrane coupling via ALIX/syntenin/syndecan-4 required for completion of cytokinesis. *Nat Commun* 11: 1941
- Agajanian MJ, Walker MP, Axtman AD, Ruela-de-Sousa RR, Serafin DS, Rabinowitz AD, Graham DM, Ryan MB, Tamir T, Nakamichi Y *et al* (2019) WNT Activates the AAK1 Kinase to Promote Clathrin-Mediated Endocytosis of LRP6 and Establish a Negative Feedback Loop. *Cell Rep* 26: 79-93 e78
- Agarwal ML, Agarwal A, Taylor WR, Stark GR (1995) p53 controls both the G2/M and the G1 cell cycle checkpoints and mediates reversible growth arrest in human fibroblasts. *Proc Natl Acad Sci U S A* 92: 8493-8497
- Alberts B, Johnson A, Lewis J, Martin Raff M, Roberts K, Walter P (2007) *Molecular biology of the cell*
- Alfieri C, Chang L, Zhang Z, Yang J, Maslen S, Skehel M, Barford D (2016) Molecular basis of APC/C regulation by the spindle assembly checkpoint. *Nature* 536: 431-436
- Andersen JL, Johnson CE, Freel CD, Parrish AB, Day JL, Buchakjian MR, Nutt LK, Thompson JW, Moseley MA, Kornbluth S (2009) Restraint of apoptosis during mitosis through interdomain phosphorylation of caspase-2. *EMBO J* 28: 3216-3227
- Anvarian Z, Mykytyn K, Mukhopadhyay S, Pedersen LB, Christensen ST (2019) Cellular signalling by primary cilia in development, organ function and disease. *Nat Rev Nephrol* 15: 199-219
- Arno B, Grassivaro F, Rossi C, Bergamaschi A, Castiglioni V, Furlan R, Greter M, Favaro R, Comi G, Becher B *et al* (2014) Neural progenitor cells orchestrate microglia migration and positioning into the developing cortex. *Nat Commun* 5: 5611
- Arquint C, Gabryjonczyk AM, Nigg EA (2014) Centrosomes as signalling centres. *Philos Trans R Soc Lond B Biol Sci* 369
- Balestra FR, Domínguez-Calvo A, Wolf B, Busso C, Buff A, Averink T, Lipsanen-Nyman M, Huertas P, Ríos RM, Gönczy P (2021) TRIM37 prevents formation of centriolar protein assemblies by regulating Centrobin. *Elife* 10
- Balestra FR, Strnad P, Flückiger I, Gönczy P (2013) Discovering regulators of centriole biogenesis through siRNA-based functional genomics in human cells. *Dev Cell* 25: 555-571
- Barrera JA, Kao LR, Hammer RE, Seemann J, Fuchs JL, Megraw TL (2010) CDK5RAP2 regulates centriole engagement and cohesion in mice. *Dev Cell* 18: 913-926
- Baschieri F, Porshneva K, Montagnac G (2020) Frustrated clathrin-mediated endocytosis - causes and possible functions. *J Cell Sci* 133

Baudoin JP, Viou L, Launay PS, Luccardini C, Espeso Gil S, Kiyasova V, Irinopoulou T, Alvarez C, Rio JP, Boudier T *et al* (2012) Tangentially migrating neurons assemble a primary cilium that promotes their reorientation to the cortical plate. *Neuron* 76: 1108-1122

Bazinet C, Katzen AL, Morgan M, Mahowald AP, Lemmon SK (1993) The *Drosophila* clathrin heavy chain gene: clathrin function is essential in a multicellular organism. *Genetics* 134: 1119-1134

Beattie EC, Howe CL, Wilde A, Brodsky FM, Mobley WC (2000) NGF signals through TrkA to increase clathrin at the plasma membrane and enhance clathrin-mediated membrane trafficking. *J Neurosci* 20: 7325-7333

Benmerah A, Lamaze C, Begue B, Schmid SL, Dautry-Varsat A, Cerf-Bensussan N (1998) AP-2/Eps15 interaction is required for receptor-mediated endocytosis. *J Cell Biol* 140: 1055-1062

Bera S, Cambor-Perujo S, Calleja Barca E, Negrete-Hurtado A, Racho J, De Bruyckere E, Wittich C, Ellrich N, Martins S, Adjaye J *et al* (2020) AP-2 reduces amyloidogenesis by promoting BACE1 trafficking and degradation in neurons. *EMBO Rep* 21: e47954

Berdnik D, Török T, González-Gaitán M, Knoblich JA (2002) The Endocytic Protein α -Adaptin Is Required for Numb-Mediated Asymmetric Cell Division in *Drosophila*. *Dev Cell* 3: 221-231

Bergstralh DT, St Johnston D (2014) Spindle orientation: what if it goes wrong? *Semin Cell Dev Biol* 34: 140-145

Berlin RD, Oliver JM (1980) Surface functions during mitosis. II. Quantitation of pinocytosis and kinetic characterization of the mitotic cycle with a new fluorescence technique. *J Cell Biol* 85: 660-671

Bettencourt-Dias M, Glover DM (2007) Centrosome biogenesis and function: centrosomes brings new understanding. *Nat Rev Mol Cell Biol* 8: 451-463

Bettencourt-Dias M, Hildebrandt F, Pellman D, Woods G, Godinho SA (2011) Centrosomes and cilia in human disease. *Trends Genet* 27: 307-315

Blitzer JT, Nusse R (2006) A critical role for endocytosis in Wnt signaling. *BMC Cell Biol* 7: 28

Bloom AB, Zaman MH (2014) Influence of the microenvironment on cell fate determination and migration. *Physiol Genomics* 46: 309-314

Booth DG, Hood FE, Prior IA, Royle SJ (2011) A TACC3/ch-TOG/clathrin complex stabilises kinetochore fibres by inter-microtubule bridging. *EMBO J* 30: 906-919

Boucrot E, Ferreira AP, Almeida-Souza L, Debard S, Vallis Y, Howard G, Bertot L, Sauvonnet N, McMahon HT (2015) Endophilin marks and controls a clathrin-independent endocytic pathway. *Nature* 517: 460-465

Boucrot E, Howes MT, Kirchhausen T, Parton RG (2011) Redistribution of caveolae during mitosis. *J Cell Sci* 124: 1965-1972

Boucrot E, Kirchhausen T (2007) Endosomal recycling controls plasma membrane area during mitosis. *Proc Natl Acad Sci U S A* 104: 7939-7944

Bourke E, Dodson H, Merdes A, Cuffe L, Zachos G, Walker M, Gillespie D, Morrison CG (2007) DNA damage induces Chk1-dependent centrosome amplification. *EMBO Rep* 8: 603-609

Bower JJ, Vance LD, Psioda M, Smith-Roe SL, Simpson DA, Ibrahim JG, Hoadley KA, Perou CM, Kaufmann WK (2017) Patterns of cell cycle checkpoint deregulation associated with intrinsic molecular subtypes of human breast cancer cells. *NPJ Breast Cancer* 3: 9

Brodsky FM, Chen CY, Knuehl C, Towler MC, Wakeham DE (2001) Biological basket weaving: formation and function of clathrin-coated vesicles. *Annu Rev Cell Dev Biol* 17: 517-568

Brown CJ, Lain S, Verma CS, Fersht AR, Lane DP (2009) Awakening guardian angels: drugging the p53 pathway. *Nat Rev Cancer* 9: 862-873

Buckley CM, King JS (2017) Drinking problems: mechanisms of macropinosome formation and maturation. *FEBS J* 284: 3778-3790

Burigotto M, Mattivi A, Migliorati D, Magnani G, Valentini C, Rocuzzo M, Offterdinger M, Pizzato M, Schmidt A, Villunger A *et al* (2021) Centriolar distal appendages activate the centrosome-PIDDosome-p53 signalling axis via ANKRD26. *EMBO J* 40: e104844

Burrows RC, Lillien L, Levitt P (2000) Mechanisms of progenitor maturation are conserved in the striatum and cortex. *Dev Neurosci* 22: 7-15

Buser DP, Ritz MF, Moes S, Tostado C, Frank S, Spiess M, Mariani L, Jenö P, Boulay JL, Hutter G (2019) Quantitative proteomics reveals reduction of endocytic machinery components in gliomas. *EBioMedicine* 46: 32-41

Cabral G, Sans SS, Cowan CR, Dammermann A (2013) Multiple mechanisms contribute to centriole separation in *C. elegans*. *Curr Biol* 23: 1380-1387

Cai T, Cinkornpumin JK, Yu Z, Villarreal OD, Pastor WA, Richard S (2021) Deletion of RBMX RGG/RG motif in Shashi-XLID syndrome leads to aberrant p53 activation and neuronal differentiation defects. *Cell Rep* 36: 109337

Calegari F, Haubensak W, Haffner C, Huttner WB (2005) Selective lengthening of the cell cycle in the neurogenic subpopulation of neural progenitor cells during mouse brain development. *J Neurosci* 25: 6533-6538

Calegari F, Huttner WB (2003) An inhibition of cyclin-dependent kinases that lengthens, but does not arrest, neuroepithelial cell cycle induces premature neurogenesis. *J Cell Sci* 116: 4947-4955

Capalbo L, Mela I, Abad MA, Jeyaprakash AA, Edwardson JM, D'Avino PP (2016) Coordinated regulation of the ESCRT-III component CHMP4C by the chromosomal passenger complex and centralspindlin during cytokinesis. *Open Biol* 6

- Carazo-Salas RE, Guarguaglini G, Gruss OJ, Segref A, Karsenti E, Mattaj IW (1999) Generation of GTP-bound Ran by RCC1 is required for chromatin-induced mitotic spindle formation. *Nature* 400: 178-181
- Carlton JG, Caballe A, Agromayor M, Kloc M, Martin-Serrano J (2012) ESCRT-III governs the Aurora B-mediated abscission checkpoint through CHMP4C. *Science* 336: 220-225
- Castedo M, Perfettini JL, Roumier T, Valent A, Raslova H, Yakushijin K, Horne D, Feunteun J, Lenoir G, Medema R *et al* (2004) Mitotic catastrophe constitutes a special case of apoptosis whose suppression entails aneuploidy. *Oncogene* 23: 4362-4370
- Castrillon DH, Wasserman SA (1994) Diaphanous Is Required for Cytokinesis in *Drosophila* and Shares Domains of Similarity with the Products of the Limb Deformity Gene. *Development* 120: 3367-3377
- Caviness VS, Jr., Goto T, Tarui T, Takahashi T, Bhide PG, Nowakowski RS (2003) Cell output, cell cycle duration and neuronal specification: a model of integrated mechanisms of the neocortical proliferative process. *Cereb Cortex* 13: 592-598
- Cayrol C, Cougoule C, Wright M (2002) The beta2-adaptin clathrin adaptor interacts with the mitotic checkpoint kinase BubR1. *Biochem Biophys Res Commun* 298: 720-730
- Chao WT, Kunz J (2009) Focal adhesion disassembly requires clathrin-dependent endocytosis of integrins. *FEBS Lett* 583: 1337-1343
- Chavali M, Klingener M, Kokkosis AG, Garkun Y, Felong S, Maffei A, Aguirre A (2018) Non-canonical Wnt signaling regulates neural stem cell quiescence during homeostasis and after demyelination. *Nat Commun* 9: 36
- Chavali PL, Pütz M, Gergely F (2014) Small organelle, big responsibility: the role of centrosomes in development and disease. *Philos Trans R Soc Lond B Biol Sci* 369
- Cheeseman LP, Harry EF, McAinsh AD, Prior IA, Royle SJ (2013) Specific removal of TACC3-ch-TOG-clathrin at metaphase deregulates kinetochore fiber tension. *J Cell Sci* 126: 2102-2113
- Chen F, Wu J, Iwanski MK, Jurriens D, Sandron A, Pasolli M, Puma G, Kromhout JZ, Yang C, Nijenhuis W *et al* (2022) Self-assembly of pericentriolar material in interphase cells lacking centrioles. *Elife* 11
- Chen H, Fre S, Slepnev VI, Capua MR, Takei K, Butler MH, Di Fiore PP, De Camilli P (1998) Epsin is an EH-domain-binding protein implicated in clathrin-mediated endocytosis. *Nature* 394: 793-797
- Chen H, Ko G, Zatti A, Di Giacomo G, Liu L, Raiteri E, Perucco E, Collesi C, Min W, Zeiss C *et al* (2009) Embryonic arrest at midgestation and disruption of Notch signaling produced by the absence of both epsin 1 and epsin 2 in mice. *Proc Natl Acad Sci U S A* 106: 13838-13843
- Chen X, Irani NG, Friml J (2011) Clathrin-mediated endocytosis: the gateway into plant cells. *Curr Opin Plant Biol* 14: 674-682

Chiba K, Yuki S, Masataka K, Toshiharu S, Seiich U (2014) Simple and Direct Assembly of Kymographs from Movies Using KYMOMAKER. *Traffic* 15: 1-11

Chinen T, Yamazaki K, Hashimoto K, Fujii K, Watanabe K, Takeda Y, Yamamoto S, Nozaki Y, Tsuchiya Y, Takao D *et al* (2021) Centriole and PCM cooperatively recruit CEP192 to spindle poles to promote bipolar spindle assembly. *J Cell Biol* 220

Christ L, Wenzel EM, Liestøl K, Raiborg C, Campsteijn C, Stenmark H (2016) ALIX and ESCRT-I/II function as parallel ESCRT-III recruiters in cytokinetic abscission. *J Cell Biol* 212: 499-513

Classon M, Harlow E (2002) The retinoblastoma tumour suppressor in development and cancer. *Nat Rev Cancer* 2: 910-917

Commisso C, Davidson SM, Soydaner-Azeloglu RG, Parker SJ, Kamphorst JJ, Hackett S, Grabocka E, Nofal M, Drebin JA, Thompson CB *et al* (2013) Macropinocytosis of protein is an amino acid supply route in Ras-transformed cells. *Nature* 497: 633-637

Conduit PT, Wainman A, Raff JW (2015) Centrosome function and assembly in animal cells. *Nat Rev Mol Cell Biol* 16: 611-624

Conner SD, Schmid SL (2002) Identification of an adaptor-associated kinase, AAK1, as a regulator of clathrin-mediated endocytosis. *J Cell Biol* 156: 921-929

Conner SD, Schmid SL (2003a) Differential requirements for AP-2 in clathrin-mediated endocytosis. *J Cell Biol* 162: 773-779

Conner SD, Schmid SL (2003b) Regulated portals of entry into the cell. *Nature* 422: 37-44

Cosker KE, Eickholt BJ (2007) Phosphoinositide 3-kinase signalling events controlling axonal morphogenesis. *Biochem Soc Trans* 35: 207-210

Cosker KE, Segal RA (2014) Neuronal signaling through endocytosis. *Cold Spring Harb Perspect Biol* 6: a020669-a020669

D'Aquino KE, Monje-Casas F, Paulson J, Reiser V, Charles GM, Lai L, Shokat KM, Amon A (2005) The protein kinase Kin4 inhibits exit from mitosis in response to spindle position defects. *Mol Cell* 19: 223-234

Damke H, Baba T, Warnock DE, Schmid SL (1994) Induction of mutant dynamin specifically blocks endocytic coated vesicle formation. *J Cell Biol* 127: 915-934

Daumke O, Roux A, Haucke V (2014) BAR domain scaffolds in dynamin-mediated membrane fission. *Cell* 156: 882-892

De Franceschi N, Arjonen A, Elkhatib N, Denessiouk K, Wrobel AG, Wilson TA, Pouwels J, Montagnac G, Owen DJ, Ivaska J (2016) Selective integrin endocytosis is driven by interactions between the integrin α -chain and AP2. *Nat Struct Mol Biol* 23: 172-179

del Pozo MA, Alderson NB, Kiosses WB, Chiang HH, Anderson RG, Schwartz MA (2004) Integrins regulate Rac targeting by internalization of membrane domains. *Science* 303: 839-842

des Portes V, Pinard JM, Billuart P, Vinet MC, Koulakoff A, Carrie A, Gelot A, Dupuis E, Motte J, Berwald-Netter Y *et al* (1998) A novel CNS gene required for neuronal migration and involved in X-linked subcortical laminar heterotopia and lissencephaly syndrome. *Cell* 92: 51-61

Dionne LK, Shim K, Hoshi M, Cheng T, Wang J, Marthiens V, Knoten A, Basto R, Jain S, Mahjoub MR (2018) Centrosome amplification disrupts renal development and causes cystogenesis. *J Cell Biol* 217: 2485-2501

Donaldson JG (2019) Macropinosome formation, maturation and membrane recycling: lessons from clathrin-independent endosomal membrane systems. *Philos Trans R Soc Lond B Biol Sci* 374: 20180148

Downes CS, Clarke DJ, Mullinger AM, Giménez-Abián JF, Creighton AM, Johnson RT (1994) A topoisomerase II-dependent G2 cycle checkpoint in mammalian cells/. *Nature* 372: 467-470

Doxsey S, McCollum D, Theurkauf W (2005) Centrosomes in cellular regulation. *Annu Rev Cell Dev Biol* 21: 411-434

Edeling MA, Smith C, Owen D (2006) Life of a clathrin coat: insights from clathrin and AP structures. *Nat Rev Mol Cell Biol* 7: 32-44

Egami Y, Taguchi T, Maekawa M, Arai H, Araki N (2014) Small GTPases and phosphoinositides in the regulatory mechanisms of macropinosome formation and maturation. *Front Physiol* 5: 374

Ehlén Å, Rosselló CA, von Stedingk K, Höög G, Nilsson E, Pettersson HM, Jirström K, Alvarado-Kristensson M (2012) Tumors with nonfunctional retinoblastoma protein are killed by reduced γ -tubulin levels. *J Biol Chem* 287: 17241-17247

Elias LA, Wang DD, Kriegstein AR (2007) Gap junction adhesion is necessary for radial migration in the neocortex. *Nature* 448: 901-907

Eriksson PS, Perfilieva E, Björk-Eriksson T, Alborn AM, Nordborg C, Peterson DA, Gage FH (1998) Neurogenesis in the adult human hippocampus. *Nat Med* 4: 1313-1317

Evans LT, Anglen T, Scott P, Lukasik K, Loncarek J, Holland AJ (2021) ANKRD26 recruits PIDD1 to centriolar distal appendages to activate the PIDDosome following centrosome amplification. *EMBO J* 40: e105106

Ezratty EJ, Bertaux C, Marcantonio EE, Gundersen GG (2009) Clathrin mediates integrin endocytosis for focal adhesion disassembly in migrating cells. *J Cell Biol* 187: 733-747

Fang K, Fu W, Beardsley AR, Sun X, Lisanti MP, Liu J (2007) Overexpression of caveolin-1 inhibits endothelial cell proliferation by arresting the cell cycle at G0/G1 phase. *Cell Cycle* 6: 199-204

Farsad K, Ringstad N, Takei K, Floyd SR, Rose K, De Camilli P (2001) Generation of high curvature membranes mediated by direct endophilin bilayer interactions. *J Cell Biol* 155: 193-200

Feng B, Schwarz H, Jesuthasan S (2002) Furrow-specific endocytosis during cytokinesis of zebrafish blastomeres. *Exp Cell Res* 279: 14-20

Ferguson SM, Brasnjo G, Hayashi M, Wolfel M, Collesi C, Giovedi S, Raimondi A, Gong LW, Ariel P, Paradise S *et al* (2007) A selective activity-dependent requirement for dynamin 1 in synaptic vesicle endocytosis. *Science* 316: 570-574

Ferguson SM, Raimondi A, Paradise S, Shen H, Mesaki K, Ferguson A, Destaing O, Ko G, Takasaki J, Cremona O *et al* (2009) Coordinated actions of actin and BAR proteins upstream of dynamin at endocytic clathrin-coated pits. *Dev Cell* 17: 811-822

Ferreira APA, Boucrot E (2018) Mechanisms of Carrier Formation during Clathrin-Independent Endocytosis. *Trends Cell Biol* 28: 188-200

Fielding AB, Royle SJ (2013) Mitotic inhibition of clathrin-mediated endocytosis. *Cell Mol Life Sci* 70: 3423-3433

Fielding AB, Willox AK, Okeke E, Royle SJ (2012) Clathrin-mediated endocytosis is inhibited during mitosis. *Proc Natl Acad Sci U S A* 109: 6572-6577

Foraker AB, Camus SM, Evans TM, Majeed SR, Chen CY, Taner SB, Corrêa IR, Doxsey SJ, Brodsky FM (2012) Clathrin promotes centrosome integrity in early mitosis through stabilization of centrosomal ch-TOG. *J Cell Biol* 198: 591-605

Ford MG, Mills IG, Peter BJ, Vallis Y, Praefcke GJ, Evans PR, McMahon HT (2002) Curvature of clathrin-coated pits driven by epsin. *Nature* 419: 361-366

Foster DA, Yellen P, Xu L, Saqcena M (2010) Regulation of G1 Cell Cycle Progression: Distinguishing the Restriction Point from a Nutrient-Sensing Cell Growth Checkpoint(s). *Genes Cancer* 1: 1124-1131

Franco SJ, Muller U (2013) Shaping our minds: stem and progenitor cell diversity in the mammalian neocortex. *Neuron* 77: 19-34

Fridlyanskaya I, Alekseenko L, Nikolsky N (2015) Senescence as a general cellular response to stress: A mini-review. *Exp Gerontol* 72: 124-128

Friocourt G, Chafey P, Billuart P, Koulakoff A, Vinet MC, Schaar BT, McConnell SK, Francis F, Chelly J (2001) Doublecortin interacts with mu subunits of clathrin adaptor complexes in the developing nervous system. *Mol Cell Neurosci* 18: 307-319

Fu W, Tao W, Zheng P, Fu J, Bian M, Jiang Q, Clarke PR, Zhang C (2010) Clathrin recruits phosphorylated TACC3 to spindle poles for bipolar spindle assembly and chromosome alignment. *J Cell Sci* 123: 3645-3651

Fujii M, Kawai K, Egami Y, Araki N (2013) Dissecting the roles of Rac1 activation and deactivation in macropinocytosis using microscopic photo-manipulation. *Sci Rep* 3: 2385

Fujita H, Yoshino Y, Chiba N (2016) Regulation of the centrosome cycle. *Mol Cell Oncol* 3: e1075643

Fukasawa K (2007) Oncogenes and tumour suppressors take on centrosomes. *Nat Rev Cancer* 7: 911-924

Gad H, Ringstad N, Low P, Kjaerulff O, Gustafsson J, Wenk M, Di Paolo G, Nemoto Y, Crun J, Ellisman MH *et al* (2000) Fission and uncoating of synaptic clathrin-coated vesicles are perturbed by disruption of interactions with the SH3 domain of endophilin. *Neuron* 27: 301-312

Gallop JL, Jao CC, Kent HM, Butler PJ, Evans PR, Langen R, McMahon HT (2006) Mechanism of endophilin N-BAR domain-mediated membrane curvature. *EMBO J* 25: 2898-2910

Ganem NJ, Godinho SA, Pellman D (2009) A mechanism linking extra centrosomes to chromosomal instability. *Nature* 460: 278-282

Gartenmann L, Vicente CC, Wainman A, Novak ZA, Sieber B, Richens JH, Raff JW (2020) Sas-6, Ana2 and Sas-4 self-organise into macromolecular structures that can be used to probe centriole and centrosome assembly. *J Cell Sci* 133

Gertler FB, Bennett RL, Clark MJ, Hoffmann FM (1989) Drosophila abl tyrosine kinase in embryonic CNS axons: a role in axonogenesis is revealed through dosage-sensitive interactions with disabled. *Cell* 58: 103-113

Ghossoub R, Lindbæk L, Molla-Herman A, Schmitt A, Christensen ST, Benmerah A (2016) Morphological and Functional Characterization of the Ciliary Pocket by Electron and Fluorescence Microscopy. *Methods Mol Biol* 1454: 35-51

Gilbert SF, Barresi MJF (2016) *Developmental biology*. Sinauer Associates is an imprint of Oxford University Press

Gorvin CM, Rogers A, Stewart M, Paudyal A, Hough TA, Teboul L, Wells S, Brown SD, Cox RD, Thakker RV (2017) N-ethyl-N-nitrosourea-Induced Adaptor Protein 2 Sigma Subunit 1 (*JBMR Plus* 1: 3-15

Gotz M, Huttner WB (2005) The cell biology of neurogenesis. *Nat Rev Mol Cell Biol* 6: 777-788

Gregg C, Weiss S (2003) Generation of functional radial glial cells by embryonic and adult forebrain neural stem cells. *J Neurosci* 23: 11587-11601

Griffith E, Walker S, Martin CA, Vagnarelli P, Stiff T, Vernay B, Al Sanna N, Saggari A, Hamel B, Earnshaw WC *et al* (2008) Mutations in pericentrin cause Seckel syndrome with defective ATR-dependent DNA damage signaling. *Nat Genet* 40: 232-236

Griner EM, Kazanietz MG (2007) Protein kinase C and other diacylglycerol effectors in cancer. *Nat Rev Cancer* 7: 281-294

Gu M, LaJoie D, Chen OS, von Appen A, Ladinsky MS, Redd MJ, Nikolova L, Bjorkman PJ, Sundquist WI, Ullman KS *et al* (2017) LEM2 recruits CHMP7 for ESCRT-mediated nuclear envelope closure in fission yeast and human cells. *Proc Natl Acad Sci U S A* 114: E2166-E2175

Guo J, Higginbotham H, Li J, Nichols J, Hirt J, Ghukasyan V, Anton ES (2015) Developmental disruptions underlying brain abnormalities in ciliopathies. *Nat Commun* 6: 7857

Güttinger S, Laurell E, Kutay U (2009) Orchestrating nuclear envelope disassembly and reassembly during mitosis. *Nat Rev Mol Cell Biol* 10: 178-191

Haditsch U, Anderson MP, Freewoman J, Cord B, Babu H, Brakebusch C, Palmer TD (2013) Neuronal Rac1 is required for learning-evoked neurogenesis. *J Neurosci* 33: 12229-12241

Harrington AW, Ginty DD (2013) Long-distance retrograde neurotrophic factor signalling in neurons. *Nat Rev Neurosci* 14: 177-187

Hartwell LH, Weinert TA (1989) Checkpoints: controls that ensure the order of cell cycle events. *Science* 246: 629-634

Haubensak W, Attardo A, Denk W, Huttner WB (2004) Neurons arise in the basal neuroepithelium of the early mammalian telencephalon: a major site of neurogenesis. *Proc Natl Acad Sci U S A* 101: 3196-3201

Hayashi MT, Karlseder J (2013) DNA damage associated with mitosis and cytokinesis failure. *Oncogene* 32: 4593-4601

He G, Gupta S, Yi M, Michaely P, Hobbs HH, Cohen JC (2002) ARH is a modular adaptor protein that interacts with the LDL receptor, clathrin, and AP-2. *J Biol Chem* 277: 44044-44049

Henne WM, Boucrot E, Meinecke M, Evergren E, Vallis Y, Mittal R, McMahon HT (2010) FCHO proteins are nucleators of clathrin-mediated endocytosis. *Science* 328: 1281-1284

Herrick TM, Cooper JA (2002) A hypomorphic allele of dab1 reveals regional differences in reelin-Dab1 signaling during brain development. *Development* 129: 787-796

Higginbotham H, Eom TY, Mariani LE, Bachleda A, Hirt J, Gukassyan V, Cusack CL, Lai C, Caspary T, Anton ES (2012) Arl13b in primary cilia regulates the migration and placement of interneurons in the developing cerebral cortex. *Dev Cell* 23: 925-938

Hinze C, Boucrot E (2018) Local actin polymerization during endocytic carrier formation. *Biochem Soc Trans* 46: 565-576

Hobert O (2008) Regulatory logic of neuronal diversity: terminal selector genes and selector motifs. *Proc Natl Acad Sci U S A* 105: 20067-20071

Hobert O (2011) Regulation of terminal differentiation programs in the nervous system. *Annu Rev Cell Dev Biol* 27: 681-696

Honing S, Ricotta D, Krauss M, Spate K, Spolaore B, Motley A, Robinson M, Robinson C, Haucke V, Owen DJ (2005) Phosphatidylinositol-(4,5)-bisphosphate regulates sorting signal recognition by the clathrin-associated adaptor complex AP2. *Mol Cell* 18: 519-531

Hood FE, Royle SJ (2009) Functional equivalence of the clathrin heavy chains CHC17 and CHC22 in endocytosis and mitosis. *J Cell Sci* 122: 2185-2190

Horgusluoglu E, Nudelman K, Nho K, Saykin AJ (2017) Adult neurogenesis and neurodegenerative diseases: A systems biology perspective. *Am J Med Genet B Neuropsychiatr Genet* 174: 93-112

- Houart C, Caneparo L, Heisenberg CP, Barth KA, Take-Uchi M, Wilson SW (2002) Establishment of the telencephalon during gastrulation by local antagonism of Wnt signaling. *Neuron* 35: 255-265
- Howe CL, Valletta JS, Rusnak AS, Mobley WC (2001) NGF signaling from clathrin-coated vesicles: Evidence that signaling endosomes serve as a platform for the Ras-MAPK pathway. *Neuron* 32: 801-814
- Howell BW, Gertler FB, Cooper JA (1997a) Mouse disabled (mDab1): a Src binding protein implicated in neuronal development. *EMBO J* 16: 121-132
- Howell BW, Hawkes R, Soriano P, Cooper JA (1997b) Neuronal position in the developing brain is regulated by mouse disabled-1. *Nature* 389: 733-737
- Hořejší B, Vinopal S, Sládková V, Dráberová E, Sulimenko V, Sulimenko T, Vosecká V, Philimonenko A, Hozák P, Katsetos CD *et al* (2012) Nuclear γ -tubulin associates with nucleoli and interacts with tumor suppressor protein C53. *J Cell Physiol* 227: 367-382
- Hubbard K, Ozer HL (1999) Mechanism of immortalization. *Age (Omaha)* 22: 65-69
- Höglinger GU, Rizk P, Muriel MP, Duyckaerts C, Oertel WH, Caille I, Hirsch EC (2004) Dopamine depletion impairs precursor cell proliferation in Parkinson disease. *Nat Neurosci* 7: 726-735
- Höög G, Zarrizi R, von Stedingk K, Jonsson K, Alvarado-Kristensson M (2011) Nuclear localization of γ -tubulin affects E2F transcriptional activity and S-phase progression. *FASEB J* 25: 3815-3827
- Insolera R, Bazzi H, Shao W, Anderson KV, Shi SH (2014) Cortical neurogenesis in the absence of centrioles. *Nat Neurosci* 17: 1528-1535
- Ishikawa Y, Maeda M, Pasham M, Aguet F, Tacheva-Grigorova SK, Masuda T, Yi H, Lee SU, Xu J, Teruya-Feldstein J *et al* (2015) Role of the clathrin adaptor PICALM in normal hematopoiesis and polycythemia vera pathophysiology. *Haematologica* 100: 439-451
- Izawa D, Pines J (2015) The mitotic checkpoint complex binds a second CDC20 to inhibit active APC/C. *Nature* 517: 631-634
- Jaiswal S, Singh P (2021) Centrosome dysfunction in human diseases. *Semin Cell Dev Biol* 110: 113-122
- Jeffery CJ (2003) Moonlighting proteins: old proteins learning new tricks. *Trends Genet* 19: 415-417
- Jin K, Minami M, Lan JQ, Mao XO, Batteur S, Simon RP, Greenberg DA (2001) Neurogenesis in dentate subgranular zone and rostral subventricular zone after focal cerebral ischemia in the rat. *Proc Natl Acad Sci U S A* 98: 4710-4715
- Jin K, Sun Y, Xie L, Peel A, Mao XO, Batteur S, Greenberg DA (2003) Directed migration of neuronal precursors into the ischemic cerebral cortex and striatum. *Mol Cell Neurosci* 24: 171-189

Joshi S, Perera S, Gilbert J, Smith CM, Mariana A, Gordon CP, Sakoff JA, McCluskey A, Robinson PJ, Braithwaite AW *et al* (2010) The dynamin inhibitors MiTMAB and OcTMAB induce cytokinesis failure and inhibit cell proliferation in human cancer cells. *Mol Cancer Ther* 9: 1995-2006

Jossin Y, Cooper JA (2011) Reelin, Rap1 and N-cadherin orient the migration of multipolar neurons in the developing neocortex. *Nat Neurosci* 14: 697-703

Kadlecova Z, Spielman SJ, Loerke D, Mohanakrishnan A, Reed DK, Schmid SL (2017) Regulation of clathrin-mediated endocytosis by hierarchical allosteric activation of AP2. *J Cell Biol* 216: 167-179

Kaindl AM, Passemard S, Kumar P, Kraemer N, Issa L, Zwirner A, Gerard B, Verloes A, Mani S, Gressens P (2010) Many roads lead to primary autosomal recessive microcephaly. *Prog Neurobiol* 90: 363-383

Kaksonen M, Roux A (2018) Mechanisms of clathrin-mediated endocytosis. *Nat Rev Mol Cell Biol* 19: 313-326

Kamiguchi H, Yoshihara F (2001) The role of endocytic I1 trafficking in polarized adhesion and migration of nerve growth cones. *J Neurosci* 21: 9194-9203

Kandasamy M, Couillard-Despres S, Raber KA, Stephan M, Lehner B, Winner B, Kohl Z, Rivera FJ, Nguyen HP, Riess O *et al* (2010) Stem cell quiescence in the hippocampal neurogenic niche is associated with elevated transforming growth factor-beta signaling in an animal model of Huntington disease. *J Neuropathol Exp Neurol* 69: 717-728

Kaplan OI, Doroquez DB, Cevik S, Bowie RV, Clarke L, Sanders AA, Kida K, Rappoport JZ, Sengupta P, Blacque OE (2012) Endocytosis genes facilitate protein and membrane transport in *C. elegans* sensory cilia. *Curr Biol* 22: 451-460

Karasmanis EP, Hwang D, Nakos K, Bowen JR, Angelis D, Spiliotis ET (2019) A Septin Double Ring Controls the Spatiotemporal Organization of the ESCRT Machinery in Cytokinetic Abscission. *Curr Biol* 29: 2174-2182.e2177

Kato J (1999) Induction of S phase by G1 regulatory factors. *Front Biosci* 4: D787-792

Kelly BT, McCoy AJ, Spate K, Miller SE, Evans PR, Honing S, Owen DJ (2008) A structural explanation for the binding of endocytic dileucine motifs by the AP2 complex. *Nature* 456: 976-979

Keung AJ, de Juan-Pardo EM, Schaffer DV, Kumar S (2011) Rho GTPases mediate the mechanosensitive lineage commitment of neural stem cells. *Stem Cells* 29: 1886-1897

Khodjakov A, Rieder CL (1999) The sudden recruitment of gamma-tubulin to the centrosome at the onset of mitosis and its dynamic exchange throughout the cell cycle, do not require microtubules. *J Cell Biol* 146: 585-596

Kirchhausen T (1999) Adaptors for clathrin-mediated traffic. *Annu Rev Cell Dev Biol* 15: 705-732

- Kirchhausen T (2000) Three ways to make a vesicle. *Nat Rev Mol Cell Biol* 1: 187-198
- Kirchhausen T (2009) Imaging endocytic clathrin structures in living cells. *Trends Cell Biol* 19: 596-605
- Klein AL, Zilian O, Suter U, Taylor V (2004) Murine numb regulates granule cell maturation in the cerebellum. *Dev Biol* 266: 161-177
- Koch U, Lehal R, Radtke F (2013) Stem cells living with a Notch. *Development* 140: 689-704
- Koh TW, Verstreken P, Bellen HJ (2004) Dap160/intersectin acts as a stabilizing scaffold required for synaptic development and vesicle endocytosis. *Neuron* 43: 193-205
- Kononenko NL, Claßen GA, Kuijpers M, Puchkov D, Maritzen T, Tempes A, Malik AR, Skalecka A, Bera S, Jaworski J *et al* (2017) Retrograde transport of TrkB-containing autophagosomes via the adaptor AP-2 mediates neuronal complexity and prevents neurodegeneration. *Nature Communications* 8: 1-16
- Kononenko NL, Diril MK, Puchkov D, Kintscher M, Koo SJ, Pfuhl G, Winter Y, Wienisch M, Klingauf J, Breustedt J *et al* (2013) Compromised fidelity of endocytic synaptic vesicle protein sorting in the absence of stonin 2. *Proceedings of the National Academy of Sciences of the United States of America* 110: E526-535
- Kononenko NL, Haucke V (2015) Molecular mechanisms of presynaptic membrane retrieval and synaptic vesicle reformation. *Neuron* 85: 484-496
- Konopka CA, Schleede JB, Skop AR, Bednarek SY (2006) Dynamin and cytokinesis. *Traffic* 7: 239-247
- Koo SJ, Markovic S, Puchkov D, Mahrenholz CC, Beceren-Braun F, Maritzen T, Dervede J, Volkmer R, Oschkinat H, Haucke V (2011) SNARE motif-mediated sorting of synaptobrevin by the endocytic adaptors clathrin assembly lymphoid myeloid leukemia (CALM) and AP180 at synapses. *Proc Natl Acad Sci U S A* 108: 13540-13545
- Koppel DE, Oliver JM, Berlin RD (1982) Surface functions during mitosis. III. Quantitative analysis of ligand-receptor movement into the cleavage furrow: diffusion vs. flow. *J Cell Biol* 93: 950-960
- Koutsopoulos OS, Kretz C, Weller CM, Roux A, Mojzisova H, Bohm J, Koch C, Toussaint A, Heckel E, Stemkens D *et al* (2013) Dynamin 2 homozygous mutation in humans with a lethal congenital syndrome. *Eur J Hum Genet* 21: 637-642
- Kovtun O, Tillu VA, Ariotti N, Parton RG, Collins BM (2015) Cavin family proteins and the assembly of caveolae. *J Cell Sci* 128: 1269-1278
- Kriegstein A, Noctor S, Martínez-Cerdeño V (2006) Patterns of neural stem and progenitor cell division may underlie evolutionary cortical expansion. *Nat Rev Neurosci* 7: 883-890
- Kuhn HG, Dickinson-Anson H, Gage FH (1996) Neurogenesis in the dentate gyrus of the adult rat: age-related decrease of neuronal progenitor proliferation. *J Neurosci* 16: 2027-2033

Kung AL, Sherwood SW, Schimke RT (1990) Cell line-specific differences in the control of cell cycle progression in the absence of mitosis. *Proc Natl Acad Sci U S A* 87: 9553-9557

Kusek G, Campbell M, Doyle F, Tenenbaum SA, Kiebler M, Temple S (2012) Asymmetric segregation of the double-stranded RNA binding protein Staufen2 during mammalian neural stem cell divisions promotes lineage progression. *Cell Stem Cell* 11: 505-516

Kuwabara T, Hsieh J, Muotri A, Yeo G, Warashina M, Lie DC, Moore L, Nakashima K, Asashima M, Gage FH (2009) Wnt-mediated activation of NeuroD1 and retro-elements during adult neurogenesis. *Nat Neurosci* 12: 1097-1105

Lambrus BG, Daggubati V, Uetake Y, Scott PM, Clutario KM, Sluder G, Holland AJ (2016) A USP28-53BP1-p53-p21 signaling axis arrests growth after centrosome loss or prolonged mitosis. *J Cell Biol* 214: 143-153

Lancaster MA, Knoblich JA (2012) Spindle orientation in mammalian cerebral cortical development. *Curr Opin Neurobiol* 22: 737-746

Lange C, Huttner WB, Calegari F (2009) Cdk4/cyclinD1 overexpression in neural stem cells shortens G1, delays neurogenesis, and promotes the generation and expansion of basal progenitors. *Cell Stem Cell* 5: 320-331

Langen UH, Pitulescu ME, Kim JM, Enriquez-Gasca R, Sivaraj KK, Kusumbe AP, Singh A, Di Russo J, Bixel MG, Zhou B *et al* (2017) Cell-matrix signals specify bone endothelial cells during developmental osteogenesis. *Nat Cell Biol* 19: 189-201

Le Belle JE, Orozco NM, Paucar AA, Saxe JP, Mottahedeh J, Pyle AD, Wu H, Kornblum HI (2011) Proliferative neural stem cells have high endogenous ROS levels that regulate self-renewal and neurogenesis in a PI3K/Akt-dependant manner. *Cell Stem Cell* 8: 59-71

Le Roy C, Wrana JL (2005) Clathrin- and non-clathrin-mediated endocytic regulation of cell signalling. *Nat Rev Mol Cell Biol* 6: 112-126

Lee HH, Elia N, Ghirlando R, Lippincott-Schwartz J, Hurley JH (2008) Midbody targeting of the ESCRT machinery by a noncanonical coiled coil in CEP55. *Science* 322: 576-580

Lee JC, Jin Y, Jin J, Kang BG, Nam DH, Joo KM, Cha CI (2011) Functional neural stem cell isolation from brains of adult mutant SOD1 (SOD1(G93A)) transgenic amyotrophic lateral sclerosis (ALS) mice. *Neurol Res* 33: 33-37

Lehtonen S, Shah M, Nielsen R, Iino N, Ryan JJ, Zhou H, Farquhar MG (2008) The endocytic adaptor protein ARH associates with motor and centrosomal proteins and is involved in centrosome assembly and cytokinesis. *Mol Biol Cell* 19: 2949-2961

Lesca C, Germanier M, Raynaud-Messina B, Pichereaux C, Etievant C, Emond S, Burlet-Schiltz O, Monsarrat B, Wright M, Defais M (2005) DNA damage induce gamma-tubulin-RAD51 nuclear complexes in mammalian cells. *Oncogene* 24: 5165-5172

Li W, Puertollano R, Bonifacino JS, Overbeek PA, Everett ET (2010) Disruption of the murine Ap2 β 1 gene causes nonsyndromic cleft palate. *Cleft Palate Craniofac J* 47: 566-573

- Lian G, Dettenhofer M, Lu J, Downing M, Chenn A, Wong T, Sheen V (2016) Filamin A- and formin 2-dependent endocytosis regulates proliferation via the canonical Wnt pathway. *Development* 143: 4509-4520
- Lim JP, Gleeson PA (2011) Macropinocytosis: an endocytic pathway for internalising large gulps. *Immunol Cell Biol* 89: 836-843
- Lim Y, Dorstyn L, Kumar S (2021) The p53-caspase-2 axis in the cell cycle and DNA damage response. *Exp Mol Med* 53: 517-527
- Lin CH, Hu CK, Shih HM (2010) Clathrin heavy chain mediates TACC3 targeting to mitotic spindles to ensure spindle stability. *J Cell Biol* 189: 1097-1105
- Lin M, Xie SS, Chan KY (2022) An updated view on the centrosome as a cell cycle regulator. *Cell Div* 17: 1
- Lingle WL, Lutz WH, Ingle JN, Maihle NJ, Salisbury JL (1998) Centrosome hypertrophy in human breast tumors: implications for genomic stability and cell polarity. *Proc Natl Acad Sci U S A* 95: 2950-2955
- Liu Z, Roche PA (2015) Macropinocytosis in phagocytes: regulation of MHC class-II-restricted antigen presentation in dendritic cells. *Front Physiol* 6: 1
- Liu Z, Zheng Y (2009) A requirement for epsin in mitotic membrane and spindle organization. *J Cell Biol* 186: 473-480
- Lizarraga SB, Margossian SP, Harris MH, Campagna DR, Han AP, Blevins S, Mudbhary R, Barker JE, Walsh CA, Fleming MD (2010) Cdk5rap2 regulates centrosome function and chromosome segregation in neuronal progenitors. *Development* 137: 1907-1917
- Loncarek J, Hergert P, Khodjakov A (2010) Centriole reduplication during prolonged interphase requires procentriole maturation governed by Plk1. *Curr Biol* 20: 1277-1282
- Lopez-Hernandez T, Puchkov D, Krause E, Maritzen T, Haucke V (2020) Endocytic regulation of cellular ion homeostasis controls lysosome biogenesis. *Nat Cell Biol* 22: 815-827
- Luders J, Stearns T (2007) Microtubule-organizing centres: a re-evaluation. *Nat Rev Mol Cell Biol* 8: 161-167
- Ludueña RF (2013) A hypothesis on the origin and evolution of tubulin. *Int Rev Cell Mol Biol* 302: 41-185
- Luo K, Yuan J, Chen J, Lou Z (2009) Topoisomerase IIalpha controls the decatenation checkpoint. *Nat Cell Biol* 11: 204-210
- Luo X, Chen J, Song WX, Tang N, Luo J, Deng ZL, Sharff KA, He G, Bi Y, He BC *et al* (2008) Osteogenic BMPs promote tumor growth of human osteosarcomas that harbor differentiation defects. *Lab Invest* 88: 1264-1277

- Mani M, Lee SY, Lucast L, Cremona O, Di Paolo G, De Camilli P, Ryan TA (2007) The dual phosphatase activity of synaptojanin1 is required for both efficient synaptic vesicle endocytosis and reavailability at nerve terminals. *Neuron* 56: 1004-1018
- Maqsood MI, Matin MM, Bahrami AR, Ghasroldasht MM (2013) Immortality of cell lines: challenges and advantages of establishment. *Cell Biol Int* 37: 1038-1045
- Maro B, Johnson MH, Pickering SJ, Louvard D (1985) Changes in the distribution of membranous organelles during mouse early development. *J Embryol Exp Morphol* 90: 287-309
- Marthiens V, Rujano MA, Pannetier C, Tessier S, Paul-Gilloteaux P, Basto R (2013) Centrosome amplification causes microcephaly. *Nat Cell Biol* 15: 731-740
- Martinez-Cerdeno V, Noctor SC (2018) Neural Progenitor Cell Terminology. *Front Neuroanat* 12: 104
- Matsumoto M, Sawada M, García-González D, Herranz-Pérez V, Ogino T, Bang Nguyen H, Quynh Thai T, Narita K, Kumamoto N, Ugawa S *et al* (2019) Dynamic Changes in Ultrastructure of the Primary Cilium in Migrating Neuroblasts in the Postnatal Brain. *J Neurosci* 39: 9967-9988
- Matsumura S, Kojidani T, Kamioka Y, Uchida S, Haraguchi T, Kimura A, Toyoshima F (2016) Interphase adhesion geometry is transmitted to an internal regulator for spindle orientation via caveolin-1. *Nat Commun* 7: ncomms11858
- Mattaloni SM, Ferretti AC, Tonucci FM, Favre C, Goldenring JR, Larocca MC (2013) Centrosomal AKAP350 modulates the G1/S transition. *Cell Logist* 3: e26331
- Mattera R, Boehm M, Chaudhuri R, Prabhu Y, Bonifacino JS (2011) Conservation and diversification of dileucine signal recognition by adaptor protein (AP) complex variants. *J Biol Chem* 286: 2022-2030
- Mayor S, Parton RG, Donaldson JG (2014) Clathrin-independent pathways of endocytosis. *Cold Spring Harb Perspect Biol* 6: a016758-a016758
- Mazia D (1987) The chromosome cycle and the centrosome cycle in the mitotic cycle. *Int Rev Cytol* 100: 49-92
- McMahon HT, Boucrot E (2011) Molecular mechanism and physiological functions of clathrin-mediated endocytosis. *Nat Rev Mol Cell Biol* 12: 517-533
- Meinecke M, Boucrot E, Camdere G, Hon WC, Mittal R, McMahon HT (2013) Cooperative recruitment of dynamin and BIN/amphiphysin/Rvs (BAR) domain-containing proteins leads to GTP-dependent membrane scission. *J Biol Chem* 288: 6651-6661
- Meitinger F, Anzola JV, Kaulich M, Richardson A, Stender JD, Benner C, Glass CK, Dowdy SF, Desai A, Shiau AK *et al* (2016) 53BP1 and USP28 mediate p53 activation and G1 arrest after centrosome loss or extended mitotic duration. *J Cell Biol* 214: 155-166

- Meitinger F, Ohta M, Lee KY, Watanabe S, Davis RL, Anzola JV, Kabeche R, Jenkins DA, Shiao AK, Desai A *et al* (2020) TRIM37 controls cancer-specific vulnerability to PLK4 inhibition. *Nature* 585: 440-446
- Mendelsohn AR, Hamer JD, Wang ZB, Brent R (2002) Cyclin D3 activates Caspase 2, connecting cell proliferation with cell death. *Proc Natl Acad Sci U S A* 99: 6871-6876
- Menendez D, Inga A, Resnick MA (2009) The expanding universe of p53 targets. *Nat Rev Cancer* 9: 724-737
- Meraldi P, Nigg EA (2002) The centrosome cycle. *FEBS Lett* 521: 9-13
- Mercer J, Helenius A (2009) Virus entry by macropinocytosis. *Nat Cell Biol* 11: 510-520
- Mestres I, Chuang JZ, Calegari F, Conde C, Sung CH (2016) SARA regulates neuronal migration during neocortical development through L1 trafficking. *Development* 143: 3143-3153
- Mettlen M, Chen PH, Srinivasan S, Danuser G, Schmid SL (2018) Regulation of Clathrin-Mediated Endocytosis. *Annu Rev Biochem* 87: 871-896
- Meunier S, Vernos I (2012) Microtubule assembly during mitosis - from distinct origins to distinct functions? *J Cell Sci* 125: 2805-2814
- Meunier S, Vernos I (2016) Acentrosomal Microtubule Assembly in Mitosis: The Where, When, and How. *Trends Cell Biol* 26: 80-87
- Milesi C, Alberici P, Pozzi B, Oldani A, Beznoussenko GV, Raimondi A, Soppo BE, Amodio S, Caldieri G, Malabarba MG *et al* (2019) Redundant and nonredundant organismal functions of EPS15 and EPS15L1. *Life Sci Alliance* 2: e201800273
- Miller SE, Sahlender DA, Graham SC, Honing S, Robinson MS, Peden AA, Owen DJ (2011) The molecular basis for the endocytosis of small R-SNAREs by the clathrin adaptor CALM. *Cell* 147: 1118-1131
- Milosevic I, Giovedi S, Lou X, Raimondi A, Collesi C, Shen H, Paradise S, O'Toole E, Ferguson S, Cremona O *et al* (2011) Recruitment of endophilin to clathrin-coated pit necks is required for efficient vesicle uncoating after fission. *Neuron* 72: 587-601
- Mirzaa GM, Rivière JB, Dobyns WB (2013) Megalencephaly syndromes and activating mutations in the PI3K-AKT pathway: MPPH and MCAP. *Am J Med Genet C Semin Med Genet* 163C: 122-130
- Mishra SK, Keyel PA, Hawryluk MJ, Agostinelli NR, Watkins SC, Traub LM (2002a) Disabled-2 exhibits the properties of a cargo-selective endocytic clathrin adaptor. *EMBO J* 21: 4915-4926
- Mishra SK, Watkins SC, Traub LM (2002b) The autosomal recessive hypercholesterolemia (ARH) protein interfaces directly with the clathrin-coat machinery. *Proc Natl Acad Sci U S A* 99: 16099-16104

- Mitsunari T, Nakatsu F, Shioda N, Love PE, Grinberg A, Bonifacino JS, Ohno H (2005) Clathrin adaptor AP-2 is essential for early embryonal development. *Mol Cell Biol* 25: 9318-9323
- Miyata T, Kawaguchi A, Saito K, Kawano M, Muto T, Ogawa M (2004) Asymmetric production of surface-dividing and non-surface-dividing cortical progenitor cells. *Development* 131: 3133-3145
- Molla-Herman A, Ghossoub R, Blisnick T, Meunier A, Serres C, Silbermann F, Emmerson C, Romeo K, Bourdoncle P, Schmitt A *et al* (2010) The ciliary pocket: an endocytic membrane domain at the base of primary and motile cilia. *J Cell Sci* 123: 1785-1795
- Molè MA, Weberling A, Zernicka-Goetz M (2020) Comparative analysis of human and mouse development: From zygote to pre-gastrulation. *Curr Top Dev Biol* 136: 113-138
- Montagnac G, Meas-Yedid V, Irondelle M, Castro-Castro A, Franco M, Shida T, Nachury MV, Benmerah A, Olivo-Marin JC, Chavrier P (2013) α TAT1 catalyses microtubule acetylation at clathrin-coated pits. *Nature* 502: 567-570
- Moreau K, Fleming A, Imarisio S, Lopez Ramirez A, Mercer JL, Jimenez-Sanchez M, Bento CF, Puri C, Zavodszky E, Siddiqi F *et al* (2014) PICALM modulates autophagy activity and tau accumulation. *Nat Commun* 5: 4998
- Morgan DO (1995) Principles of CDK regulation. *Nature* 374: 131-134
- Moritz M, Braunfeld MB, Sedat JW, Alberts B, Agard DA (1995) Microtubule nucleation by gamma-tubulin-containing rings in the centrosome. *Nature* 378: 638-640
- Morris SM, Cooper JA (2001) Disabled-2 colocalizes with the LDLR in clathrin-coated pits and interacts with AP-2. *Traffic* 2: 111-123
- Moutinho-Pereira S, Stuurman N, Afonso O, Hornsveld M, Aguiar P, Goshima G, Vale RD, Maiato H (2013) Genes involved in centrosome-independent mitotic spindle assembly in *Drosophila* S2 cells. *Proc Natl Acad Sci U S A* 110: 19808-19813
- Mu Y, Gage FH (2011) Adult hippocampal neurogenesis and its role in Alzheimer's disease. *Mol Neurodegener* 6: 85
- Murdoch JD, Rostovsky CM, Gowrisankaran S, Arora AS, Soukup SF, Vidal R, Capece V, Freytag S, Fischer A, Verstreken P *et al* (2016) Endophilin-A Deficiency Induces the Foxo3a-Fbxo32 Network in the Brain and Causes Dysregulation of Autophagy and the Ubiquitin-Proteasome System. *Cell Rep* 17: 1071-1086
- Muroyama A, Lechler T (2017) Microtubule organization, dynamics and functions in differentiated cells. *Development* 144: 3012-3021
- Muroyama A, Seldin L, Lechler T (2016) Divergent regulation of functionally distinct gamma-tubulin complexes during differentiation. *J Cell Biol* 213: 679-692
- Musacchio A (2015) The Molecular Biology of Spindle Assembly Checkpoint Signaling Dynamics. *Curr Biol* 25: R1002-1018

Nahorski MS, Al-Gazali L, Hertecant J, Owen DJ, Borner GH, Chen YC, Benn CL, Carvalho OP, Shaikh SS, Phelan A *et al* (2015) A novel disorder reveals clathrin heavy chain-22 is essential for human pain and touch development. *Brain* 138: 2147-2160

Nahorski MS, Borner GHH, Shaikh SS, Davies AK, Al-Gazali L, Antrobus R, Woods CG (2018) Clathrin heavy chain 22 contributes to the control of neuropeptide degradation and secretion during neuronal development. *Sci Rep* 8: 2340

Nandez R, Balkin DM, Messa M, Liang L, Paradise S, Czapla H, Hein MY, Duncan JS, Mann M, De Camilli P (2014) A role of OCRL in clathrin-coated pit dynamics and uncoating revealed by studies of Lowe syndrome cells. *Elife* 3: e02975

Nano M, Basto R (2017) Consequences of Centrosome Dysfunction During Brain Development. *Adv Exp Med Biol* 1002: 19-45

Nguyen TTM, Gillet G, Popgeorgiev N (2021) Caspases in the Developing Central Nervous System: Apoptosis and Beyond. *Front Cell Dev Biol* 9: 702404

Nigg EA (1995) Cyclin-dependent protein kinases: key regulators of the eukaryotic cell cycle. *Bioessays* 17: 471-480

Nigg EA, Stearns T (2011) The centrosome cycle: Centriole biogenesis, duplication and inherent asymmetries. *Nat Cell Biol* 13: 1154-1160

Nishimura T, Kaibuchi K (2007) Numb controls integrin endocytosis for directional cell migration with aPKC and PAR-3. *Dev Cell* 13: 15-28

Noctor SC, Martinez-Cerdeno V, Ivic L, Kriegstein AR (2004) Cortical neurons arise in symmetric and asymmetric division zones and migrate through specific phases. *Nat Neurosci* 7: 136-144

Noctor SC, Martinez-Cerdeno V, Kriegstein AR (2008) Distinct behaviors of neural stem and progenitor cells underlie cortical neurogenesis. *J Comp Neurol* 508: 28-44

O'Neill AC, Uzbass F, Antognolli G, Merino F, Draganova K, Jäck A, Zhang S, Pedini G, Schessner JP, Cramer K *et al* (2022) Spatial centrosome proteome of human neural cells uncovers disease-relevant heterogeneity. *Science* 376: eabf9088

O'Toole E, Greenan G, Lange KI, Srayko M, Muller-Reichert T (2012) The role of gamma-tubulin in centrosomal microtubule organization. *PLoS One* 7: e29795

Oakley BR, Paolillo V, Zheng Y (2015) gamma-Tubulin complexes in microtubule nucleation and beyond. *Mol Biol Cell* 26: 2957-2962

Oakley CE, Oakley BR (1989) Identification of gamma-tubulin, a new member of the tubulin superfamily encoded by mipA gene of *Aspergillus nidulans*. *Nature* 338: 662-664

Okamoto CT, McKinney J, Jeng YY (2000) Clathrin in mitotic spindles. *Am J Physiol Cell Physiol* 279: C369-374

Oliver TG, Meylan E, Chang GP, Xue W, Burke JR, Humpton TJ, Hubbard D, Bhutkar A, Jacks T (2011) Caspase-2-mediated cleavage of Mdm2 creates a p53-induced positive feedback loop. *Mol Cell* 43: 57-71

Olmos Y, Hodgson L, Mantell J, Verkade P, Carlton JG (2015) ESCRT-III controls nuclear envelope reformation. *Nature* 522: 236-239

Olszewski MB, Chandris P, Park BC, Eisenberg E, Greene LE (2014) Disruption of clathrin-mediated trafficking causes centrosome overduplication and senescence. *Traffic* 15: 60-77

Otsuki L, Brand AH (2018) Cell cycle heterogeneity directs the timing of neural stem cell activation from quiescence. *Science* 360: 99-102

Owen DJ, Collins BM, Evans PR (2004) Adaptors for clathrin coats: structure and function. *Annu Rev Cell Dev Biol* 20: 153-191

Pardee AB (1989) G1 events and regulation of cell proliferation. *Science* 246: 603-608

Pechstein A, Gerth F, Milosevic I, Japel M, Eichhorn-Grunig M, Vorontsova O, Bacetic J, Maritzen T, Shupliakov O, Freund C *et al* (2015) Vesicle uncoating regulated by SH3-SH3 domain-mediated complex formation between endophilin and intersectin at synapses. *EMBO Rep* 16: 232-239

Pedersen LB, Mogensen JB, Christensen ST (2016) Endocytic Control of Cellular Signaling at the Primary Cilium. *Trends Biochem Sci* 41: 784-797

Pereira G, Schiebel E (2005) Kin4 kinase delays mitotic exit in response to spindle alignment defects. *Mol Cell* 19: 209-221

Petry S, Vale RD (2015) Microtubule nucleation at the centrosome and beyond. *Nat Cell Biol* 17: 1089-1093

Petsalaki E, Dandoulaki M, Zachos G (2018) The ESCRT protein Chmp4c regulates mitotic spindle checkpoint signaling. *J Cell Biol* 217: 861-876

Phan TP, Maryniak AL, Boatwright CA, Lee J, Atkins A, Tijhuis A, Spierings DC, Bazzi H, Foijer F, Jordan PW *et al* (2021) Centrosome defects cause microcephaly by activating the 53BP1-USP28-TP53 mitotic surveillance pathway. *EMBO J* 40: e106118

Pihan GA, Purohit A, Wallace J, Knecht H, Woda B, Quesenberry P, Doxsey SJ (1998) Centrosome defects and genetic instability in malignant tumors. *Cancer Res* 58: 3974-3985

Ping XL, Sun BF, Wang L, Xiao W, Yang X, Wang WJ, Adhikari S, Shi Y, Lv Y, Chen YS *et al* (2014) Mammalian WTAP is a regulatory subunit of the RNA N6-methyladenosine methyltransferase. *Cell Res* 24: 177-189

Plotnikova OV, Pugacheva EN, Golemis EA (2009) Primary cilia and the cell cycle. *Methods Cell Biol* 94: 137-160

Polo S, Di Fiore PP (2006) Endocytosis conducts the cell signaling orchestra. *Cell* 124: 897-900

Prasad K, Barouch W, Greene L, Eisenberg E (1993) A Protein Cofactor Is Required for Uncoating of Clathrin Baskets by Uncoating Atpase. *J Biol Chem* 268: 23758-23761

Prosseda PP, Luo N, Wang B, Alvarado JA, Hu Y, Sun Y (2017) Loss of OCRL increases ciliary PI(4,5)P2 in Lowe oculocerebrorenal syndrome. *J Cell Sci* 130: 3447-3454

Puehringer D, Orel N, Luningschror P, Subramanian N, Herrmann T, Chao MV, Sendtner M (2013) EGF transactivation of Trk receptors regulates the migration of newborn cortical neurons. *Nat Neurosci* 16: 407-415

R Ferreira R, Fukui H, Chow R, Vilfan A, Vermot J (2019) The cilium as a force sensor-myth versus reality. *J Cell Sci* 132

Raab M, Gentili M, de Belly H, Thiam HR, Vargas P, Jimenez AJ, Lautenschlaeger F, Voituriez R, Lennon-Duménil AM, Manel N *et al* (2016) ESCRT III repairs nuclear envelope ruptures during cell migration to limit DNA damage and cell death. *Science* 352: 359-362

Raimondi A, Ferguson SM, Lou X, Armbruster M, Paradise S, Giovedi S, Messa M, Kono N, Takasaki J, Cappello V *et al* (2011) Overlapping role of dynamin isoforms in synaptic vesicle endocytosis. *Neuron* 70: 1100-1114

Rakic P (1971) Guidance of neurons migrating to the fetal monkey neocortex. *Brain Res* 33: 471-476

Rakic P (1974) Neurons in rhesus monkey visual cortex: systematic relation between time of origin and eventual disposition. *Science* 183: 425-427

Rao AN, Falnikar A, O'Toole ET, Morphew MK, Hoenger A, Davidson MW, Yuan X, Baas PW (2016) Sliding of centrosome-unattached microtubules defines key features of neuronal phenotype. *J Cell Biol* 213: 329-341

Rasin MR, Gazula VR, Breunig JJ, Kwan KY, Johnson MB, Liu-Chen S, Li HS, Jan LY, Jan YN, Rakic P *et al* (2007) Numb and Numbl are required for maintenance of cadherin-based adhesion and polarity of neural progenitors. *Nat Neurosci* 10: 819-827

Rauch A, Thiel CT, Schindler D, Wick U, Crow YJ, Ekici AB, van Essen AJ, Goecke TO, Al-Gazali L, Chrzanowska KH *et al* (2008) Mutations in the pericentrin (PCNT) gene cause primordial dwarfism. *Science* 319: 816-819

Redlingshofer L, McLeod F, Chen Y, Camus MD, Burden JJ, Palomer E, Briant K, Dannhauser PN, Salinas PC, Brodsky FM (2020) Clathrin light chain diversity regulates membrane deformation in vitro and synaptic vesicle formation in vivo. *Proc Natl Acad Sci U S A* 117: 23527-23538

Reider A, Wendland B (2011) Endocytic adaptors--social networking at the plasma membrane. *J Cell Sci* 124: 1613-1622

Renard HF, Simunovic M, Lemiere J, Boucrot E, Garcia-Castillo MD, Arumugam S, Chambon V, Lamaze C, Wunder C, Kenworthy AK *et al* (2015) Endophilin-A2 functions in membrane scission in clathrin-independent endocytosis. *Nature* 517: 493-496

- Rhinn M, Zapata-Bodalo I, Klein A, Plassat JL, Knauer-Meyer T, Keyes WM (2022) Aberrant induction of p19Arf-mediated cellular senescence contributes to neurodevelopmental defects. *PLoS Biol* 20: e3001664
- Rice DS, Curran T (2001) Role of the reelin signaling pathway in central nervous system development. *Annu Rev Neurosci* 24: 1005-1039
- Ricotta D, Conner SD, Schmid SL, von Figura K, Honing S (2002) Phosphorylation of the AP2 mu subunit by AAK1 mediates high affinity binding to membrane protein sorting signals. *J Cell Biol* 156: 791-795
- Ringstad N, Gad H, Low P, Di Paolo G, Brodin L, Shupliakov O, De Camilli P (1999) Endophilin/SH3p4 is required for the transition from early to late stages in clathrin-mediated synaptic vesicle endocytosis. *Neuron* 24: 143-154
- Robbins E, Jentsch G, Micali A (1968) The centriole cycle in synchronized HeLa cells. *J Cell Biol* 36: 329-339
- Robinson HM, Black EJ, Brown R, Gillespie DA (2007) DNA mismatch repair and Chk1-dependent centrosome amplification in response to DNA alkylation damage. *Cell Cycle* 6: 982-992
- Robinson MS (2004) Adaptable adaptors for coated vesicles. *Trends Cell Biol* 14: 167-174
- Rohde G, Wenzel D, Haucke V (2002) A phosphatidylinositol (4,5)-bisphosphate binding site within mu2-adaptin regulates clathrin-mediated endocytosis. *J Cell Biol* 158: 209-214
- Rondelet A, Lin YC, Singh D, Porfetye AT, Thakur HC, Hecker A, Brinkert P, Schmidt N, Bendre S, Muller F *et al* (2020) Clathrin's adaptor interaction sites are repurposed to stabilize microtubules during mitosis. *J Cell Biol* 219
- Rosse C, Linch M, Kermorgant S, Cameron AJ, Boeckeler K, Parker PJ (2010) PKC and the control of localized signal dynamics. *Nat Rev Mol Cell Biol* 11: 103-112
- Royle SJ (2011) Mitotic moonlighting functions for membrane trafficking proteins. *Traffic* 12: 791-798
- Royle SJ (2012) The role of clathrin in mitotic spindle organisation. *J Cell Sci* 125: 19-28
- Royle SJ, Bright NA, Lagnado L (2005) Clathrin is required for the function of the mitotic spindle. *Nature* 434: 1152-1157
- Royle SJ, Lagnado L (2006) Trimerisation is important for the function of clathrin at the mitotic spindle. *J Cell Sci* 119: 4071-4078
- Sager PR, Brown PA, Berlin RD (1984) Analysis of transferrin recycling in mitotic and interphase HeLa cells by quantitative fluorescence microscopy. *Cell* 39: 275-282

Sakaba T, Kononenko NL, Bacetic J, Pechstein A, Schmoranzer J, Yao L, Barth H, Shupliakov O, Kobler O, Aktories K *et al* (2013) Fast neurotransmitter release regulated by the endocytic scaffold intersectin. *Proc Natl Acad Sci U S A* 110: 8266-8271

Salcini AE, Confalonieri S, Doria M, Santolini E, Tassi E, Minenkova O, Cesareni G, Pelicci PG, Di Fiore PP (1997) Binding specificity and in vivo targets of the EH domain, a novel protein-protein interaction module. *Genes Dev* 11: 2239-2249

Sallee MD, Feldman JL (2021) Microtubule organization across cell types and states. *Curr Biol* 31: R506-R511

Salomoni P, Calegari F (2010) Cell cycle control of mammalian neural stem cells: putting a speed limit on G1. *Trends Cell Biol* 20: 233-243

Santolini E, Puri C, Salcini AE, Gagliani MC, Pelicci PG, Tacchetti C, Di Fiore PP (2000) Numb is an endocytic protein. *J Cell Biol* 151: 1345-1352

Schaar BT, McConnell SK (2005) Cytoskeletal coordination during neuronal migration. *Proc Natl Acad Sci U S A* 102: 13652-13657

Schmid EM, McMahon HT (2007) Integrating molecular and network biology to decode endocytosis. *Nature* 448: 883-888

Schreiber S, Fleischer J, Breer H, Boekhoff I (2000) A possible role for caveolin as a signaling organizer in olfactory sensory membranes. *J Biol Chem* 275: 24115-24123

Schuske KR, Richmond JE, Matthies DS, Davis WS, Runz S, Rube DA, van der Blik AM, Jorgensen EM (2003) Endophilin is required for synaptic vesicle endocytosis by localizing synaptojanin. *Neuron* 40: 749-762

Schöneberg J, Pavlin MR, Yan S, Righini M, Lee IH, Carlson LA, Bahrami AH, Goldman DH, Ren X, Hummer G *et al* (2018) ATP-dependent force generation and membrane scission by ESCRT-III and Vps4. *Science* 362: 1423-1428

Serrano M (2010) Shifting senescence into quiescence by turning up p53. *Cell Cycle* 9: 4256-4257

Shats I, Milyavsky M, Cholostoy A, Brosh R, Rotter V (2007) Myocardin in tumor suppression and myofibroblast differentiation. *Cell Cycle* 6: 1141-1146

Shen Q, Temple S (2002) Creating asymmetric cell divisions by skewing endocytosis. *Sci STKE* 2002: pe52

Shen Q, Zhong WM, Jan YN, Temple S (2002) Asymmetric Numb distribution is critical for asymmetric cell division of mouse cerebral cortical stem cells and neuroblasts. *Development* 129: 4843-4853

Shieh JC, Schaar BT, Srinivasan K, Brodsky FM, McConnell SK (2011) Endocytosis regulates cell soma translocation and the distribution of adhesion proteins in migrating neurons. *PLoS One* 6: e17802

Shohayeb B, Diab M, Ahmed M, Ng DCH, 2018. Factors that influence adult neurogenesis as potential therapy. *BioMed Central*, pp. 4-4.

Sidi S, Sanda T, Kennedy RD, Hagen AT, Jette CA, Hoffmans R, Pascual J, Imamura S, Kishi S, Amatruda JF *et al* (2008) Chk1 suppresses a caspase-2 apoptotic response to DNA damage that bypasses p53, Bcl-2, and caspase-3. *Cell* 133: 864-877

Silkworth WT, Nardi IK, Scholl LM, Cimini D (2009) Multipolar spindle pole coalescence is a major source of kinetochore mis-attachment and chromosome mis-segregation in cancer cells. *PLoS One* 4: e6564

Sir JH, Pütz M, Daly O, Morrison CG, Dunning M, Kilmartin JV, Gergely F (2013) Loss of centrioles causes chromosomal instability in vertebrate somatic cells. *J Cell Biol* 203: 747-756

Skoufias DA, Lacroix FB, Andreassen PR, Wilson L, Margolis RL (2004) Inhibition of DNA decatenation, but not DNA damage, arrests cells at metaphase. *Mol Cell* 15: 977-990

Smith CM, Haucke V, McCluskey A, Robinson PJ, Chircop M (2013) Inhibition of clathrin by pitstop 2 activates the spindle assembly checkpoint and induces cell death in dividing HeLa cancer cells. *Mol Cancer* 12: 4

Sorensen EB, Conner SD (2008) AAK1 regulates Numb function at an early step in clathrin-mediated endocytosis. *Traffic* 9: 1791-1800

Soukup SF, Kuenen S, Vanhauwaert R, Manetsberger J, Hernandez-Diaz S, Swerts J, Schoovaerts N, Vilain S, Goukko NV, Vints K *et al* (2016) A LRRK2-Dependent EndophilinA Phosphoswitch Is Critical for Macroautophagy at Presynaptic Terminals. *Neuron* 92: 829-844

Soykan T, Kaempf N, Sakaba T, Vollweiter D, Goerdeler F, Puchkov D, Kononenko NL, Haucke V (2017) Synaptic Vesicle Endocytosis Occurs on Multiple Timescales and Is Mediated by Formin-Dependent Actin Assembly. *Neuron* 93: 854-866 e854

Spassky N, Han YG, Aguilar A, Strehl L, Besse L, Laclef C, Ros MR, Garcia-Verdugo JM, Alvarez-Buylla A (2008) Primary cilia are required for cerebellar development and Shh-dependent expansion of progenitor pool. *Dev Biol* 317: 246-259

Stoufflet J, Chaulet M, Doulazmi M, Fouquet C, Dubacq C, Métin C, Schneider-Maunoury S, Trembleau A, Vincent P, Caillé I (2020) Primary cilium-dependent cAMP/PKA signaling at the centrosome regulates neuronal migration. *Sci Adv* 6

Strome S, Powers J, Dunn M, Reese K, Malone CJ, White J, Seydoux G, Saxton W (2001) Spindle dynamics and the role of gamma-tubulin in early *Caenorhabditis elegans* embryos. *Mol Biol Cell* 12: 1751-1764

Sudakin V, Chan GK, Yen TJ (2001) Checkpoint inhibition of the APC/C in HeLa cells is mediated by a complex of BUBR1, BUB3, CDC20, and MAD2. *J Cell Biol* 154: 925-936

Sueda R, Kageyama R (2020) Regulation of active and quiescent somatic stem cells by Notch signaling. *Dev Growth Differ* 62: 59-66

- Sulimenko V, Dráberová E, Dráber P (2022) γ -Tubulin in microtubule nucleation and beyond. *Front Cell Dev Biol* 10: 880761
- Swanson JA (2008) Shaping cups into phagosomes and macropinosomes. *Nat Rev Mol Cell Biol* 9: 639-649
- Swanson JA, Yoshida S (2019) Macropinosomes as units of signal transduction. *Philos Trans R Soc Lond B Biol Sci* 374: 20180157
- Sweet HO, Bronson RT, Johnson KR, Cook SA, Davisson MT (1996) Scrambler, a new neurological mutation of the mouse with abnormalities of neuronal migration. *Mamm Genome* 7: 798-802
- Takahashi T, Nowakowski RS, Caviness VS (1994) Mode of cell proliferation in the developing mouse neocortex. *Proc Natl Acad Sci U S A* 91: 375-379
- Takei K, Mundigl O, Daniell L, De Camilli P (1996) The synaptic vesicle cycle: a single vesicle budding step involving clathrin and dynamin. *J Cell Biol* 133: 1237-1250
- Tanaka T, Serneo FF, Higgins C, Gambello MJ, Wynshaw-Boris A, Gleeson JG (2004) Lis1 and doublecortin function with dynein to mediate coupling of the nucleus to the centrosome in neuronal migration. *J Cell Biol* 165: 709-721
- Taylor KR, Holzer AK, Bazan JF, Walsh CA, Gleeson JG (2000) Patient mutations in doublecortin define a repeated tubulin-binding domain. *J Biol Chem* 275: 34442-34450
- Taylor SS, McKeon F (1997) Kinetochore localization of murine Bub1 is required for normal mitotic timing and checkpoint response to spindle damage. *Cell* 89: 727-735
- Terzi MY, Izmirli M, Gogebakan B (2016) The cell fate: senescence or quiescence. *Mol Biol Rep* 43: 1213-1220
- Thawani A, Petry S (2021) Molecular insight into how γ -TuRC makes microtubules. *J Cell Sci* 134
- Thompson HM, Cao H, Chen J, Euteneuer U, McNiven MA (2004) Dynamin 2 binds gamma-tubulin and participates in centrosome cohesion. *Nat Cell Biol* 6: 335-342
- Thornton GK, Woods CG (2009) Primary microcephaly: do all roads lead to Rome? *Trends Genet* 25: 501-510
- Tobin JL, Di Franco M, Eichers E, May-Simera H, Garcia M, Yan J, Quinlan R, Justice MJ, Hennekam RC, Briscoe J *et al* (2008) Inhibition of neural crest migration underlies craniofacial dysmorphology and Hirschsprung's disease in Bardet-Biedl syndrome. *Proc Natl Acad Sci U S A* 105: 6714-6719
- Tovey CA, Tubman CE, Hamrud E, Zhu Z, Dyas AE, Butterfield AN, Fyfe A, Johnson E, Conduit PT (2018) γ -TuRC Heterogeneity Revealed by Analysis of Mozart1. *Curr Biol* 28: 2314-2323.e2316
- Tsai LH, Gleeson JG, 2005. Nucleokinesis in neuronal migration. *Cell Press*, pp. 383-388.

Tsou MF, Stearns T (2006) Mechanism limiting centrosome duplication to once per cell cycle. *Nature* 442: 947-951

Tyanova S, Temu T, Cox J (2016a) The MaxQuant computational platform for mass spectrometry-based shotgun proteomics. *Nat Protoc* 11: 2301-2319

Tyanova S, Temu T, Sinitcyn P, Carlson A, Hein MY, Geiger T, Mann M, Cox J (2016b) The Perseus computational platform for comprehensive analysis of (prote)omics data. *Nat Methods* 13: 731-740

Umeshima H, Hirano T, Kengaku M (2007) Microtubule-based nuclear movement occurs independently of centrosome positioning in migrating neurons. *Proc Natl Acad Sci U S A* 104: 16182-16187

Ungewickell E, Ungewickell H, Holstein SE, Lindner R, Prasad K, Barouch W, Martin B, Greene LE, Eisenberg E (1995) Role of auxilin in uncoating clathrin-coated vesicles. *Nature* 378: 632-635

van der Vaart A, Rademakers S, Jansen G (2015) DLK-1/p38 MAP Kinase Signaling Controls Cilium Length by Regulating RAB-5 Mediated Endocytosis in *Caenorhabditis elegans*. *PLoS Genet* 11: e1005733

Veltman DM, Williams TD, Bloomfield G, Chen BC, Betzig E, Insall RH, Kay RR (2016) A plasma membrane template for macropinocytic cups. *Elife* 5: e20085

Ventimiglia LN, Cuesta-Geijo MA, Martinelli N, Caballe A, Macheboeuf P, Miguet N, Parnham IM, Olmos Y, Carlton JG, Weissenhorn W *et al* (2018) CC2D1B Coordinates ESCRT-III Activity during the Mitotic Reformation of the Nuclear Envelope. *Dev Cell* 47: 547-563.e546

Verstreken P, Kjaerulff O, Lloyd TE, Atkinson R, Zhou Y, Meinertzhagen IA, Bellen HJ (2002) Endophilin mutations block clathrin-mediated endocytosis but not neurotransmitter release. *Cell* 109: 101-112

Verstreken P, Koh TW, Schulze KL, Zhai RG, Hiesinger PR, Zhou Y, Mehta SQ, Cao Y, Roos J, Bellen HJ (2003) Synaptojanin is recruited by endophilin to promote synaptic vesicle uncoating. *Neuron* 40: 733-748

Vicente JJ, Wordeman L (2015) Mitosis, microtubule dynamics and the evolution of kinesins. *Exp Cell Res* 334: 61-69

Vietri M, Schink KO, Campsteijn C, Wegner CS, Schultz SW, Christ L, Thoresen SB, Brech A, Raiborg C, Stenmark H (2015) Spastin and ESCRT-III coordinate mitotic spindle disassembly and nuclear envelope sealing. *Nature* 522: 231-235

Vitriol EA, Zheng JQ (2012) Growth cone travel in space and time: the cellular ensemble of cytoskeleton, adhesion, and membrane. *Neuron* 73: 1068-1081

von Appen A, LaJoie D, Johnson IE, Trnka MJ, Pick SM, Burlingame AL, Ullman KS, Frost A (2020) LEM2 phase separation promotes ESCRT-mediated nuclear envelope reformation. *Nature* 582: 115-118

- Waite K, Eickholt BJ (2010) The neurodevelopmental implications of PI3K signaling. *Curr Top Microbiol Immunol* 346: 245-265
- Walther K, Diril MK, Jung N, Haucke V (2004) Functional dissection of the interactions of stonin 2 with the adaptor complex AP-2 and synaptotagmin. *Proc Natl Acad Sci U S A* 101: 964-969
- Wang RH, Yu H, Deng CX (2004) A requirement for breast-cancer-associated gene 1 (BRCA1) in the spindle checkpoint. *Proc Natl Acad Sci U S A* 101: 17108-17113
- Warecki B, Ling X, Bast I, Sullivan W (2020) ESCRT-III-mediated membrane fusion drives chromosome fragments through nuclear envelope channels. *J Cell Biol* 219
- Watanabe S, Mamer LE, Raychaudhuri S, Luvsanjav D, Eisen J, Trimbuch T, Sohl-Kielczynski B, Fenske P, Milosevic I, Rosenmund C *et al* (2018) Synaptojanin and Endophilin Mediate Neck Formation during Ultrafast Endocytosis. *Neuron* 98: 1184-1197 e1186
- Watanabe S, Meitinger F, Shiau AK, Oegema K, Desai A (2020) Centriole-independent mitotic spindle assembly relies on the PCNT-CDK5RAP2 pericentriolar matrix. *J Cell Biol* 219
- Watanabe S, Rost BR, Camacho-Perez M, Davis MW, Sohl-Kielczynski B, Rosenmund C, Jorgensen EM (2013) Ultrafast endocytosis at mouse hippocampal synapses. *Nature* 504: 242-247
- Watanabe S, Trimbuch T, Camacho-Perez M, Rost BR, Brokowski B, Sohl-Kielczynski B, Felies A, Davis MW, Rosenmund C, Jorgensen EM (2014) Clathrin regenerates synaptic vesicles from endosomes. *Nature* 515: 228-233
- Webb DJ, Parsons JT, Horwitz AF (2002) Adhesion assembly, disassembly and turnover in migrating cells -- over and over and over again. *Nat Cell Biol* 4: E97-100
- Weinberg RA (1995) The retinoblastoma protein and cell cycle control. *Cell* 81: 323-330
- West MA, Prescott AR, Eskelinen E-L, Ridley AJ, Watts C (2000) Rac is required for constitutive macropinocytosis by dendritic cells but does not control its downregulation. *Curr Biol* 10: 839-848
- Wheway G, Nazlamova L, Hancock JT (2018) Signaling through the Primary Cilium. *Front Cell Dev Biol* 6: 8
- Wickman G, Julian L, Olson MF (2012) How apoptotic cells aid in the removal of their own cold dead bodies. *Cell Death Differ* 19: 735-742
- Wilkinson RS, Lin MY (2004) Endocytosis and synaptic plasticity: might the tail wag the dog? *Trends Neurosci* 27: 171-174
- Willaredt MA, Hasenpusch-Theil K, Gardner HA, Kitanovic I, Hirschfeld-Warneken VC, Gojak CP, Gorgas K, Bradford CL, Spatz J, Wöfl S *et al* (2008) A crucial role for primary cilia in cortical morphogenesis. *J Neurosci* 28: 12887-12900
- Winey M (1999) Cell cycle: driving the centrosome cycle. *Curr Biol* 9: R449-452

Woods CG, Basto R (2014) Microcephaly. *Curr Biol* 24: R1109-1111

Wu S, Majeed SR, Evans TM, Camus MD, Wong NM, Schollmeier Y, Park M, Muppidi JR, Reboldi A, Parham P *et al* (2016) Clathrin light chains' role in selective endocytosis influences antibody isotype switching. *Proc Natl Acad Sci U S A* 113: 9816-9821

Xie S, Reinecke JB, Farmer T, Bahl K, Yeow I, Nichols BJ, McLamarrah TA, Naslavsky N, Rogers GC, Caplan S (2018) Vesicular trafficking plays a role in centriole disengagement and duplication. *Mol Biol Cell* 29: 2622-2631

Yabuno Y, Uchihashi T, Sasakura T, Shimizu H, Naito Y, Fukushima K, Ota K, Kogo M, Nojima H, Yabuta N (2019) Clathrin heavy chain phosphorylated at T606 plays a role in proper cell division. *Cell Cycle* 18: 1976-1994

Yamashita N, Kuruvilla R (2016) Neurotrophin signaling endosomes: biogenesis, regulation, and functions. *Curr Opin Neurobiol* 39: 139-145

Yap CC, Digilio L, Kruczek K, Roszkowska M, Fu XQ, Liu JS, Winckler B (2018) A dominant dendrite phenotype caused by the disease-associated G253D mutation in doublecortin (DCX) is not due to its endocytosis defect. *J Biol Chem* 293: 18890-18902

Yap CC, Vakulenko M, Kruczek K, Motamedi B, Digilio L, Liu JS, Winckler B (2012) Doublecortin (DCX) mediates endocytosis of neurofascin independently of microtubule binding. *J Neurosci* 32: 7439-7453

Yap CC, Winckler B (2012) Harnessing the power of the endosome to regulate neural development. *Neuron* 74: 440-451

Yap CC, Winckler B (2015) Adapting for endocytosis: roles for endocytic sorting adaptors in directing neural development. *Front Cell Neurosci* 9: 119

Yeh E, Skibbens RV, Cheng JW, Salmon ED, Bloom K (1995) Spindle dynamics and cell cycle regulation of dynein in the budding yeast, *Saccharomyces cerevisiae*. *J Cell Biol* 130: 687-700

Yeow ZY, Lambrus BG, Marlow R, Zhan KH, Durin MA, Evans LT, Scott PM, Phan T, Park E, Ruiz LA *et al* (2020) Targeting TRIM37-driven centrosome dysfunction in 17q23-amplified breast cancer. *Nature* 585: 447-452

Yin HL, Janmey PA (2003) Phosphoinositide regulation of the actin cytoskeleton. *Annu Rev Physiol* 65: 761-789

Yoneshima H, Nagata E, Matsumoto M, Yamada M, Nakajima K, Miyata T, Ogawa M, Mikoshiba K (1997) A novel neurological mutant mouse, yotari, which exhibits reeler-like phenotype but expresses CR-50 antigen/Reelin. *Neuroscience Research* 29: 217-223

Young RA (2011) Control of the embryonic stem cell state. *Cell* 144: 940-954

Yu H, Li Y, Li L, Huang J, Wang X, Tang R, Jiang Z, Lv L, Chen F, Yu C *et al* (2021) Functional reciprocity of proteins involved in mitosis and endocytosis. *FEBS J* 288: 5850-5866

- Yue S, Tang LY, Tang Y, Tang Y, Shen QH, Ding J, Chen Y, Zhang Z, Yu TT, Zhang YE *et al* (2014) Requirement of Smurf-mediated endocytosis of Patched1 in sonic hedgehog signal reception. *Elife* 3
- Zakrzewski W, Dobrzyński M, Szymonowicz M, Rybak Z (2019) Stem cells: past, present, and future. *Stem Cell Res Ther* 10: 68
- Zein-Sabatto H, Lerit DA (2021) The Identification and Functional Analysis of mRNA Localizing to Centrosomes. *Front Cell Dev Biol* 9: 782802
- Zhang S, Hemmerich P, Grosse F (2007) Centrosomal localization of DNA damage checkpoint proteins. *J Cell Biochem* 101: 451-465
- Zhang X, He X, Li Q, Kong X, Ou Z, Zhang L, Gong Z, Long D, Li J, Zhang M *et al* (2017) PI3K/AKT/mTOR Signaling Mediates Valproic Acid-Induced Neuronal Differentiation of Neural Stem Cells through Epigenetic Modifications. *Stem Cell Reports* 8: 1256-1269
- Zheng J, Shen WH, Lu TJ, Zhou Y, Chen Q, Wang Z, Xiang T, Zhu YC, Zhang C, Duan S *et al* (2008) Clathrin-dependent endocytosis is required for TrkB-dependent Akt-mediated neuronal protection and dendritic growth. *J Biol Chem* 283: 13280-13288
- Zhou P, Alfaro J, Chang EH, Zhao X, Porcionatto M, Segal RA (2011) Numb links extracellular cues to intracellular polarity machinery to promote chemotaxis. *Dev Cell* 20: 610-622
- Zhou P, Porcionatto M, Pilapil M, Chen Y, Choi Y, Toliaas KF, Bikoff JB, Hong EJ, Greenberg ME, Segal RA (2007a) Polarized signaling endosomes coordinate BDNF-induced chemotaxis of cerebellar precursors. *Neuron* 55: 53-68
- Zhou Y, Atkins JB, Rompani SB, Bancescu DL, Petersen PH, Tang H, Zou K, Stewart SB, Zhong W (2007b) The mammalian Golgi regulates numb signaling in asymmetric cell division by releasing ACBD3 during mitosis. *Cell* 129: 163-178
- Zilian O, Saner C, Hagedorn L, Lee HY, Sauberli E, Suter U, Sommer L, Aguet M (2001) Multiple roles of mouse Numb in tuning developmental cell fates. *Curr Biol* 11: 494-501
- Zucco AJ, Pozzo VD, Afinogenova A, Hart RP, Devinsky O, D'Arcangelo G (2018) Neural progenitors derived from Tuberous Sclerosis Complex patients exhibit attenuated PI3K/AKT signaling and delayed neuronal differentiation. *Mol Cell Neurosci* 92: 149-163

8. PUBLICATIONS

Cambior-Perujo S. and Kononenko N.L. Brain-specific functions of the endocytic machinery (The FEBS Journal, 2021)

Sanchez-Mendoza, E.H., **Cambior-Perujo, S.**, Martins Nascentes-Melo, L. et al. Compromised Hippocampal Neuroplasticity in the Interferon- α and Toll-like Receptor-3 Activation-Induced Mouse Depression Model. (Molecular Neurobiology, 2020)

Bera, S., **Cambior-Perujo, S.**, Calleja Barca, E., Negrete-Hurtado, A., Racho, J., De Bruyckere, E., Wittich, C., Ellrich, N., Martins, S., Adjaye, J., Kononenko, N. L. AP-2 reduces amyloidogenesis by promoting BACE1 trafficking and degradation in neurons (EMBO reports, 2020)

ACKNOWLEDGMENTS

Foremost all I would like to thank my supervisor Prof. Dr. Natalia L. Kononenko who gave me the opportunity to work in her group. Our scientific discussions have been the main engine of this project and she trusted my criteria allowing our research to go to a territory uncharted for our lab. My time in her lab under her supervision help me to evolve as a scientist, for which I am truly grateful.

I would like to thank Prof Dr Elena Rugarli and Prof. Dr Peter Kloppenburg who kindly agreed to take part of my dissertation committee and Prof Dr Jan Riemer, supervisor of my graduate school, and Dr Susanne Vorhagen, coordinator of the graduate school, for its involvement and dedication to the program, providing courses, scientific lectures, and support for presenting the research outside the lab. I am also greatly thankful for Dr. Hisham Bazzi constant advice and help during the developing of this project.

I thank CECAD's facility, mostly from the animal caretakers, the imaging facility, and the proteomics facility. Their excellent work helped keep the research going forward smoothly.

In addition, I would like to thank former members of Kononenko's lab, especially Dr Sujoy Bera and Dr Albert Negrete Hurtado who helped me greatly during my beginning in the lab, and all the people part of our lab, especially Dr Melina Overhoff and Marvin Schäfer who have support me not only scientifically but also at a personal level resulting in a kind friendship outside the lab also. This thesis would not have been possible without their help.

Finally, on a more personal note, I would like to thank my friends and family, who have always believed in me and always supported me in my pursue of a scientific career.

EIDESSTATTLICHE ERKLÄRUNG

Ich versichere, dass ich die von mir vorgelegte Dissertation selbständig angefertigt, die benutzten Quellen und Hilfsmittel vollständig angegeben und die Stellen der Arbeit – einschließlich Tabellen, Karten und Abbildungen –, die anderen Werken im Wortlaut oder dem Sinn nach entnommen sind, in jedem Einzelfall als Entlehnung kenntlich gemacht habe; dass diese Dissertation noch keiner anderen Fakultät oder Universität zur Prüfung vorgelegen hat; dass sie – abgesehen von unten angegebenen Teilpublikationen – noch nicht veröffentlicht worden ist, sowie, dass ich eine solche Veröffentlichung vor Abschluss des Promotionsverfahrens nicht vornehmen werde. Die Bestimmungen der Promotionsordnung sind mir bekannt. Die von mir vorgelegte Dissertation ist von Dr Natalia L. Kononenko betreut worden.

Teilpublikationen sind in Kapitel 8 angegeben

Ich versichere, dass ich alle Angaben wahrheitsgemäß nach bestem Wissen und Gewissen gemacht habe und verpflichte mich, jedmögliche, die obigen Angaben betreffende Veränderungen dem Promotionsausschuss unverzüglich

07.11.2022

Datum

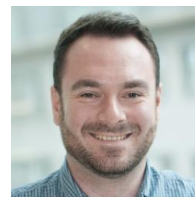
Santiago Manuel Cambor Perujo

Unterschrift

CV

Santiago Manuel Camblor Perujo

Berrenrather Str. 572, 50354 Hürth, (NRW) Germany
 +49 173 47 69 713
 santiagocamblorperujo@gmail.com



PROFILE:

- Highly self-motivated Ph.D. candidate with demonstrated research expertise in neurobiology and stem cells.
- Strong interpersonal skills, good communicator, independent -worker, able to learn and adapt quickly.
- Experimental techniques: primary cell cultures (NPCs/NSCs, Neurons, MEFs, Astrocytes), stem cells induction and differentiation, microscopy and live-cell imaging, organotypic cultures, electrophysiology stereotactic injections, and behavioral experiments.
- Computer skills: data analysis, imaging processing and analysis, and basic programming skills.

EDUCATION:

- **University of Cologne, Cologne, Germany**
Ph.D. Biological Sciences, December 2022 (expected)
- **Ruhr-Universität Bochum (RUB), Bochum, Germany (GPA: 2.0 | German System)**
M.Sc. Molecular and Developmental Stem Cell Biology International Master Program, 2017
Ml.Grant "Convenium" for abroad studies (2015)
- **Universidad de Oviedo, Oviedo, Spain (GPA: 7/10)**
B.Sc. Biology, 2015

RESEARCH

- Neurogenesis and neuronal stem cells
- Neurodevelopment and related disorders
- Senescence and quiescence in stem cells
- Tissue engineering and regenerative medicine

SCIENTIFIC RESEARCH EXPERIENCE:

CECAD (University of Cologne), Cologne, Germany

Ph.D. Candidate, 2018-present

Project: The endocytic adaptor AP-2 interacts with γ -TuRC components to maintain centrosome integrity in neural progenitor cells

Supervisor: Prof. Dr. Natalia Kononenko

- Investigating a novel endocytosis-independent role of AP-2 in neurogenesis, neuronal determination, and neuronal migration by regulating centrosomes, microtubule dynamics, and cell cycle progression.
- Contributed to a team researching an endocytosis-independent function of AP-2 regulating BACE1 endosomal trafficking and delivery to lysosomes in Alzheimer's Disease.
- Experience in diverse cell cultures, live-imaging microscopy, behavioral experiments, and organotypic cultures.

Chair of Vascular Neurology/NeuroScienceLab (UK-Essen), Essen, Germany

Internship, 2016-2017 | **Master Thesis**, Apr-Oct 2017 | **Ph.D. Candidate**, 2017-2018

Project: Molecular mechanisms of exosome-induced axonal branching

Supervisor: Dr Eduardo Sánchez-Mendoza

- Investigated how EPO influences axon development by exosomal release.
- Contributed to a team researching how IFN- α and poly(I:C) influence neuroplasticity in immune response-induced depression.
- Experience in neuronal and neurosphere cultures, biochemical techniques, electrophysiology, thalamic injections, mice surgery, and ischemia models (in vitro and in vivo).

Department of Anatomy and Embryology (RUB), Bochum, Germany

iPSCs practical course Mar-Apr 2016

- Instructed in how to generate iPSCs and how to work with them (transfection, differentiation, and characterization)

Experimental Eye Research Institute (Knappschaftskrankenhaus), Bochum, Germany

Practical course, Dec 2015

- Instructed in how to extract, culture and work with retinal organotypic cultures.

Centro Comunitario de Sangre y Tejidos de Asturias / FIO Fernández-Vega, Oviedo, Spain **Internship,** May-Jul 2014 | **Bachelor Thesis,** 2014-2015

Project: Design of scaffolds from hemoglobin for tissue engineering

Supervisor: Dr Álvaro Meana

- Contributed to developing a new scaffold derived from hemoglobin and testing it in vitro and in vivo.
- Basic training in tissue engineering

SUPERVISION EXPERIENCE:

CECAD (University of Cologne), Cologne, Germany

- Practical module supervision, Oct-Dec 2021
- Practical module supervision, Nov-Dec 2020
- Master thesis supervision, Feb-Sep 2020
- Practical module supervision, July 2019

MAJOR COURSES:

- FELASA-A (Lab animal experimentation) 2018

PUBLICATIONS:

- Cambior-Perujo S, Kononenko NL. Brain-specific functions of the endocytic machinery. FEBS J. 2021 Apr 25. doi: 10.1111/febs.15897.
- Sanchez-Mendoza EH, Cambior-Perujo S, Martins Nascentes-Melo L, Dzyubenko E, Fleischer M, Silva de Carvalho T, Schmitt LI, Leo M, Hagenacker T, Herring A, Keyvani K, Bera S, Kononenko N, Kleinschnitz C, Hermann DM. Compromised Hippocampal Neuroplasticity in the Interferon- α and Toll-like Receptor-3 Activation-Induced Mouse Depression Model. Mol Neurobiol. 2020 Jul;57(7):3171-3182. doi: 10.1007/s12035-020-01927-0.
- Bera S, Cambior-Perujo S, Calleja Barca E, Negrete-Hurtado A, Racho J, De Bruyckere E, Wittich C, Ellrich N, Martins S, Adjaye J, Kononenko NL. AP-2 reduces amyloidogenesis by promoting BACE1 trafficking and degradation in neurons. EMBO Rep. 2020 Jun 4;21(6):e47954. doi: 10.15252/embr.201947954.

ORAL PRESENTATIONS:

- **Pint of Science Cologne (May 2022)** How to make a brain?
- **EURON PhD days (February 2022)**
Parallel session ("Mitochondria in Parkinson's disease: Exploring cellular mechanisms beyond mitophagy")
- **14th Göttingen Meeting of the German Neuroscience Society (March 2021)**
Symposium 14 (Post-translational modifications of proteome in neuronal development)

POSTER PRESENTATIONS:

- **EMBO Workshop: Neural stem cells: From basic understanding to translational applications (June 2022)**
The endocytic adaptor AP-2 interacts with γ -TuRC components to maintain centrosome integrity in neural progenitor cells
- **EURON PhD days (February 2022)**
Regulation of Neuronal Cell Fate Determination by Endocytic Adaptor AP-2
- **Groningen-Jena Aging Meeting (G-Jam) (October 2021)**
Regulation of Neuronal Cell Fate Determination by Endocytic Adaptor AP-2
- **14th Göttingen Meeting of the German Neuroscience Society (March 2021)**
Regulation of Neuronal Cell Fate Determination by Endocytic Adaptor AP-2
- **INSIDE – The dark side of the cell (February 2021)**
Regulation of Neuronal Cell Fate Determination by Endocytic Adaptor AP-2
- **11th FENS Forum of Neuroscience (July 2018)**
Interferon alpha (IFN- α) and Polyinosinic:polycytidylic acid (Poly I:C) alter AMPA1 receptor phosphorylation and neuronal structure as a mechanism of inflammation mediated depression.